LAPPEENRANTA-LAHTI UNIVERSITY OF TECHNOLOGY LUT
School of Energy Systems
Department of Energy Technology
Master's Thesis

Petteri Aalto

Utilization of seawater heat pumps in buildings – system energy study of heating & cooling performance

Examiners: D.Sc (Tech.) Teemu Turunen-Saaresti
Docent Aki Grönman

Supervisors: D.Sc (Tech.) Teemu Turunen-Saaresti
M.Sc (Tech.) Santeri Siren

ABSTRACT

Lappeenranta-Lahti University of Technology LUT
LUT School of Energy Systems
Master's Degree Programme in Energy Technology

Petteri Aalto

Utilization of seawater heat pumps in buildings – system energy study of heating & cooling performance

Master's Thesis 2021

111 pages, 77 figures, and 20 tables.

Examiners: D.Sc. (Tech.) Teemu Turunen-Saaresti, Docent Aki Grönman
Supervisors: D.Sc. (Tech.) Teemu Turunen-Saaresti, M.Sc. (Tech.) Santeri Siren

Keywords: heat pump, district heating, heat exchanger, seawater, waterways, buildings, energy modeling, simulation, life cycle costing, authorization, environmental impacts.

In this master's thesis is a seawater heat pump (SWHP) system's heating & cooling performance studied in buildings. A simulation model of the system is created in IDA ICE, where real performance data for heat pumps, circulation pumps, and seawater heat exchangers are implemented. The created system consists of both heat pumps and district heating and is compared to a district heating-only system, where system performance, life cycle costing and emissions are examined. Authorization of these systems requires a Water Permit from the Regional State Administrative Agency (AVI). No substantial issues to get a permit was noticed. The only issue can be with lakes, where the size, hydrology, and social activities may impact the permit approval.

Two ways of utilizing seawater were recognized: open- and closed-loop, where open-loop generally use a separate heat exchanger and closed-loop consist of a collector pipe anchored on the bottom of the waterbody. Corrosion, fouling, and freezing risks are higher in an open-loop configuration. By choosing proper steel materials and intake filtration can these issues be resolved to a certain extent. Freezing risk is highest during wintertime when seawater temperatures are low. Methods for decreasing the risk are by enabling a high mass flow rate and adequate pressure loss in the primary side of the heat exchanger. These features provide high turbulent flow and enable great shear force in the heat exchanger.

The studied case was a generic 14 400 k-m^2 residential building block with a heating demand of 1225 MWh and 45 MWh of cooling demand. The heat pumps contributed to the total heating demand with a 77 % energy coverage and 89 % of the cooling demand was covered by free cooling. The LCC analysis resulted to be more beneficial for the SWHP system. The payback time was 11,6 years and the system had significantly lower CO_2 emissions. The system performance studied in this work seems promising from a perspective to produce cleaner energy.

TIIVISTELMÄ

Lappeenranta-Lahti University of Technology LUT
LUT School of Energy Systems
Energiatekniikan koulutusohjelma

Petteri Aalto

Merivesilämpöpumppujen hyödyntäminen rakennuksissa -järjestelmän energiaselvitys lämmityksessä & jäähdytyksessä

Diplomityö 2021

111 sivua, 77 kuvaa, ja 20 taulukkoa.

Tarkastajat: TkT Teemu Turunen-Saaresti, Dosentti Aki Grönman
Ohjaajat: TkT Teemu Turunen-Saaresti, DI Santeri Siren

Hakusanat: lämpöpumppu, kaukolämpö, lämmönvaihdin, merivesi, vesistöt, rakennukset, energiamallinnus, simulointi, elinkaarikustannuslaskelma, lupa-asiat, ympäristövaikutukset.

Tässä diplomityössä tarkasteltiin merivesilämpöpumppujärjestelmän suorituskykyä rakennusten lämmityksessä & jäähdytyksessä. Järjestelmästä tehtiin simulointimalli IDA ICE-ohjelmalla, jossa käytettiin oikeita suorituskykyarvoja järjestelmän pääkomponenteissa. Malli koostui lämpöpumppujen ja kaukolämmön yhteiskäytöstä, jota vertailtiin pelkkään kaukolämpöjärjestelmään tarkastelemalla suorituskykyä, elinkaarikustannuksia ja syntyneitä päästöjä. Työssä tutkittu järjestelmä vaatii vesiluvan, jonka aluehallintovirasto myöntää. Merkittäviä haasteita järjestelmän toteuttamisessa ei ilmaantunut. Ainoa huomio on vesistöjen kanssa, missä alueen koko, hydrologia ja sosiaaliset aktiviteetit voivat herkemmin vaikuttaa luvan saamiseen.

Kaksi menetelmää hyödyntää merivettä ovat avoimella ja suljetulla kierrolla. Avoimessa kierrossa käytetään yleensä erillistä lämmönvaihdinta. Suljetussa kierrossa on keruuputkisto ankkuroitu vesilähteen pohjaan. Avoimessa kierrossa korroosio, likaantuminen ja jäätymisriski ovat suuremmat. Näitä ongelmia voidaan ehkäistä käyttämällä korroosiota kestäviä materiaaleja ja imupuolen suodatusta. Ratkaisuja jäätymistä vastaan on korkea meriveden massavirta ja painehäviö, joka tekee virtauksesta turbulenttista ja mahdollistaa suuret leikkausvoimat vaihtimessa. Jäätymisriski on suurimmillaan talvella, kun meriveden lämpötila on alhaisimmillaan.

Työssä tarkasteltiin 14 400 k-m^2 kokoista geneeristä asuinkerrostalokorttelia, jonka kokonaisenergiatarve oli 1225 MWh lämmitykselle ja 45 MWh jäähdytykselle. Lämpöpumppujen energiapeitto oli 77 % lämmitystarpeesta ja jäähdytyksen energiatarve tuotettiin 89 % vapaajäähdytyksen avulla. Elinkaarikustannusten tulokset osoittivat merivesipumppujärjestelmän kannattavaksi. Takaisinmaksuajaksi saatiin 11,6 vuotta ja tuotannosta syntyneet päästöt olivat huomattavasti alhaisemmat. Kyseisen järjestelmän suorituskyky vaikuttaa lupaavalta puhtaamman energiantuotannon näkökulmasta.

ACKNOWLEDGEMENTS

Completion of my master's degree at LUT-University was supported by Ramboll Finland Oy that kindly provided a thesis topic. Special thanks to my supervisor Santeri Siren who supported and gave valuable insights along the entire process. I would also like to thank the Ramboll Energy team, especially Erkki Karjalainen for the IDA ICE support, and Jukka Kopra for giving support in Excel and viewpoints to different subjects that arose from time to time.

From LUT-University I would like to thank Teemu Turunen-Saaresti for providing academic insight and overall support for my work during the whole thesis process.

Finally, I would like to show my gratitude to my family, friends, and colleagues throughout my whole study journey, who have encouraged and supported me in different times of my life. Without Your support, I might not have achieved this goal.

Petteri Aalto

Espoo, 31.05.2021

TABLE OF CONTENTS

LIST OF SYMBOLS

Roman

A_{GFA}	gross floor area	k-m^2
a_n	discount factor	
c_p	specific heat	J/kgK
C_{sys}	system energy cost	€/MWh
E	energy	Wh
I	investment	€
t	tons	
P	electrical power	W
p	pressure	kPa
q_m	mass flow rate	kg/s
Q	heat flow rate	W
T	temperature	°C, K

Greek

Δ	delta

Subscripts

a	annual
avg	average
comp	compressor
e	electricity
h	high
in	inlet
l	low
out	outlet
th	thermal

Superscripts

2	square
3	cubic

Abbreviations

AHU	Air handling unit
ASHRAE	American Society of Heating, Refrigerating and Air-Conditioning Engineers
AVI	Regional State Administrative Agency
BAT	Best available technique
CAPEX	Capital expenditure
COP	Coefficient of power
DH	District heating
DWH	Domestic water heating
EC	European Commission
EG	Ethylene-glycol
EED	Energy Efficiency Directive
EER	Energy efficiency rating
EPBD	Energy Performance of Buildings Directive
ESR	Effort sharing regulation
ETS	Emission trading system
EU	European Union
GFA	Gross floor area
GHG	Greenhouse gas
GWP	Greenhouse warming potential
HP	Heat pump
HX	Heat exchanger
IDA ICE	IDA Indoor Climate and Energy
LCC	Life cycle costing
NECP	Nation Energy and Climate Plan
NPV	Net present value
nZEB	Nearly Zero-Energy Building

ODP	Ozone depletion potential
OPEX	Operating expenses
PBT	Payback time
PU	Pump
RED	Renewable energy directive
RES	Renewable energy share
SCOP	Seasonal coefficient of power
SEER	Seasonal energy efficiency ratio
SPF	Seasonal performance factor
SWHP	Seawater water heat pump
TEWI	Total equivalent warming impact
TFEU	Treaty on the Functioning of the European Union
UNEP	United Nations Environment Programme
VAT	Value-added tax
VHC	Volumetric heating capacity
WAM	With Additional Measures

1 INTRODUCTION

As the world's population grows the demand for energy supply is also increased. Through decades has energy been produced mostly via fossil fuels, which has caused a major issue in our climate. Governments worldwide have made action plans to decrease their emissions by shifting their energy sector towards renewable energy sources. (REN21, 2018, p. 15)

Demand for energy-efficient production with low emissions is highly requested when designing new plants and systems. In residential and office buildings are efficient and reliable heating, cooling and ventilation solutions becoming more critical when indoor climate requirements are increasing. (REHVA, 2016) Decarbonization in the energy sector is happening nationally and worldwide, with the common goal of restraining climate change (Ministry of the Environment and Statistics Finland, 2017).

Responding to the continuously straining climate goals stresses implementation and use of new low emission technologies for heating and cooling energy production. The development and execution of smaller-scale seawater heat pumps (SWHP) have not been studied comprehensively in Scandinavia. These systems are not that common in facilities or residential buildings. Building stock located near water basins might offer a great potential to produce cost-effectively and low emission heating and cooling. One issue that has caused rejection to these in the Nordic climate is the low water temperature during the heating season.

The object of this study is to investigate the feasibility in practice of SWHP systems in heating and cooling production, possible risks, energy production potential, profitability calculation, and potential decrease in emissions in energy production. A look into environmental aspects on what regulations and restrictions may affect the placement of these systems.

The goal of this study is to increase knowledge of SWHP systems in Finnish climate conditions. Via simulations and calculations, the goal is to build a simulation model that can be calibrated against a real SWHP system. Possible advantages and feasibility of this system can be demonstrated and compared to other mature heating & cooling production systems. Raising awareness among seawater utilization is and these systems are also an important

matter. With these actions could the share of renewable energy production in Finland be increased and result in positive climate impact.

1.1 European Union and national legislation

1.1.1 European Union (EU)

The European Commission (EC) installed in 2009 the Renewable energy directive (RED) to act in the greenhouse gas (GHG) emission reduction, where the energy sector is responsible for 75 % of the emissions in the EU. The directive (EU Directive 2009/28/EC) sets an overall policy for the production and promotion of energy from renewable sources in the EU. (European Commission, 2020a) The directive included three main key targets for the year 2020: reduction in GHG emissions (from 1990 levels), an increase of renewable share, and improvement in energy efficiency.

Every EU country has an own individual target value, which depends on starting points, renewable energy (REN) potential, and economic performance of the nation (Eurostat Newsrelease, 2020a). These target values were supposed to be achieved by the end of the year 2020 (European Commission, 2020a). Every EU member state is committed to set national energy and climate plan (NECP), where is described how the nation will meet these targets.

In 2018 a revised renewable energy directive (2018/2001/EU) was put into effect. The revised directive (RED II) includes updated key target values for the year 2030, sustainability and GHG criteria for biofuels, and introduction of advanced biofuels share to the target value for transport fuels (European Commission - EU Science Hub, 2019). This directive aims to help the EU to meet its emissions reduction obligations under the Paris Agreement. This directive needs to be transposed into national law by member states by June 2021 (European Commission, 2020a) In Table 1 are shown the key targets values for 2020 and 2030.

Table 1. EU Renewable energy directive key targets for 2020 and 2030.

Sector	2020 (RED I)	2030 (RED II)
GHG emissions reduction (from 1990 levels)	20 %	40 %
Share of REN	20 %	32 %
Energy efficiency improvement	20 %	32,5 %
Share of REN in transport	10 %	14 %

The installed target values are legally binding for the EU, not for the individual member states. Updated regulations for the EU was made by the Treaty of Lisbon, where under Treaty on the Functioning of the European Union (TFEU) Article 194 is stated that EU legislation shall not affect a Member State's right to regulate its choice between different energy sources and the general structure of its energy supply. This constraint had lead to important consequences for the legal appeal of the REN target. RED I projected a legally binding target for the individual Member States, where RED II only offers an overall target value for the whole EU (Monti & Romera, 2020)

Figure 1 shows the situation in 2018 share of renewable energy for every nation and the target values. Share for Finland was set to 38 %, and in 2018 was it over 40 %. The share of renewable energy in the EU was 18 % in 2018 and the target was to reach 20 % in the year 2020 seems to be unachieved.

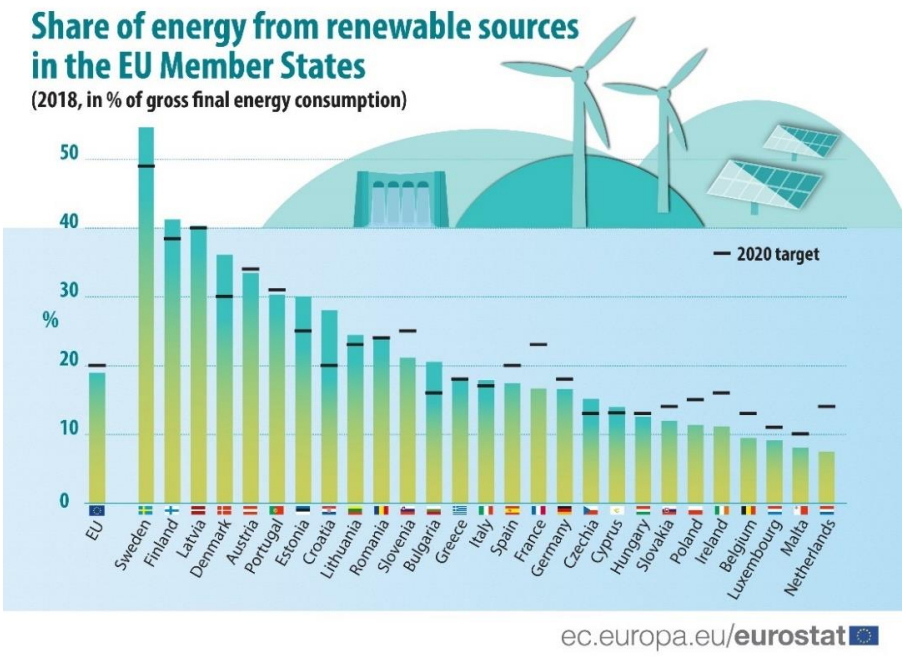

Figure 1. Share of gross final energy consumption for renewable sources in the EU Member states in 2018 (Eurostat Newsrelease, 2020a)

In 2012 energy efficiency directive (Directive 2012/27/EU) was established to give more specific measurements to help the EU reach its 20 % energy efficiency target in 2020. Member states are required to do energy-saving actions at all steps in the energy chain, such as generation, transmission, distribution, and end-use consumption. (European Commission, 2020b) Every member state needs to draw up a national energy efficiency action plan (NEEAP) every third year and report annually of the progress (European Commission, 2020c). To highlight a few measurements in the directive:

- Minimum energy efficiency standards for different products, such as household appliances, boilers, and lightning.
- Mandatory energy efficiency certificates corresponding to the sale and rental of buildings
- Strategies for long-term renovation strategies for building stock in every EU country (European Commission, 2020b).

The amended energy efficiency directive (EED) (EU)2018/2012 was put into effect in 2018, where different measurements are updated from the 2012 directive. Following revisions were introduced:

- New target for energy efficiency improvement of 32,5 % in the EU
- Member states will have to achieve new energy savings of 0,8 % every year of final energy consumption during 2021-2030
- More specific rules for metering and billing of thermal energy, especially in multi-apartment buildings, by giving consumers clearer rights and regular information on how to follow their energy consumption
- National rules for heating, cooling, and how water consumption are required to be more transparent and publicly available (European Commission, 2020b).

The building stock in the EU is roughly 75 % energy inefficient. This means that a big share of the energy goes to waste. To tackle this, are improvements made for existing buildings, and in the new building stock are smart solutions and energy-efficient materials implemented to minimize energy loss. Renovation of existing buildings is currently on average 1 % nationally. The rate should be doubled, in order to meet the climate and energy objectives. This would also reduce the total energy consumption by 5-6 % and CO_2 emissions by 5 %. (European Commission, 2020d)

Acting on this matter, the EU has established The Energy Performance of Buildings Directive (EPBD) 2010/31/EU. The directive has been revised (2018/844/EU) as part of the Clean Energy for all Europeans' package. The directive includes an extensive range of policies and many supportive measures to help national governments to improve the existing building stock. In the following are few measurements listed:

- Member states are required to establish long-term renovation strategies to support the renovation of their building stock into vastly energy-efficient and decarbonized building stock by 2050. The strategies should support the NECP energy efficiency targets.
- All new buildings must be nearly zero-energy buildings (nZEB) from 31 December 2020. All new public buildings already since 31 December of 2018.
- Energy performance certificates must be delivered when a building is sold or rented. Inspection schemes for heating and air conditioning systems must be formed.
- Promoting smart technologies through requirements on the installation of building automation and control systems, and devices that regulate room temperature.
- Building user's health and well-being are considered for example via air quality and ventilation (European Commission, 2020e).

Heat pumps are considered to have a significant role in decarbonizing the building sector. CO_2 emissions from heat pumps can be measured as zero when the supplied electricity is from renewable sources. (Thomaßen, et al., 2021) Figure 2 shows the development of energy source utilization of heat pumps, where useful-heat productions per unit of primary energy input are compared. It can be recognized from the figure that heat pumps have been since 2005 more efficient in energy conversion than new heating appliances, for example boiler heating. The data is provided by the Joint Research Centre Integrated Database of the European Energy System (JRC IDEES).

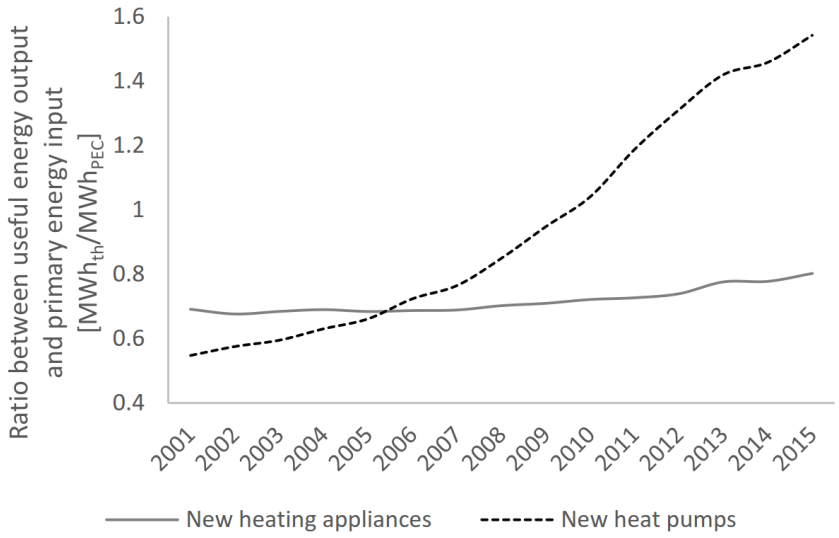

Figure 2. Primary energy consumption performance of heat pumps in comparison to the average new heating appliance in EU countries residential sector (Kavvadias, et al., 2019)

Finland and Sweden have promising development trends in heat pumps, where both nations strive at shares beyond 40 % for 2030. According to Thomaßen, et al. study can 32 %, corresponding to 1,1 $TW_{th,}$ of space heating demand in buildings be covered within EU27 and UK with heat pumps. Carbon emission reduction by 10-15% is possible in several member states. An additional emission cut by 8 % is possible if heat pump demand is met by carbon-neutral electricity. (Thomaßen, et al., 2021)

The residential heat pump market in 21 European countries has grown constantly since 2012. A 12–13% growth in sales can be seen since 2014. Figure 3 presents the sales development from 2009 to 2018. The statistics are made by the European Heat pump Association (EHPA). The market is growing stronger within the building renovation sector, where new product offerings are carried out (EHPA, 2021).

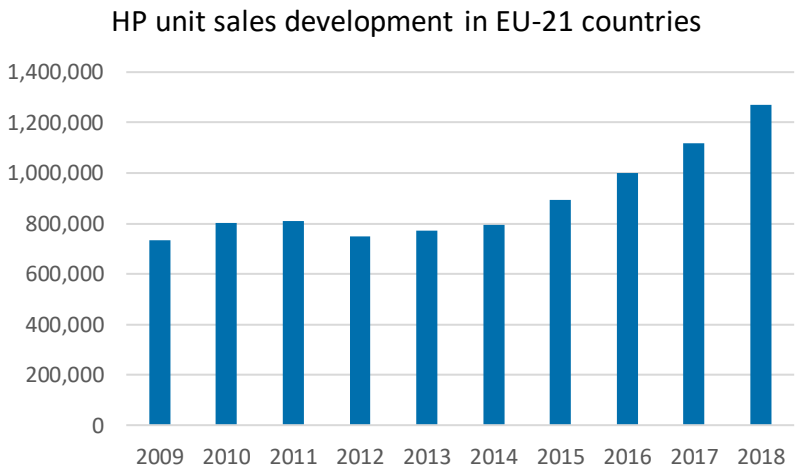

Figure 3. The sales development of heat pumps in Europe. (EHPA, 2020)

Figure 4 presents the share of units by heat source and country and it can be recognized that air-source heat pump dominates across the market. The share of sanitary water or domestic water heating units is also important in several countries. Ground source heat pumps have a noticeable share in the Nordic countries.

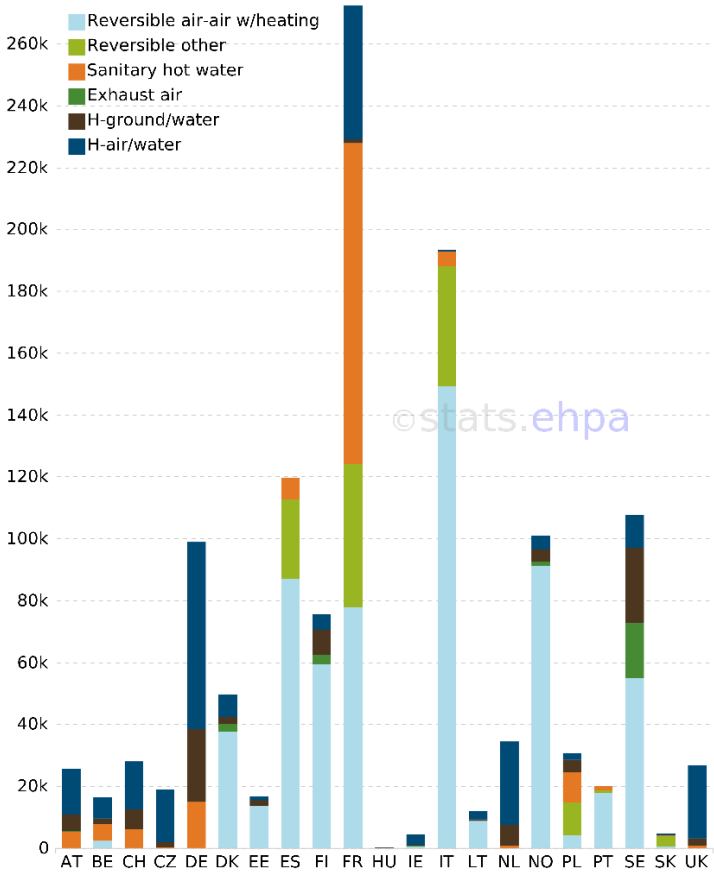

Figure 4. Units sold by market and type in European countries 2018. (EHPA, 2020)

1.1.2 National implementation

In Finland's Integrated Energy and Climate Plan (NECP) published by the Ministry of Economic Affairs and Employment in 2019 is stated two strategic themes on carbon neutrality: Finland will achieve carbon neutrality in 2035 and aims to be the world's first fossil-free welfare society. The target for GHG emission reduction for 2030 is 39 % compared to 2005 levels in line with the EU's Effort Sharing Regulation (ESR). This binding target is supposed to be reached over the period 2021-2030. The renewable energy target is set at 51 % for 2030, because of good development in the field of renewable energy and particularly wind power. (Ministry of Economic Affairs and Employment, 2019) Table 2 shows the estimated path of Renewable Energy Share (RES) target for the period 2020-2030.

Table 2. Finland RES target progression (Ministry of Economic Affairs and Employment, 2019, p. 48)

	2020	**2022**	**2025**	**2027**	**2030**
Finland's EU obligation	20 %				
Finland's RES target for 2030 and the minimum level for the intermediate years		41 %	44 %	47 %	51 %

Finland's energy efficiency target for 2020, in line with EED, was set to 310 TWh for final energy consumption and 417 TWh for primary energy consumption. In 2017 had Finland achieved a consumption of 294 TWh for final energy production, corresponding to 371 TWh for primary energy production. In other words, the estimated consumptions were higher than the real consumption. This means that energy-efficient solutions have been applied. Following up on the energy efficiency targets is to some extent challenging. The varying conditions weather conditions, especially during the winter season, can the heating degree days vary depending on mild or cold winter periods. Therefore, the heating demand can vary remarkably, more than 5 % in final energy consumption. (Ministry of Economic Affairs and Employment, 2019)

The heating source distribution within space heating is divided into four major categories, district heating, electricity, heat pumps, and wood. The market share of space heating is still dominated by district heating, as Figure 6 illustrates. In the year 2020 heat pump production was around 12 TWh, which corresponds to over 15 % of the space heating share (The Finnish Heat Pump Association (SULPU), 2021b).

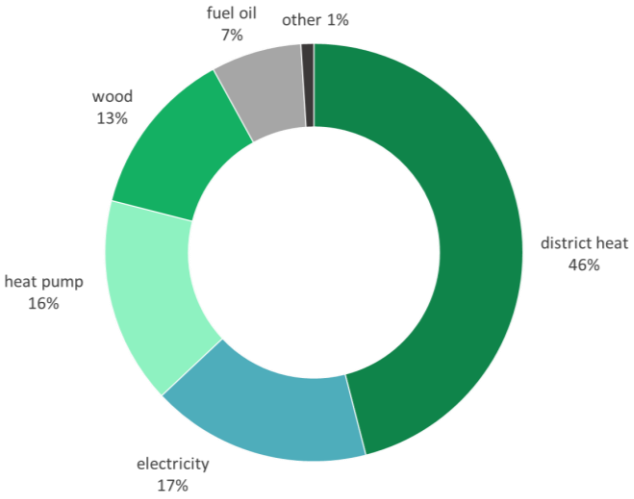

Figure 5. Market share of space heating 2018. Including residential, commercial, and public buildings. (Finnish Energy, 2021)

Figure 6 illustrates a starting trend in the new building stock, where the share of heat pump systems has started to increase since 2016. District heating does still have a strong market share in new buildings. However, a small decrease in district heating can be also recognized from the graph.

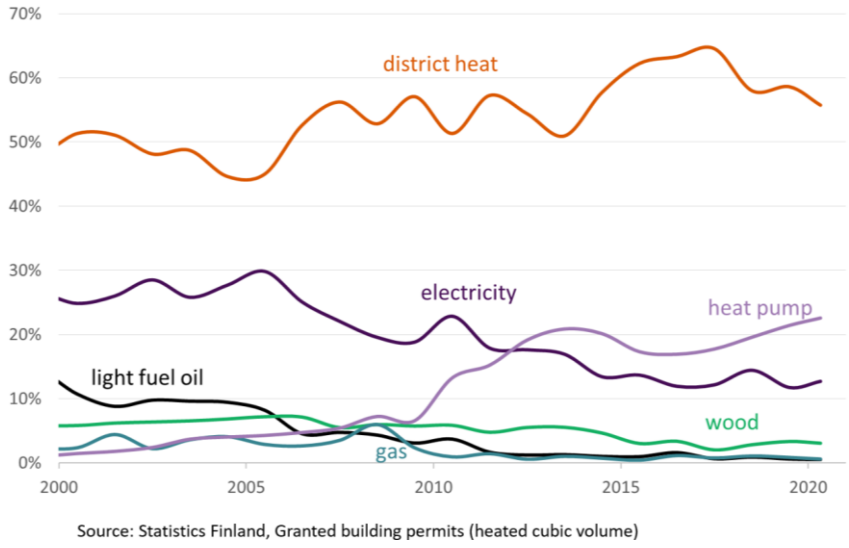

Figure 6. Market share development of heating source in new buildings. (Finnish Energy, 2021)

Investments in heat pump units have increased constantly during the past decade. Figure 7 presents the cumulative investments of heat pump units by private consumers from 1996 to 2020. In recent years investments have grown considerably in all heat pump unit types.

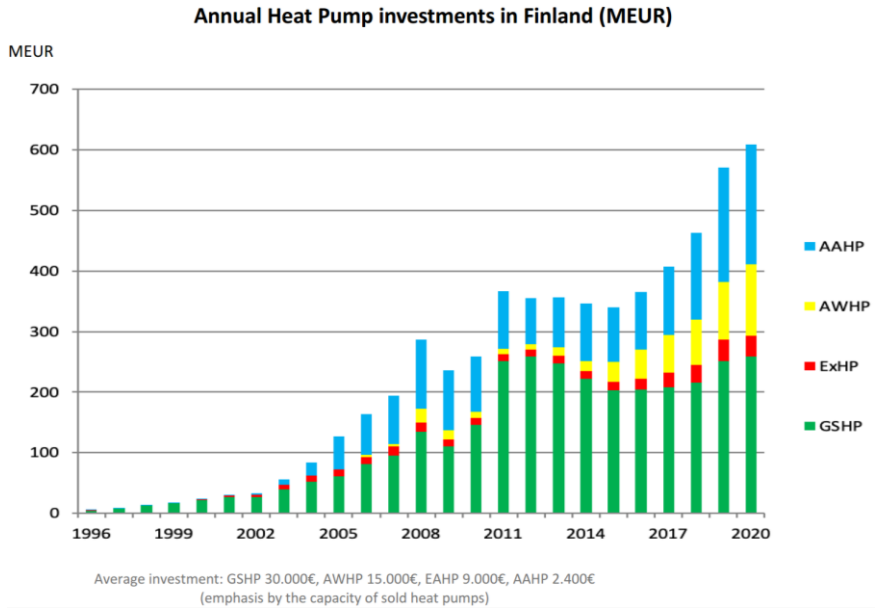

Figure 7. Cumulative heat pump investments by private consumers. AAHP: Air-to-air heat pump, AWHP: Air-to-water heat pump, ExHP: Exhaust-air heat pump, GSHP: Ground source heat pump. (The Finnish Heat Pump Association (SULPU), 2021a)

2 HEAT PUMP TECHNOLOGY

2.1 Working principle

Heat pump is a device that transfers heat from a low-temperature source to a high-temperature source, through an external energy source. (Cengel & Boles, 2011, pp. 282-283) A working fluid is used to transfer heat from heat source to heat sink. The working principle of the heat pump is the following: Compressor pressurizes low-temperature fluid (vapor state) from the evaporator, which is located at the low-temperature side, to a high temperature and pressure that flows through a condenser, the high-temperature side. In the condenser is the heat extracted to the application and phase change from gas to liquid. The high-pressure fluid goes then through an expansion valve, which lowers the pressure and temperature. The working fluid enters the evaporator and the process starts again. Figure 8 shows the working principle and *p-h* (pressure-enthalpy) diagram of a vapor compression heat pump.

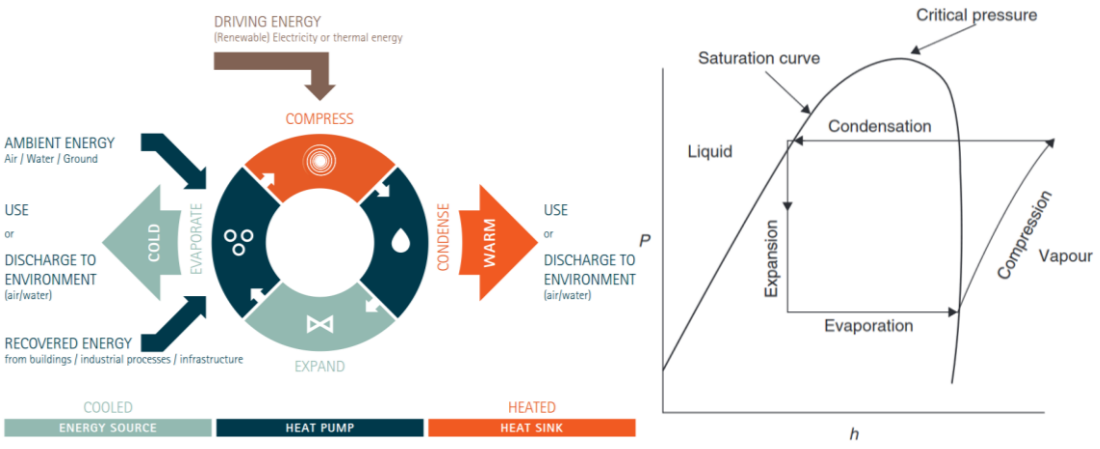

Figure 8. Working principle for a vapor compression cycle heat pump and p-h diagram (Nowak, 2018) (Hundy, et al., 2008, p. 16)

2.2 Performance measurement

When comparing heat pump performance Coefficient of Performance (COP) and Energy efficiency ratio (EER) values are used. COP value measures the energy efficiency in heating performance and EER for cooling performance. The definitions are the following for heat pumps (Cengel & Boles, 2011, pp. 283-284):

Cooling:

$$EER = \frac{Q_L}{P_{net,in}} = \frac{Q_L}{Q_H - Q_L} = \frac{1}{\frac{Q_H}{Q_L} - 1} \quad (1)$$

where,

Q_L heat amount in the low-temperature medium

Q_H heat amount in the high-temperature medium

P_{net} input power for the compressor

Heating:

$$COP = \frac{Q_H}{P_{net,in}} = \frac{Q_H}{Q_H - Q_L} = \frac{1}{1 - \frac{Q_L}{Q_H}} \quad (2)$$

In Figure 9 an example of the impact on COP value is presented, when ΔT between evaporator and condenser is increased. COP value decreases as ΔT difference increases. The reference values emulate real heat pump unit COP values. For illustration was Q_H 200 kW and Q_L from 195 to 30 kW. The smaller difference between the source and the sink is, the less work must be done by the compressor, which again increases the performance of the heat pump (Nowak, 2018).

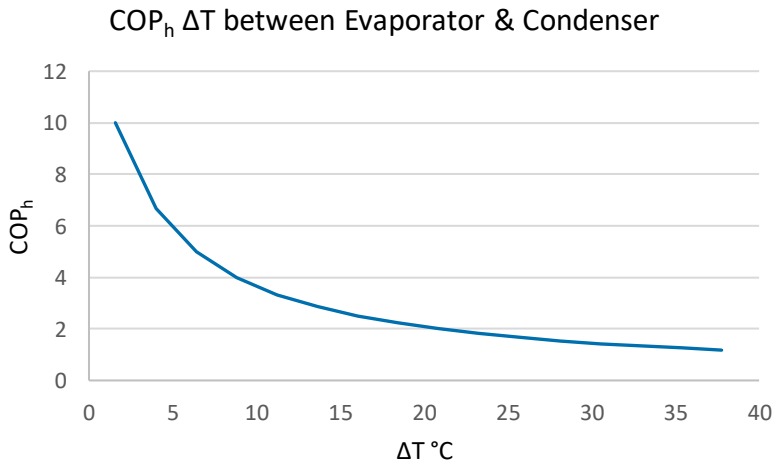

Figure 9. Function of ΔT related to COP.

Several factors affect COP value. Firstly, the temperature difference between the heat source and the sink determines the efficiency. The smaller the difference, the higher the COP. The applied working fluid also influences the efficiency of the system. Different working fluids have different evaporation and condensation temperatures. ASHRAE (American Society of Heating, Refrigerating and Air-Conditioning Engineers) reviewed available literature of installed heat pumps in Scandinavian climates, seasonal COP varied between 2 to 4 for SWHP systems. Hence, the overall system efficiency depends on the design, management, and performance of the heat pump. (Xin, et al., 2018)

Other comparison factors are the Seasonal Coefficient of Performance (SCOP) and Seasonal Performance Factor (SPF) for heat pump applications. SCOP describes the average COP during a heating period. Correspondingly Seasonal Energy Efficiency Ratio (SEER) is used for a specific cooling period. The definition varies, depending on what other parts are included in the system. SPF describes the COP during a specific period. It is defined as the ratio of the heat delivered and the total consumed energy during the season. It is usually used for the evaluation or estimation of real performance. SPF can also be used to compare conventional heating systems, for example, boilers, concerning primary energy saving and reduced CO_2 emissions. (IEA-Heat pump technologies, 2020) (Kärkkäinen, 2012) In SFS-standard 14825:2018 the following formulas are defined for SCOP and SEER

$$SCOP_{HP} = \frac{Q_H}{Q_{HE}}, \qquad SEER_{HP} = \frac{Q_C}{Q_{CE}} \tag{3}$$

Where,

Q_H	annual heating demand [kWh]
Q_{HE}	annual energy consumption for heating [kWh]
Q_C	annual cooling demand [kWh]
Q_{CE}	annual energy consumption for cooling [kWh]

SPF can in simple terms be determined as following (Nordman, 2012):

$$SPF = \frac{Useful\ energy}{Energy\ input} = \frac{Heating\&Cooling\ production}{Total\ enegy\ input} \tag{4}$$

Boundaries are needed when calculating SPF. Defined boundaries have a direct impact on the measurement equipment needed to measure the required parameters for the calculation of the different SPF. Project SEPEMO (Seasonal Performance factor and Monitoring), supported by Intelligent Energy Europe (IEE), formed a general system boundary setup for measurement and calculation for SPF, as shown in Figure 10. (Nordman, 2012)

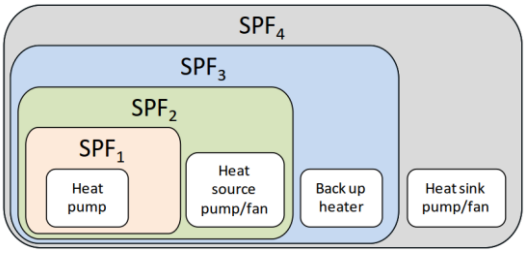

Figure 10. SPF boundaries. (Nordman, 2012)

The four boundaries were as following in the SEPEMO project (Nordman, 2012):

- SPF_1 = Heat pump unit itself
- SPF_2 = Heat pump and the needed applications to make the heat source available for the heat pump
- SPF_3 = SPF_1 + SPF_2 and the back-up heater
- SPF_4 = SPF_1 + SPF_2 + SPF_3 and the distribution of the heat

Expressed in equations:

$$SPF_1 = \frac{Q_{HP}}{W_{HP}}$$

$$SPF_2 = \frac{Q_{HP}}{W_{HP} + W_{heat_{source_{pump}}}}$$

$$SPF_3 = \frac{Q_{HP} + Q_{backup_{heater}}}{W_{HP} + W_{heat_{source_{pump}}} + W_{backup_{heater}}}$$

$$SPF_4 = \frac{Q_{HP} + Q_{backup_{heater}}}{W_{HP} + W_{heat_{source_{pump}}} + W_{backup_{heater}} + W_{heat_{sink_{pump}}}}$$

There are numerous existing standards and regulations for calculating SPF, out of which are based on testing standard EN 14511. This standard does not take the whole system integration into account. The system boundaries are limited to the heating or cooling unit itself. Hence, these standards do not include the whole energy consumption of the auxiliary drives on the heat sink and heat source side. (Nordman, 2012) Volumetric heating capacity

(VHC) is an important measure among COP when designing a heat pump. VHC value describes the produced condenser heat capacity per processed volume of refrigerant suction vapor (Arpagaus, et al., 2018). It can be defined as following (Frate, et al., 2019):

$$VHC = \frac{Q_{cond}}{V_{comp,in}} \tag{5}$$

Where,

Q_{cond} heat rejected from the condenser and

$V_{\text{comp, in}}$ volumetric flow rate at the compressor suction.

Working fluid with a higher VHC value requires a smaller compressor, which also affects positively the investment cost. Usual VHC values in HP applications are between 3000 and 6000 kJ/m^3. The lower practical depends on the compressor type and the limit is around 1000 kJ/m^3. Higher VHC values suit better for positive displacement compressors, such as reciprocating and screw type, as it requires a reduced swept volume at a given capacity and smaller size and investment costs. (Arpagaus, et al., 2018) The VHC is in general used to compare working fluids in combination with COP. These two measures are usually different, as fluids with high COP have low VHC and contrariwise. (Frate, et al., 2019) An efficient heat pump should have both the VHC and COP as high as possible. A high COP reduces the running cost while a high VHC reduces the investment cost. (Abdesselam, et al., 2008)

Low VHC values do not put any technical restrictions. It is appropriate to use multiple compressors to achieve larger VHC values, which is a common practice in commercial refrigeration systems. The VHC can be increased at the cost of efficiency, selecting fluids not only based on COP but considering also the VHC for each operational setup. Since VHC is mainly an economic indicator, the decision between VHC and COP should be based on economic reflections. (Frate, et al., 2019)

2.3 Working fluids

Working fluid is a key component for the heat pump to operate. It enables heat transfer in the system. The medium circulates in the system to absorb, transport, and release heat. Working fluids differ with pressure: as the pressure is increased, the boiling point is also

increased. Under atmospheric pressure, working fluids have very low boiling points, -40 °C or lower. Hence, it is possible to utilize heating energy from low-temperature sources. (IEA-Heat pump technologies, 2020)

2.3.1 **Environmental measurements**

Working fluids can be toxic, flammable, explosive, or act as greenhouse gases if they are released or leaked from the heat pump. The environmental impact is measured with indicators such as Ozone Depletion Potential (ODP), Global Warming Potential (GWP), and Total Equivalent Warming Impact (TEWI). ODP indicates the expected ozone layer reduction of the reference refrigerant R-11(trichlorofluoromethane). ODP=1 refers to one substance of R-11 refrigerant.

GWP term describes the amount of heat a greenhouse gas can absorb in comparison to the same amount of CO_2. GWP value 1, is one CO_2 molecule over a time of 100 years. (IEA-Heat pump technologies, 2020)

The TEWI indicator expresses the overall environmental impact of a refrigeration system throughout the whole operational lifetime. TEWI accounts for the global warming impact as a sum of both direct and indirect emissions in kilograms of CO_2 (Makhntach & Khodabandeh, 2014).

$$TEWI = direct\ emissions + indirect\ emissions = (GWP \times L \times N) + (E_a \times \beta \times n) \quad (6)$$

Where,

GWP	Global Warming potential [kg CO_2/kg refrigerant]
L	annual leakage rate [%]
N	lifetime of the system [year]
E_a	energy consumption [kWh/year]
β	carbon dioxide emission factor [kg CO_2/kWh]
n	equipment lifetime [year]

When looking from an environmental aspect, it is worth assessing both the direct and indirect effects of the substances, as TEWI calculation enables. By using the right methods, wrong

conclusions can be avoided. A working fluid with low GWP could in fact have a higher indirect impact due to lower performance in the system. (Longhini, 2015) This index does have a downside, when trying to include many different and unclear matters, such as the magnitude of leakage and the distribution of the energy production consumed by the installation between the different forms of production. In Finland, only a part of the electricity is produced by fuels that accelerate the greenhouse effect. In a situation where a major part of the consumed energy of a refrigeration facility is produced by fossil fuels, the share of energy is multiple times bigger than the refrigerants. (Aittomäki, et al., 2012)

2.3.2 **Design properties & project environment**

Three parameters for choosing proper working fluid are essential: temperatures for the two media, heated or cooled space, and the source temperature. Also, the temperature and pressure of the working fluid on the condenser side are important factors. (Cengel & Boles, 2011, p. 621) Pricing and availability are other criterias when selecting a suitable working fluid for the system (Arpagaus, et al., 2018) Among these are also the following properties that should be considered (Aittomäki, et al., 2012):

- Thermodynamic properties
- Chemical properties
- Physiological requirements
- Environmental impact
- Reacting with oil
- Reacting with water

In the project environment, the design for working fluid selection criteria is limited to heating and cooling demands and the operative temperature range for both evaporator and condenser sides. With these values, the refrigeration designer can look for suitable options both for the heat pump and working fluid by using dimensioning software provided by different manufacturers. The chosen options can be then evaluated by the manufacturer and they can give more detailed data and alternatives for the desired parameters. In many cases, higher GWP valued working fluids are offered and finally chosen by the customer, because of availability and favorable pricing. Some refrigerants require extensive safety procedures in the case of leakage, because of the flammability class. For example, class A2L working fluids according to SFS EN-378 require a separate extract air flow system. Contractors often offer R-410A and R-134A for residential heat pump applications. Another goal when

designing refrigeration applications is lifespan. Foreseeing the applicability and possible restrictions for the designed working fluid can be challenging due to the rapid changes in refrigerant restrictions and phase-outs. (Reikko, 2020)

In projects where the goal is to achieve a sustainability rating for the building factors considering environment and energy consumption are in focus. BREEAM (Building Research Establishment Environmental Assessment Method) and LEED (Leadership in Energy and Environmental Design) certificates are common classifications for buildings and in these are working fluid selection more significant. BREEAM is based on European standards and is, therefore, the sustainability assessment standard, where LEED is globally the most used green building rating system. (Green Building Council Finland, 2020)

2.3.3 **Working fluid types**

Working fluids can be divided into two groups: single-component (pure) fluid and multicomponent mixtures, more commonly blends. Fluorocarbons are one of the most widely used synthetic compounds currently in use as working fluids. Methane and ethane are molecules that form the foundation for many of the pure working fluids. In their normal state, these two molecules contain only carbon *(C)* and hydrogen *(H)* atoms and are themselves denoted as pure hydrocarbons. If one of the hydrogens in a hydrocarbon is substituted with a halogen, for example, chlorine or fluorine, a new chlorinated or fluorinated molecule is formed. (ASHRAE, 2018, p. 76)

Chlorofluorocarbons (CFCs) are fully halogenated hydrocarbons, as all their hydrogen atoms are replaced. Examples of these are R-11, R-12 and R-114. The main properties (chemical, thermodynamic and physiological) for CFCs are generally good. As these working fluids are stable and contain chlorine, have they been banned for their large ODP potential by the United Nations Environment Programme UNEP 1987 Montreal Protocol. The protocol required that developed countries end the production of CFCs in 1996. (ASHRAE, 2018, p. 76)

Hydrochlorofluorocarbons (HCFCs) are partially halogenated hydrocarbons, as not all their hydrogen atoms are replaced. Examples of these are R-21, R-21 and R-124. These are less chemically stable compared to CFCs, but they perform in general well in vapor compression refrigeration systems. The ODP impact is much less compared to CFCs, but they still contain

some ODP. These are also put into phaseout (R-22 by the year 2020 and R-123 by 2030) as part of the Montreal Protocol. (ASHRAE, 2018, p. 76–77)

Hydrofluorocarbons (HFCs) are methane or ethane-based working fluids that do not hold any chlorine but are halogenated by the fluorine atom alone. These are also chemically very stable but their thermodynamic and transport properties vary from decent to excellent. Hence, they fit well for the vapor-compression cycle. Also, synthetic oils are required for lubrication in refrigeration systems with these working fluids. As these do not include any chlorine atoms, they do not have any ODP, but respectively they have strong GWP values. The most common working fluid in this category is R-134a as a substitute for R-12 (CFC). This category has not been scheduled for a phase-out according to the Kigali amendments to the Montreal Protocol. (ASHRAE, 2018, p. 77) A reduction for HFC quotas is in progress and should be reduced to a certain amount by 2030. R-134a is widely used among air-conditioning applications and district cooling solutions. (Laitinen, et al., 2016) Figure 11 presents the phase-down for HFC working fluids.

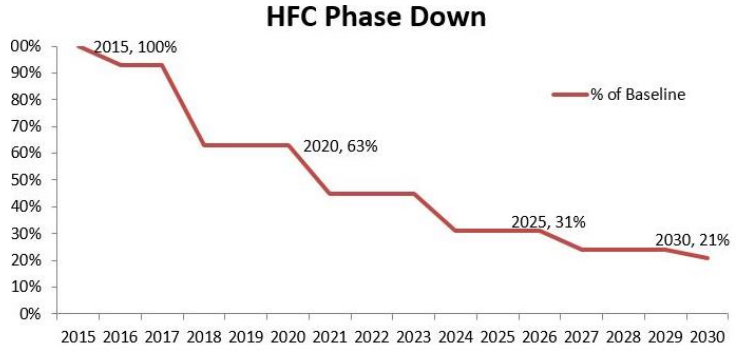

Figure 11. Reduction curve of HFC working fluids. (Sidat, 2018)

Hydrofluoroolefins (HFOs) are the newest class of halogenated working fluids containing a carbon-carbon double bond (olefin) molecular structure. The development is driven by the desire to have working fluids with no ODP but with a low GWP value. Examples of these working fluids are R-1234yf and R-1234ze. These two fluids are developed as a replacement for R-134a HFC working fluid (Laitinen, et al., 2016). This class is still relatively new and continues evolving. (ASHRAE, 2018, p. 77)

Working fluids, that do not contain halogen molecules at all, are called natural refrigerants. Refrigerants occur in nature and are not harmful to the ozone layer and their GHG impact is zero or near zero. There are two categories of natural refrigerants: HC (Hydro carbon)

refrigerants and Inorganic Compounds. To HC-refrigerants include for example propane (R-290) and butane. Examples of inorganic compounds are ammonia (R-717) and carbon dioxide (R-744). (Kapanen, 2017)

Working fluid blends or mixtures are composed of two or more pure working fluids. The development of blend working fluids is due to the demand for more environmentally friendly fluids. This enables to tailor different pure refrigerant properties to meet the desired design values, such as saturation temperature and flammability. Mixtures can be subcategorized into azeotropic mixtures, near-azeotropic mixtures, and zeotropic mixtures. (ASHRAE, 2018, p. 78–79)

Azeotropic mixtures consist of two or more pure working fluid components, when mixed in accurate proportions, these mixtures behave like pure working fluids when changing state. In other words, azeotropes evaporate and condensate at close constant temperature and the mixture structure in vapor and liquid phases remains the same. One example is R-507A, which is a 50%-50% mixture of R-125 and R-143a. (ASHRAE, 2018, p. 79)

Near-azeotropic mixtures peculiarity is temperature glide, where mixtures undergo a minor change in temperature as the working fluid changes phase. This happens because the change of state takes place at different temperature and pressure relations for each working fluid component that is included in the mixture. (ASHRAE, 2018, p. 79)

Zeotropic mixtures unveil a significant temperature variation or glide during phase change at constant pressure. Especially, as the mixture vaporizes in the evaporator the saturation temperature is increased. As the mixture condenses in the condenser the saturation is temperature decreased. (ASHRAE, 2018, p. 79–80) This glide is shown in Figure 12, where a refrigeration cycle of R-407C fluid is plotted.

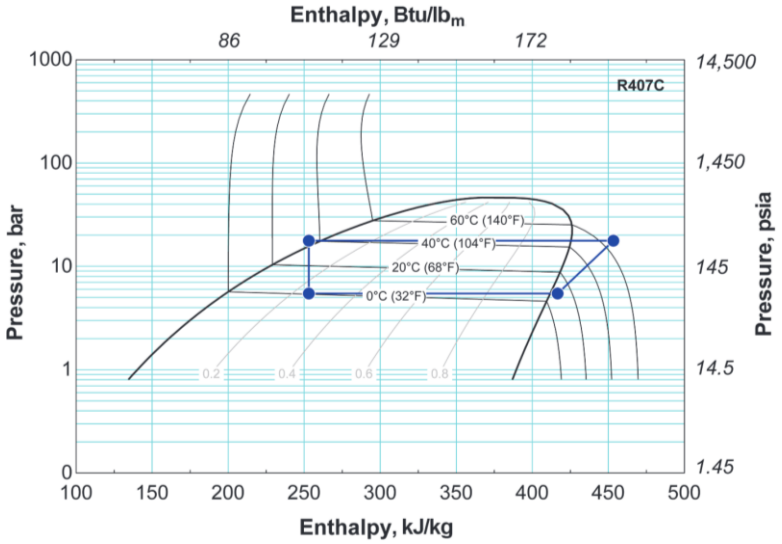

Figure 12. Zeotropic mixture P-h curve of working fluid R-407C. (ASHRAE, 2018)

Previously presented working fluids, ODP, and GHG impacts are summarized in Table 3.

Table 3. ODP and GHG impact of single-component working fluids.

Working fluid	Low or zero ozone impact	High ozone impact	Low or zero GHG content	High GHG content
CFC		X		X
HCFC	X			X
HFC	X			X
HFO	X		X	
Natural refrigerants	X		X	

2.4 Compressors

Compressors are used to increase the pressure of a fluid. They need an external source, typically electricity, to perform the work. In Figure 13 different compressor classifications could be reviewed.

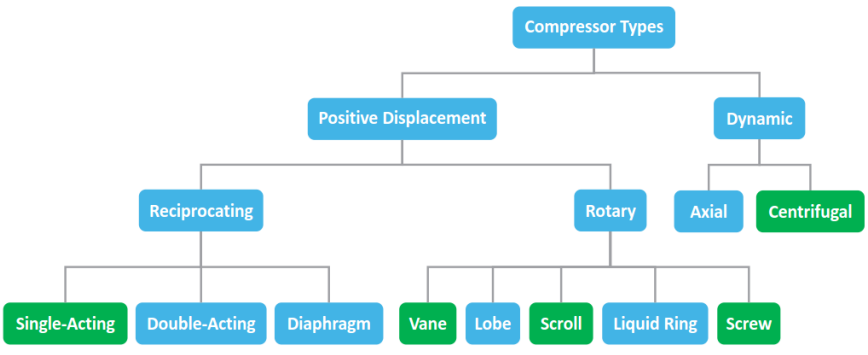

Figure 13. Classification of cooling compressor types (Lin & Avelar, 2017)

Different compressor types can be divided based on their power output to different applications, as Figure 14 shows.

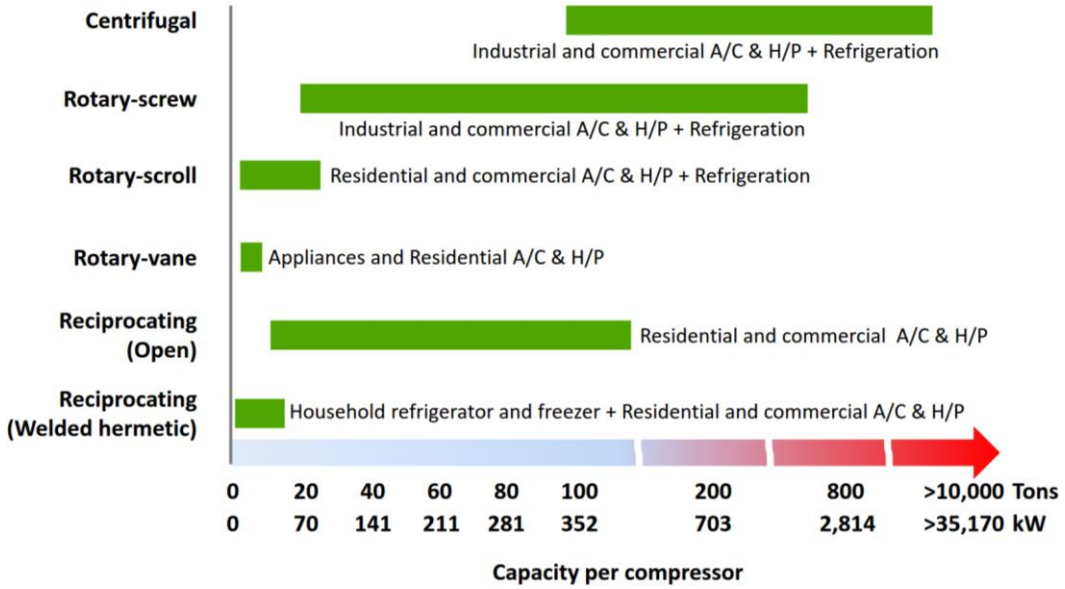

Figure 14. Compressor power chart in different applications. (Lin & Avelar, 2017)

Compressors can also be categorized by their construction type:

- Open type
- Hermetically sealed
- Semi-hermetic

In an open type compressor, the power is transferred via an axis, that goes through the compressor housing. When using ammonia as a working fluid the open type is used, mainly because motor coil cannot be manufactured to resist ammonia. Sealing of the axis is the hardest part of this type of compressor. (Aittomäki, et al., 2012)

Hermetically sealed or fully sealed compressors are entirely sealed. The machinery is in a welded, gas-proof housing, where the gas is suctioned. Advantages over an open construction are a good shield for outcoming effects, silent operation, and in general effective cooling. One disadvantage is the difficulty to repair faults. These are constructed for smaller power scales, such as refrigerators and freezers. Semi-hermetic type is used in larger power scale compressors, because of better access for maintenance. Additionally, this compressor type can be disassembled. (Aittomäki, et al., 2012)

The pressure ratio should be as low as possible for minimizing compressor power (Arpagaus, et al., 2018). Pressure ratio (PR) is defined as follows:

$$PR = \frac{p_1}{p_2} \tag{7}$$

Where,

p_1 condensing pressure

p_2 evaporating pressure

2.4.1 **Reciprocating**

A reciprocating type of compressor uses a piston to compress a substance to higher pressure. Figure 15 shows a basic working cycle of this compressor type. As the piston moves towards the outlet, volume is reduced, and pressure is increased. As the piston moves back down, the movement is reversed: volume is increased, and pressure is reduced. (Lin & Avelar, 2017)

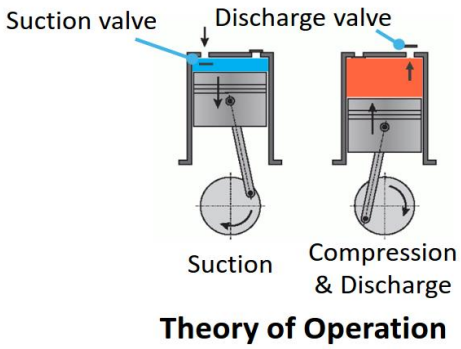

Figure 15. Reciprocating compressor working principle (Lin & Avelar, 2017)

The benefits of reciprocating compressors are the simple working principle and construction: a circular cylinder, and a piston, which can be manufactured relatively easily and with good precision. One disadvantage is the amount of moving parts creating vibrations, which are hard to be avoided. (SWEP, 2019) This type of compressor has broad applications. It can compress a wide range of substances, such as refrigerants, hydrogen, natural gas, and so on. As a result, it can be applied in various industries such as building, refrigeration, mining, and others. (Lin & Avelar, 2017)

2.4.2 **Screw**

A rotary-screw compressor utilizes rotors to compress substances to higher pressure and temperature. The work is done by male and female rotors that reduce the substance volume as they rotate. As the substance flows through the threads as the screws rotate, the pressure and temperature are increased and leaves the discharge port. Figure 16 shows the working principle of a screw compressor. (Lin & Avelar, 2017)

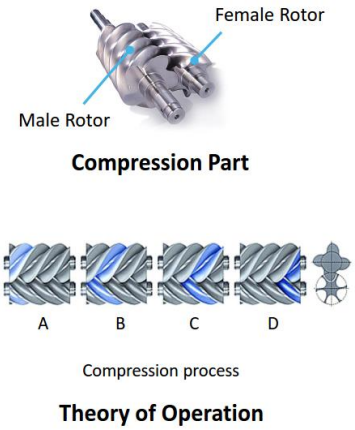

Figure 16. Working principle of a twin-screw compressor (Lin & Avelar, 2017)

This type is impractical for smaller capacities, because of the rotor processing technology. Capacity power typically from 30 to 100 kW and upwards. Advantages over recuperating compressors are construction without valves, simplicity and long maintenance intervals, also power adjustment, and stepless control. The main issue with the oil spray screw compressor is the oil that exits with the working fluid. An oil deflector is needed, and the sizing is dependent on the working fluid type. (Aittomäki, et al., 2012)

2.4.3 **Rotary-vane**

The functionality of a rotary-vane compressor is similar to piston movement, as Figure 17 illustrate. The casting is known as a cylinder. The vane, that rotates inside the cylinder, splits the space and the rolling piston into suction and discharge sections. As the piston rotates, the two volumes are increased and decreased to achieve suction, compression, and discharge to the substance in matter. (Lin & Avelar, 2017)

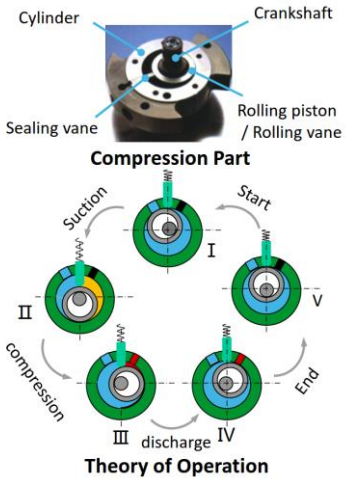

Figure 17. Working principle of a rotary-vane compressor (Lin & Avelar, 2017)

Common applications for a rotary-vane are household applications, such as refrigerators and freezers. Also, heat pumps for residential use with a limit of 18 kW capacity. Compared to other types, the rotary-vane has lower reliability due to the number of components. It has lower energy efficiency compared to the scroll compressor due to losses from clearance volume and discharge valve. The construction of a rotary-vane compressor is simple but requires high precision in manufacturing. In general, this compressor type has a higher efficiency rate than the reciprocating type. (Lin & Avelar, 2017) Recognized issues are within wear in packing and lubrication (Aittomäki, et al., 2012).

2.4.4 **Scroll**

A rotary scroll compressor is used in smaller applications between 18 to 35 kW. The working principle is the following: The substance is drawn in from outside of the fixed scroll, then compressed in between the fixed and orbital scroll, and finally discharged from the center of the fixed scroll, as Figure 18 describes.

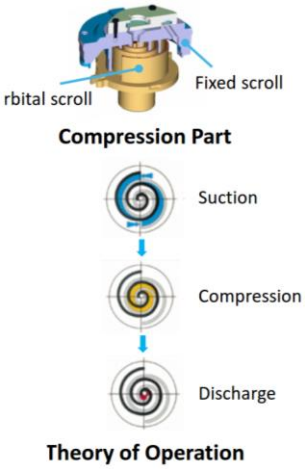

Figure 18. Working principle of a scroll compressor (Lin & Avelar, 2017)

Compared to reciprocating and rotary-vane compressors, rotary-scroll has higher reliability due to simpler structure and fewer components. This type has lower efficiency and smaller capacity compared to centrifugal and rotary-screw compressors. (Lin & Avelar, 2017)

2.4.5 **Centrifugal**

A centrifugal compressor is also called turbo or radial compressor. This type compresses a substance to high pressure and temperature by adding kinetic energy to the substance via rotating impellers. The substance is forced through an impeller, which makes the substance increase its speed. The vastly moving substance is then forced via a diffuser, where the substance volume expands and velocity decreases. This process converts the kinetic energy of the high-speed low-pressure substance to a low-speed higher pressure substance. The working principle of this type is shown in Figure 19. (Lin & Avelar, 2017)

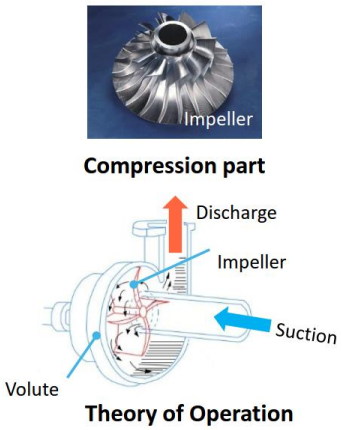

Figure 19. Centrifugal compressor working principle (Lin & Avelar, 2017)

Turbo compressor suits best for larger cooling applications above 700 kW, and it is the most common type for commercial & industrial air conditioning, and refrigeration systems (Lin & Avelar, 2017). Typical applications are for example air-conditioning cooling, which requires large power and a small pressure ratio (small temperature difference). To achieve high-pressure ratios, many stages are needed, which again increases the cost. (Aittomäki, et al., 2012)

2.5 Heat exchangers

A heat exchanger transfers thermal energy from one medium to another, in general from one liquid to another, a liquid to gas, or a liquid to a solid surface, and vice versa. They can be used for both heating and cooling purposes. There are commonly no external heat and work interactions that enable heat exchange of a fluid. (Shah & P. Sekulić, 2003, p. 1–3)

The simplest heat exchanger setup is a double-pipe arrangement, that contains two concentric pipes of different diameters, as Figure 20 shows. One fluid flow in the smaller pipe, while the other flows in the surrounding space. Two types of flow arrangement are possible in this setup, parallel and counter flow. In parallel, both cold and hot streams enter from the same end, and in counter flow again, cold and hot steams enter from the opposite ends. (Cengel & Ghajar, 2015, p. 648) The temperature profiles are shown in Figure 21.

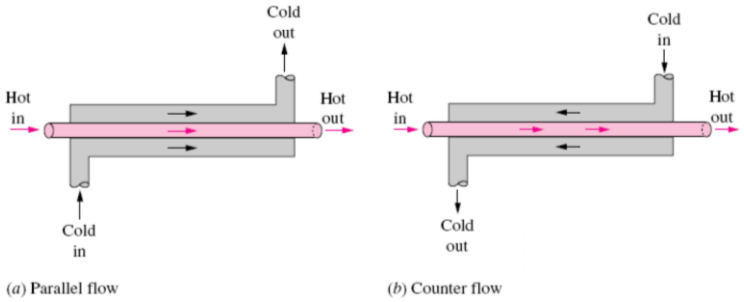

Figure 20. Flow regimes in double-pipe setup for Parallel and Counter flow. (Cengel & Ghajar, 2015, p. 648)

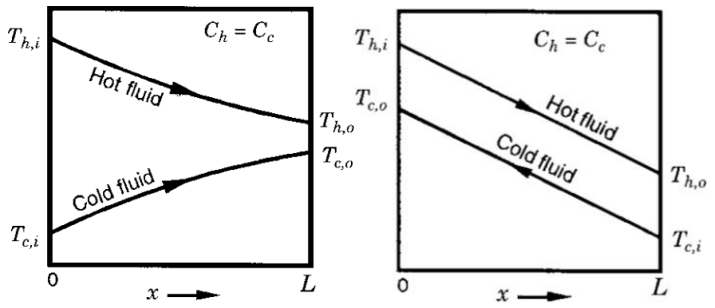

Figure 21. Temperature profiles. Left: Parallel flow. Right: Counter-flow (Shah & P. Sekulić, 2003, pp. 58-59)

Classification of heat exchangers can be done differently. Usually, they are classified by transfer process or construction type. In Figure 22 the two main transfer types are shown, indirect and direct contact types. Another way of classification is by area density β, which is the ratio of the heat transfer surface area of a heat exchanger to its volume.

A heat exchanger with $\beta > 700$ m^2/m^3 is classified as being a compact one. Examples of these are car radiators (β ~1000 m^2/m^3), glass-ceramic gas turbine heat exchangers (β ~6000 m^2/m^3) or human lungs (β ~20,000 m^2/m^3). (Cengel & Ghajar, 2015, p. 648)

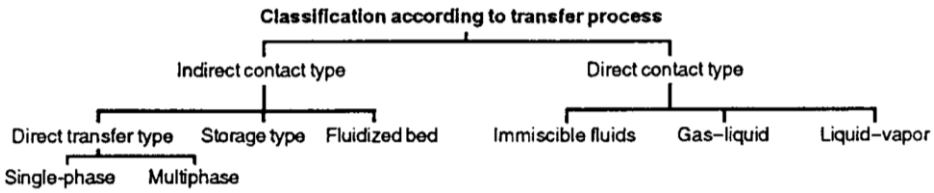

Figure 22. Classification by transfer process. (Shah & P. Sekulić, 2003)

In compact heat exchangers, the two fluids usually move vertically to each other, and this configuration is called cross-flow. This can further be classified as mixed and unmixed, depending on the setup, as Figure 23 illustrates. In setup (*a*) is the flow forced to go between the fins. In setup (*b*) is mixed, where the fluid can flow freely between the piping. (Cengel & Ghajar, 2015, p. 650)

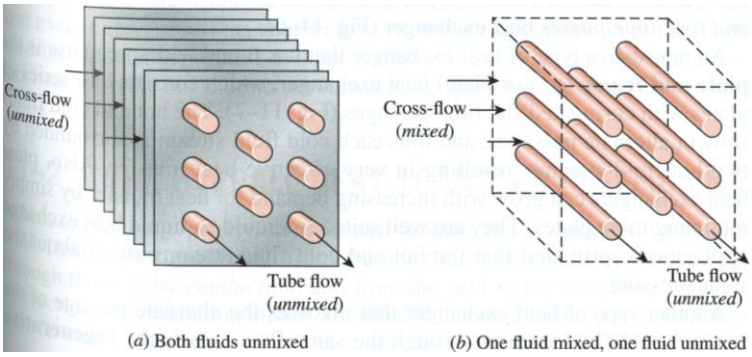

Figure 23. Flow configurations for cross-flow. (Cengel & Ghajar, 2015, p. 649)

In the following section evaporators and condensers are briefly introduced. The design of these components is not a vital part of the simulation model for the studied case, therefore can the specifics be left aside. Heat pumps for residual and commercial use are usually all-in-one units, where the condenser and evaporator sizing are performed by the manufacturer.

2.5.1 **Evaporators & condensers**

Generally, the function of an evaporator is to cool air or liquid. The purpose of an evaporator is to exchange the low pressure and temperature working fluid in thermal contact with the load side, for example, seawater. In terms evaporators are the same as heat exchangers (HX), except the second liquid is a working fluid that exchanges thermal energy with the other fluid. Evaporators are categorized in either air or liquid-cooled types.

Liquid evaporators are classified as either dry (direct) or flooded. The dry evaporator is recognized by the expansion valve that lowers the working fluid condensate. Fluid enters the evaporator as a gas-fluid mixture. As the fluid passes through it is vaporized, but it needs to be superheated a few degrees before entering the compressor to avoid liquid state.

The flooded evaporator type has a receiver circuit between the expansion valve and evaporator inlet where the vapor is separated from the liquid. This is needed to ensure that the working fluid is entirely in liquid form before entering the evaporator. The fluid typically needs to be circulated a couple of times through the evaporator and receiver before it matches inlet liquid quality requirements. (SWEP, 2019). The flooded evaporator is not completely filled with working fluid by design. This enables the working fluid to evaporate on the fluid surface (Hundy, et al., 2016, p. 123). In Figure 24 a flooded evaporation unit is shown.

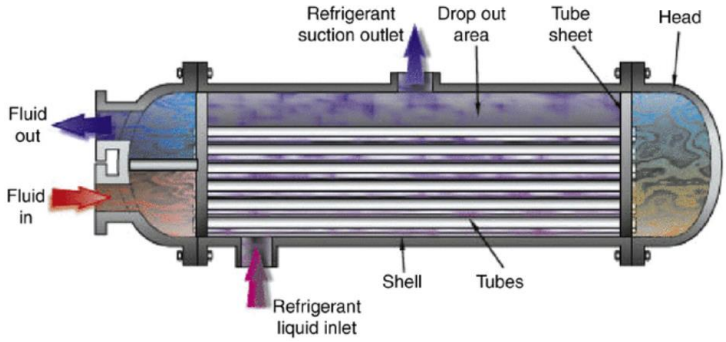

Figure 24. Flooded Shell & tube evaporator. (Hundy, et al., 2016, p. 124)

Features of a good evaporator design are stable boiling process and the low-temperature difference between refrigerant and source. This leads to a higher evaporation temperature and pressure. Decreasing the pressure difference between evaporator and condenser results in less energy consumption in the compressor, which results in better unit COP. Also, higher evaporation pressure enables increased working fluid flow in the system, due to the increase of fluid density. (SWEP, 2019)

The flooded evaporator type has the same characteristics, as described earlier. A major advantage of a flooded type is that they completely use all the latent energy of the working fluid in the phase transition between liquid and gas to cool a fluid. The flooded type is suited better for larger systems, because of the lower requirements of the compressor. Pay-back time is often measured to be too long if applied for smaller systems, despite the smaller power input. (SWEP, 2019)

Plate type evaporators function in both wet and dry configurations. With moderately narrow flow channels, the working fluid should be filtered before the evaporator. Minor freezing does not cause damage to the plate heat exchanger and the thermal exchange is still effective, thus the unit can be dimensioned in certain situations very close to the freezing point. A balanced plate distribution in a fluid-vapor mixture requires a rather high velocity, which again decreases the surface area or amount of plates. This can cause increased temperature differences with the interacting fluids. (Aittomäki, et al., 2012) In Figure 25 a typical plate & shell evaporator is presented.

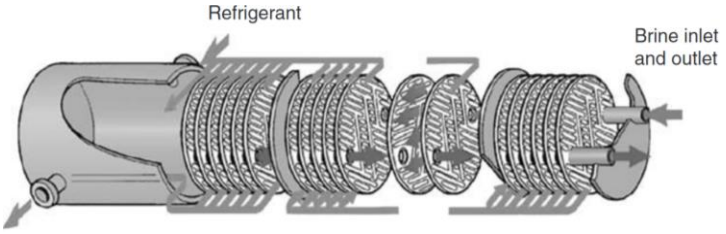

Figure 25. Plate & shell type. (Hundy, et al., 2008, p. 99)

The basis of designing an evaporator is the evaporating temperature. This is set by the required load requirements and ΔT between the evaporating working fluid and the temperature of the entering fluid to the unit. The ΔT affects the size of the evaporator: the smaller the temperature difference, the bigger is the unit. Consideration on how to prevent ice build-up on the evaporator surface should be noticed. (Hundy, et al., 2016, pp. 168-169)

The function of the condenser is to cool down hot high-pressure working fluid gas from the compressor back to liquid by condensation. The exchanged heat from the condenser is transferred through a fluid or air to the desired application. In heat pump applications plate heat exchangers are commonly used. A typical condenser unit in domestic refrigeration applications can be found in freezers or fridges, where a surface condenser is made of thin tubes placed on the back of the unit. In order to maximize COP, the condensing temperature should be as low as possible. (Hundy, et al., 2016, pp. 99,119)

Air- and water-cooled condensers are most common in commercial applications. The source for cool supply water for heat rejection can be different waterways, such as lakes or rivers. Water quality is an important factor for efficient condenser operation. When used in open sources heat exchangers are subjected to fouling, which is also the biggest disadvantage of this type. (ASHRAE, 2018, pp. 258-259)

The heat exchanger types in refrigeration machinery differ slightly. In water-cooled evaporators with small capacities, double-pipe exchangers have been used earlier. Plate exchangers are now becoming more common in small evaporators. These features apply also to heat pumps. In bigger systems are tubular or plate exchangers. (Aittomäki, et al., 2012) In refrigeration application condensers are in a more central part when the purpose is to remove heat from the process, whereas in heating applications is the function to apply heat to the process. As these processes are opposite to each other, the same heat exchanger types can be used for both evaporators and condensers, in theory, by changing the flow direction.

2.5.2 **Solutions for seawater**

The heat exchanger is a central part of the SWHP system. It enables the heat transfer between the heat source (seawater) and the heat sink. The common types are tubular, plate, and shell & plate heat exchangers. As mentioned in section 2.5.1 the same types of heat exchangers are used within evaporators, condensers, and seawater applications.

Tubular heat exchangers are mostly used for liquid-to-liquid and liquid-to-phase heat exchange applications. These have fair flexibility in design, by changing the core geometry, tube diameter, length, and arrangement. (Shah & P. Sekulić, 2003) In Figure 26 a tube and shell heat exchanger is shown. Tubes are packed in a shell with their axes parallel to that of the shell. The number of tubes can be up to many hundred. Baffles are placed to force the shell-side fluid to flow across the shell to increase heat transfer. (Cengel & Ghajar, 2015, p. 650)

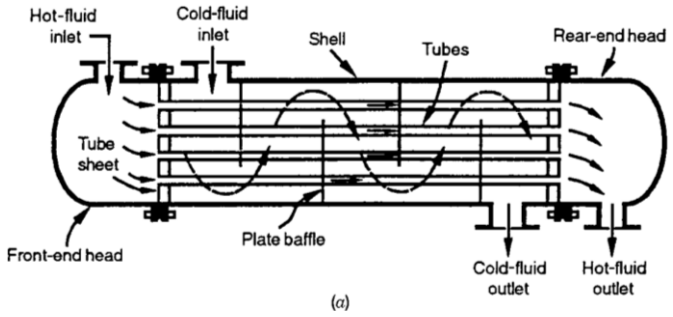

Figure 26. One pass tube and shell exchanger (Shah & P. Sekulić, 2003)

The plate heat exchanger (PHE) is another broadly used type, which consists of a series of plates with ridged flat flow passages. Hot and cold fluids flow in alternate passages, where each cold stream is surrounded by two hot streams. The amount of heat exchange can be varied by the number of plates in the pack. These suit for liquid-to-liquid heat transfer, where the fluid streams have about the same pressure. (Cengel & Ghajar, 2015, p. 650) Compared to tube & shell types, plate & shell types require much less floor space and the welded plate pair construction minimizes also the possibility of leakage. (ASHRAE, 2018, p. 220) The PHE has multiple times higher heat transfer rate compared to Shell & tube type. The essential feature of the PHE is the capability to be disassembled for cleaning. The channels between the plates are sealed by elastomeric gaskets which limit the application range. The maximum temperature is around 180 °C and the pressure around 25 bar. In Figure 27 a typical plate heat exchanger could be reviewed.

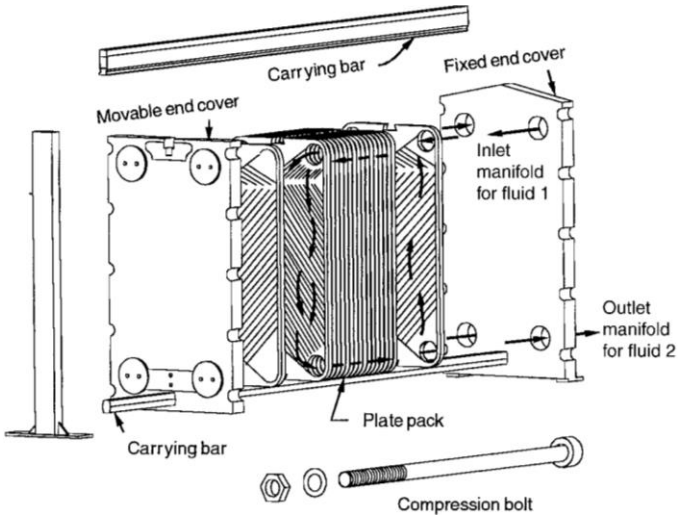

Figure 27. Plate heat exchanger (Shah & P. Sekulić, 2003)

A fully welded version of the PHE is called Plate & Shell heat exchanger (PSHE). This type can be used in many applications, for instance, general heating and cooling, as condensers or evaporators and steam heaters. Also, operating conditions beyond 400 °C and pressure up to 100 bar are possible to achieve. This fully sealed construction with rounded plates was commercially put to production in the 1990s by Vahterus Oy with their Plate & Shell heat exchanger (PSHE) (Arsenyeva, et al., 2016). Figure 28 presents the flow arrangement and construction of the PSHE.

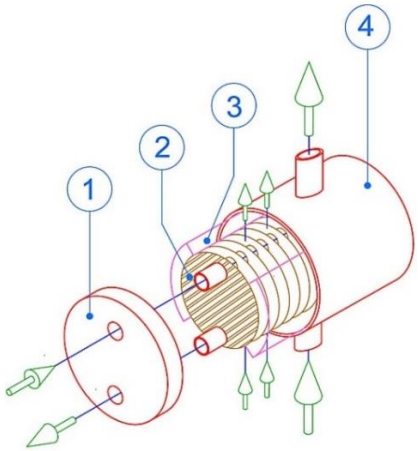

Figure 28. Vahterus Plate & Shell Heat Exchanger 1 = end plate; 2 = Z-plate; 3 = plate pack; 4 = flow directors; 5 = shell; A = shell side flow; B = plate side flow. (Vahterus Oy, 2021c)

Simplified, the construction consists of a cylindrical plate pack and a fully welded frame with no gaskets. The number of plates is dependent on the required load. The flow arrangement is typically done so that the hot source is on the plate side and the cold source on the shell side. For instance, seawater would flow on the plate side and anti-freeze fluid

on the shell side. Methods for cleaning in welded heat exchangers are for example back flushing, chemical cleaning, mechanical cleaning, and soda blasting. The method of cleaning is dependent on the type of fouling. (Vahterus Oy, 2021c)

2.5.2.1 Fouling and materials

Fouling is a common issue when using process fluid that contains impurities. Table 4 demonstrates typical fouling resistance values for different fluids within PHEs and tubular heat exchangers (THE). Fouling resistances are approximately 10 times lower in PHEs in comparison to THEs (Awad, 2011).

Table 4. Typical fouling resistances for PHEs THEs (Awad, 2011)

Process Fluid	**PHE** $[R_f, (m^2 \cdot K/kW)]$	**THE** $[R_f, (m^2 \cdot K/kW)]$
Soft water	0.018	0.18–0.35
Cooling tower water	0.044	0.18–0.35
Seawater	0.026	0.18–0.35
River water	0.044	0.35–0.53
Lube oil	0.053	0.36
Organic solvents	0.018–0.053	0.36
Steam (oil bearing)	0.009	0.18

Seawater includes a variety of different salts. Metallic components that are in contact with seawater suffer from corrosion through the electrochemical corrosion process. Corrosion-resistant materials should be used, such as titanium, nickel-based alloys, or stainless-steel alloys. These materials are expensive and replacing seawater heat exchangers with non-metallic materials is and up to date topic, for example, thermo plastics suitability has been studied. Titanium heat exchanger can be two to three times more expensive than heat exchanger made of other metallic materials. (Su, et al., 2020) Titanium is widely used around the world for seawater heat exchangers whereas high alloy steel is recommended for fresh water systems (Mitchell & Spitler, 2013).

2.5.3 Anti-freeze

Two approaches for seawater heat utilization were studied: Flooded evaporator and a seawater heat exchanger. Both approaches share the same plate & shell-type construction in this case. The original approach was to model the SWHP system with an intermediate ethylene-glycol network. Heat exchanger manufacturers suggested designing the system with flooded evaporation, without the intermediate circuit. One benefit is a more even plate

surface temperature inside the heat exchanger because of the constant saturation temperature of the working fluid. Uncertainty in the risk of freezing with the intermediate circuit was noticed. The two approaches are presented in Figure 29 and Figure 30.

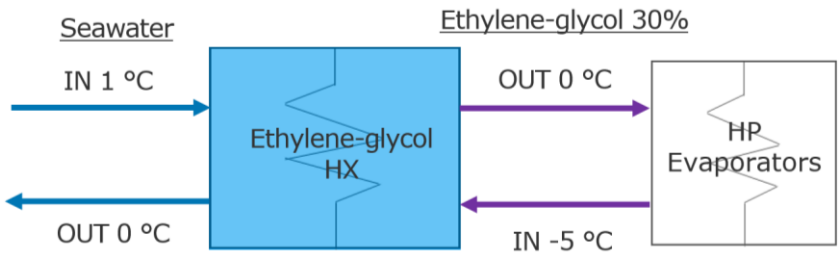

Figure 29. Seawater heat exchanger with an ethylene-glycol intermediate network approach.

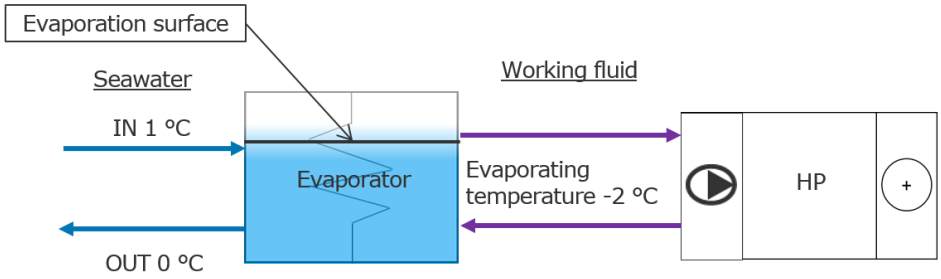

Figure 30. Flooded evaporator approach.

Freezing can be compared to a river with a high current against a low current: a high current river rarely freezes when a slowly moving current starts slowly to frost and finally freezes. The risk of freezing is utmost during periods when seawater temperature is close to 0 °C. For the seawater heat exchanger is the highest risk of freezing takes place on the primary side plates in the heat exchanger. Before actual freezing starts, is frosting starting to occur on the plate channels, which makes the fluid channels smaller. This leads to greater pressure loss inside the heat exchanger, which indicates that the freezing phase has started. The highest chance of freezing, in this case, can occur at the section between the ethylene-glycol inlet and seawater outlet. (Vahterus Oy, 2021b) In Figure 31 the risk section in the Plate & Shell heat exchanger is shown.

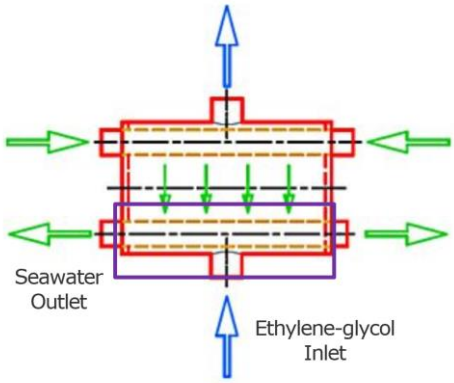

Figure 31. Purple marked section shows where freezing risk is highest in a welded Plate & Shell heat exchanger. (Vahterus Oy, 2021c)

Compared to a flooded evaporator is the temperature more even inside the shell. This originates from the working fluid saturation temperature, which is constant inside the evaporator. Evaporation occurs on the working fluid surface. In this type is the risk of freezing highest under the evaporation surface. (Vahterus Oy, 2021b)

Minimizing and preventing the risk of freezing in heat exchangers can be done by having a high mass flow rate and adequate pressure drop on the primary side which enables high turbulent flow and large shear force in the heat exchanger. The plate surface temperature should at minimum remain close to the fluid freezing point. If the surface temperature decrease below the fluid freezing point does it increase the risk of freezing. (Vahterus Oy, 2021b)

3 SEAWATER HEAT PUMP SYSTEMS

3.1 Open-loop system

In an open-loop seawater heat pump (SWHP) system sea- or lake water is pumped through a separate heat exchanger, from where the thermal energy is carried through a separate medium that circulates between the heat exchanger and evaporator, as Figure 32 shows.

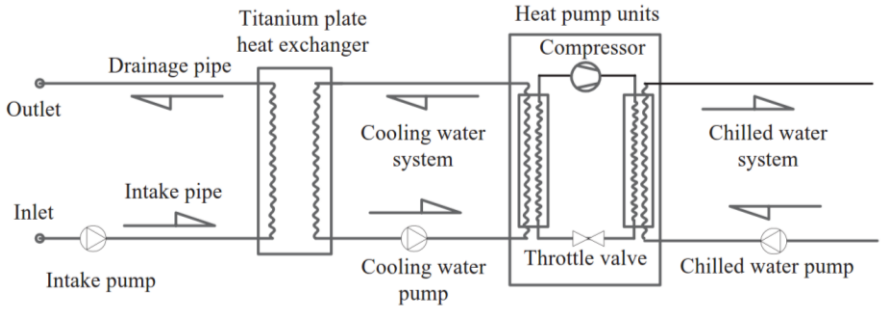

Figure 32. Conventional SWHP layout. (Liu, et al., 2019)

A typical method of utilizing seawater in industrial applications is to pump seawater through evaporators, where the seawater heat is processed to a higher temperature. During colder seasons is heat extraction more challenging when seawater temperature is near zero degrees. System options are for instance having great mass flow rates to the evaporators with minor cooling temperature or placing the heat exchanger in the sea and count on natural currents or induced flow (Eskafi, et al., 2019). An intermediate network method consists of an anti-freeze fluid that circulates between the heat exchanger and evaporators. A separate heat exchanger is needed because of the impurity and corrosive seawater. (Liu, et al., 2019)

Free cooling or direct surface water cooling (DSWC) can be utilized by open-loop systems. This means that the heat pump is bypassed, and thermal energy is exchanged from the sea water heat exchanger to the building heat exchanger. The water is then discharged back to the water source. (Mitchell & Spitler, 2013)

Since a SWHP application is geographically constrained, buildings within a certain distance from the water source can utilize produced heating or cooling energy. A long transport distance will cause excessive pumping electricity consumption. Research by Lund et al. 2016 considers that buildings within 500 m from the source have the potential to install a SWHP plant, where one individual or a few buildings are connected. Research by Shu et al. 2016

showcased that district heating systems transportation distances are longer, therefore a 5 km radius was found optimal for a SWHP system compared to a coal boiler system. (Su, et al., 2020)

Material selection for the seawater intake pump depends on many factors, including service conditions, pump design, approximate qualities of the seawater, material availability, and financial aspect. Conventional austenitic stainless steels are the most cost-effective choice for normal seawater conditions, proper precautions of minimum flow guarantee(0,9 to 1,5 m/sec) have to be maintained and avoiding stagnant conditions. (Morrow, 2010)

3.1.1 **Intake methods**

Two intake methods can be recognized for SWHP systems. Direct intake and beach-well method. In the direct intake method is the water pumped straight off the water source. The Beach-well method is based on a drilled opening at the shoreline where the seawater is infiltrated and then pumped to the heat pump unit. Figure 33 illustrates the beach well method compared to the direct intake method. (Su, et al., 2020)

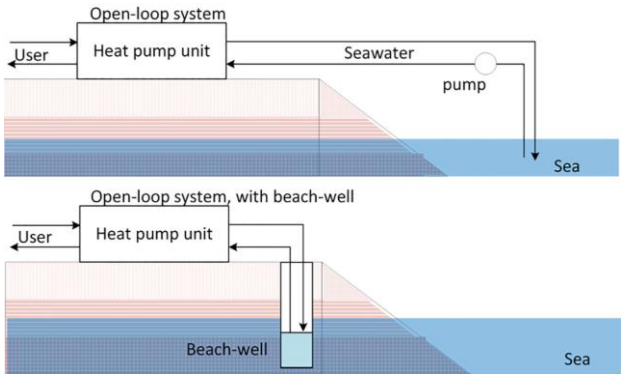

Figure 33. Intake methods. (Su, et al., 2020)

A comparison between direct and indirect water intake was studied by Xin et al. 2018, where the direct intake method consisted of a separate seawater basin between the heat exchanger and seawater intake, as shown in Figure 34. The indirect method consisted of a beach well, located 800 m from the seacoast at a depth of 42 m. The beach well setup is illustrated in Figure 35. The direct method case had a larger heating capacity than the beach well case.

The direct method case heating and cooling capacity was 4605 kW and 79 kW correspondingly. The beach well method case had capacities of 270 kW heating and 164 kW cooling. Both cases provided heating and cooling for a facility via heat pumps. The average seawater temperature during winter was around 5,83 °C for direct and 12,85 °C for indirect. The system and unit COP for the direct method was on average 2,3 and 2,9. For beach well was COP measured on average to be 3,7 for system and unit 4,66. The study showed that the beach well method had better reliability, stability, and energy efficiency. Under extreme weather conditions, with supply and return water temperatures from 1 to -0,6 °C, would the heat exchanger freeze and therefore, also heat pumps would stop running in the direct intake system. The freezing point was at –1,7 °C with 30 ‰ salinity. Beach well infiltration had better stability because of a more steady seawater inlet temperature against the direct system. Energy efficiency was also better in the beach well infiltration system when comparing to COP. This has to do with the higher average seawater inlet temperature. Higher temperatures were possible because of the thermal energy from both sea and ground. The energy-saving rate was calculated to be 38 % of the final energy consumption. (Xin, et al., 2018)

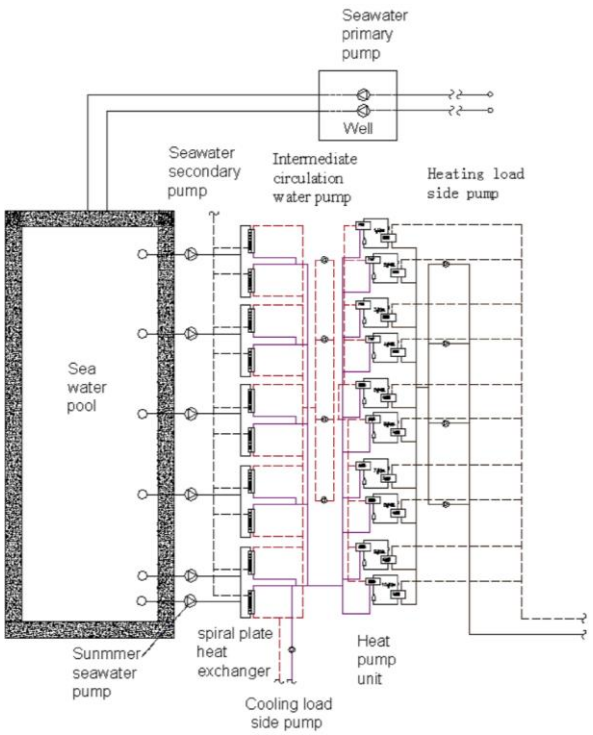

Figure 34. Direct seawater intake method. (Xin, et al., 2018)

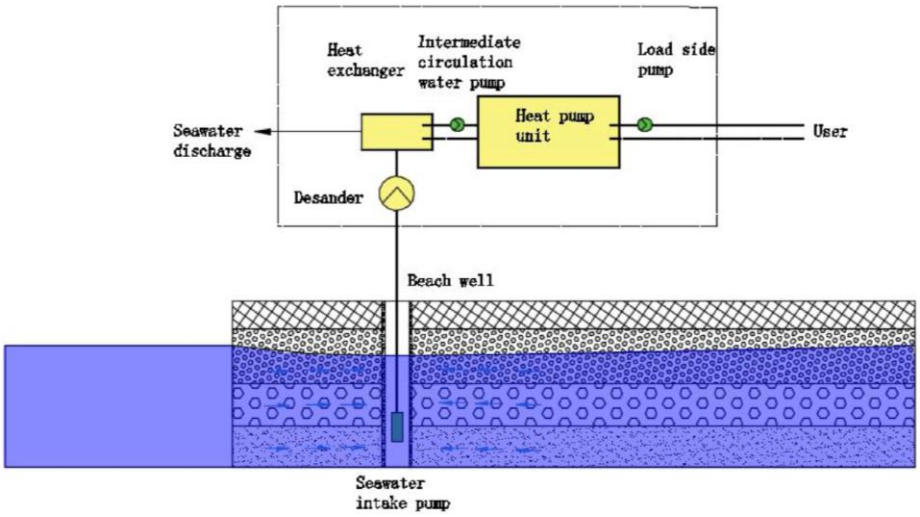

Figure 35. Beach well setup. (Xin, et al., 2018)

Wang et al. 2018 studied different water-intake designs for SWHP systems. The study was made with numerical simulations through Computational Fluid Dynamics (CFD) for examining an optimal intake design, where three designs were compared, as shown in Figure 36. An experimental intake model with single water-intake and linear water-intake port system was established. Results showed that the intake water temperature was lower with the linear intake method and the theoretical energy-saving rate was improved with this method. (Wang, et al., 2012)

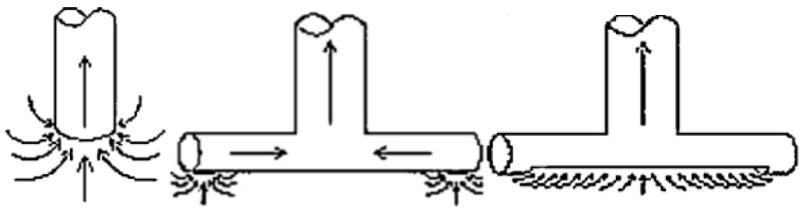

Figure 36. Intake methods. From left to right: Single water-intake point, multiple water-intake port system, linear water-intake port system. (Wang, et al., 2012)

3.1.2 **Fouling**

Intake piping in open-loop systems may encounter biofouling. This can be prevented with appropriate screening or filtration at the water intake. A radial screening structure is shown in Figure 37 where the intake pipe is installed close to the sea- or lakebed. To prevent infiltration of biological organisms, such as fish, to be drawn in the intake piping is it recommended to have a reasonable face velocity at the intake and equip it with a wedge wire screen. Sand filters have also been proven to work for smaller residential applications

(45 kW unit), where the fine sand or other porous medium filters intake water before entering the heat pump. (Mitchell & Spitler, 2013)

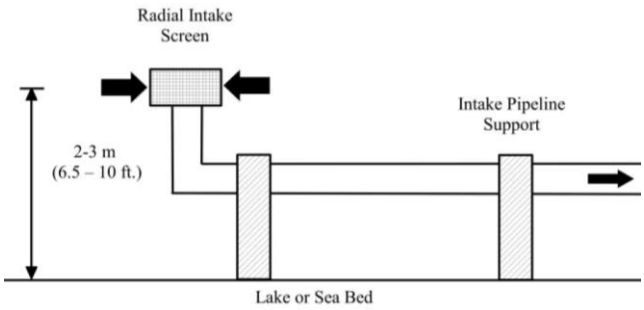

Figure 37. Intake screening. (Mitchell & Spitler, 2013)

During the summer season, when cooling is needed, seawater temperature could rise to 25 °C or above in the East China Sea, thus being an incubator for sea organisms. Microorganisms can develop a biofilm on suction piping or heat exchanger when these are in contact with seawater, eventually causing biofouling. Substantial negative effects can occur, for example, water flow blockage, mechanical damage to pumps, clogging of water tubes, and a decrease in heat transfer efficiency. (Su, et al., 2020)

Several methods for preventing biofouling in a SWHP system are available: physical screening, physical cleaning, and chemical dosing. Physical screening can be high-pressure water flushing. Physical cleaning again would be sponge rubber balls for removing biofilm. As an exception, in mechanical cleaning biocides are used. Chlorination is still the most common biocide for biofouling treatment. It is regrettably harmful to the environment and human health due to the by-products of chlorine. (Su, et al., 2020)

District heating plants that utilize seawater to produce heat energy are network shell and tube spray evaporators are used with titanium tubes. Water velocity is between 3- 4 m/s, which prevents fouling, and each tube is 22mm in diameter. The working fluid in the system is ammonia. This example is from Drammen, Norway. (Zahid, 2016) The evaporator is shown in Figure 38.

Figure 38. Spray evaporator during installation. (Zahid, 2016)

3.2 Closed-loop system

In a closed-loop configuration circulates an anti-freeze fluid in a collector pipe that is anchored on the bottom of the sea or lake. The location should be deep enough, to prevent freezing and no strong current at the location. (Forsén, 2005) In Figure 39 a serpentine and helical layout of closed-loop piping is shown.

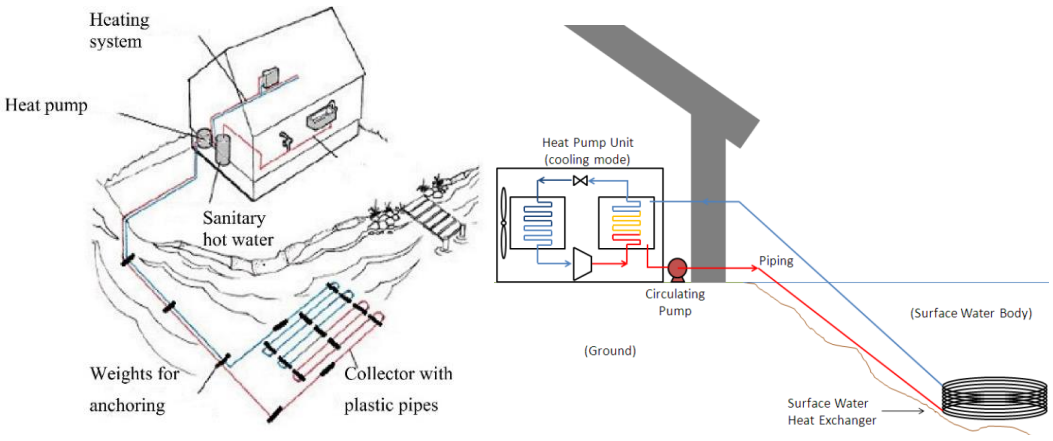

Figure 39. Closed-loop layouts: Serpentine(left) and helical(right). (Forsén, 2005) (Hansen, 2011)

The collector pipe can also be placed in a spiral helical format in the water source. Different collector pipe geometry configurations are available. Figure 40 shows a couple of different coil configurations. Closed-loop systems can tackle the corrosion damage and pipe blockage caused by marine organisms, which impact the system economy and lifetime of an open-loop configuration. (Zheng, et al., 2020) Advantages over open-loop configuration are reduced fouling in the system and pumping power because the head elevation is no longer

present. Disadvantages again are fouling outside of the heat exchanger coil and risk of damage on the coil, if located in a lake. (Kavanaugh & Rafferty, 2014, p. 138)

Figure 40. Different Spiral Helical coil geometries. (Hansen, 2011)

Liu, et al. 2019 Studied the possibility to use a capillary tube heat exchanger on the primary side instead of a titanium plate type, which has high investment costs and a large work quantity. A polypropylene random (PPR) material was used and a glycol anti-freeze fluid was circulating in the capillaries. The capillary heat exchanger was connected to the evaporator. The system and the capillary heat exchanger tube installation are shown in Figure 41. This experiment was performed in a 500 m^2 hotel building with 60 kW heating and 53 kW maximum cooling load. The result proved that it is feasible to use a capillary heat exchanger on the heat source side over a traditional titanium PHE configuration. (Liu, et al., 2019)

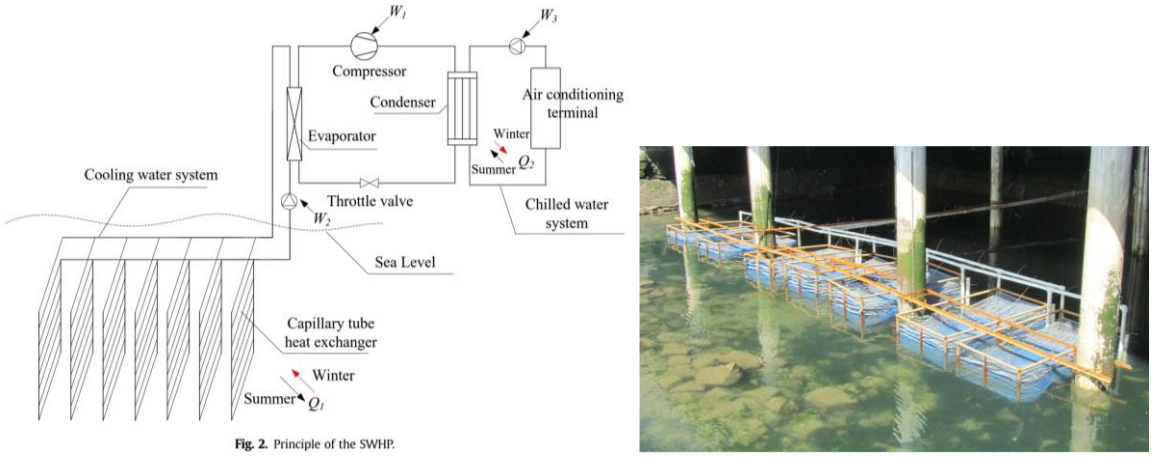

Figure 41. A capillary tube heat exchanger. (Liu, et al., 2019)

3.3 Available systems & development

The scale of SWHP system capacity varies from 0,6 MW up to 108 MW. Many of these systems are designed and fulfilled for district heating and cooling purposes. These plants are in general operating in an open-loop configuration, because of the system scale. World's largest SWHP plant is in Sweden Ropsten area is connected to the district heating network with a total system heating capacity of 215 MW. In Norway, SWHP systems are used during cold periods for heating and under summer periods for cooling. (Su, et al., 2020) Drammen in Norway has a capacity of 13 MW and in Iceland Vestmannaeyjar SWHP system of 10 MW. These systems produce high temperature (80–90 °C) water for district heating. Drammen and Vestmannaeyjar have ammonia screw compressors with two stages. Seawater temperatures are alike in both plants, never under 5 °C. With two-stage compression and steady seawater temperatures is the COP above 3 at these plants. (Eskafi, et al., 2019)

In Kopli, Tallinn is a new residential area in development, where Volkova et al. 2019 explored district heating solutions via three scenarios, these were analyzed from a technical, economic, and environmental point of view. One of the scenarios included a SWHP and gas-fired boiler, where the boiler would cover the peak loads. The setup would consist of two boilers (1950kW and 560kW) and a two-stage heat pump, with screw compressors and ammonia as the refrigerant. The heat capacity of the system was assumed to 2,1 MW and seasonal COP to 4.04 (Volkova, et al., 2019)

In Viitasaari, Finland is a closed-loop SWHP system built at a service station. Keitele lake is the heat sink for the heat pump (315 kW), where cooling and heating energy is taken from. 7500 m of piping, consisting of 25 loops each 300 m long, that are placed on the bottom of the Keitele Lake at a depth from 2 to 7 m. Average heating energy production is around 750 MWh annually. The collector fluid in the system is Thermera. (Teiniranta, 2010)

In the following section is open and closed-loop configurations compared with given study case data, which is discussed more comprehensively in Chapter 5. For the closed-loop system was information needed about thermal conductivity. Table 5 presents different maximum heat amounts for waterways in different areas of Finland. Location is divided into four weather sectors for Finland, where the first (I) is the southern area and the fourth (IV) is the most northern area. Selected maximum heat amount for a water body in the weather

sector I was 20 W/m. Estimated average piping costs (€/m) were read from a wholesale shop (Suomen Maalämpötukku, 2021).

Table 5. Available heat amount for waterway applications in Finland. (NIBE, 2014)

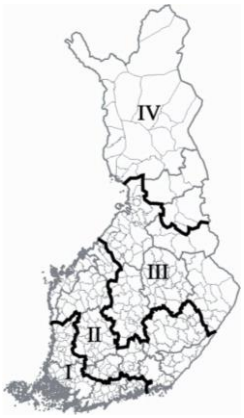

Waterway	I area	II area	III area	IV area
kWh/m	90	80	70	50
W/m	20	20–25	15–20	15–20
Fluid avg. temp, °C	+1…+2	+1…+2	+1…+2	+1…+2

Figure 42. Weather sectors. (NIBE, 2014)

Data and pricing over an open-loop system are presented in more detail in Chapter 5. Comparison results are presented in Table 6. Prices are without value-added tax (VAT). Pipe price refers to the intake and return piping in an open-loop system and collector pipe in a closed-loop. 100 m of piping was estimated for open-loop and 15 000 m for closed-loop collector pipes.

Table 6. Open-loop and closed-loop comparison

Parameter	Value	
A_{GFA}	14 400 k-m^2	
$Q_{HP,tot}$	300 kW	
	Open-loop	**Closed-loop**
qm	75 kg/s(seawater)	12,85 kg/s (anti-freeze)
Pipe amount	100 m	15 000 m
Pipe price	57,12 €/m (DN200)	1,97 €/m (DN40)
Piping cost	5 700 €	29 507
HX_{price}	35 000 €	-
Total	40 700	29 507 €

The investment price difference is higher with the made estimations for the open-loop system. Value for maximum heat amount has an impact on collector pipe length, which also affects investment price.

3.4 Lake water and seawater features

3.4.1 Lake water

One problem when utilizing thermal energy from lakes is the low temperature during the winter period. When the energy demand is at its highest, the water temperature is under 4 °C or in lower shallow waters is under 2 °C. (Aittomäki, 1983)

Finnish lakes are dimictic, referring that lakes have two turnovers per year. The turnovers occur in spring and fall (Leppävirta, et al., 2017). In winter the colder water is closer to the surface and in summer is vice versa. During winter and spring stratification water volumes are layered isothermally of density differences and no vertical convection appears. During spring and fall turnover water volumes are mixed in consequence of heating of the water surface in spring and cooling in fall. Wind conditions also affect the water turnover. (Aittomäki, 1983) The yearly turnover of a lake is shown in Figure 43.

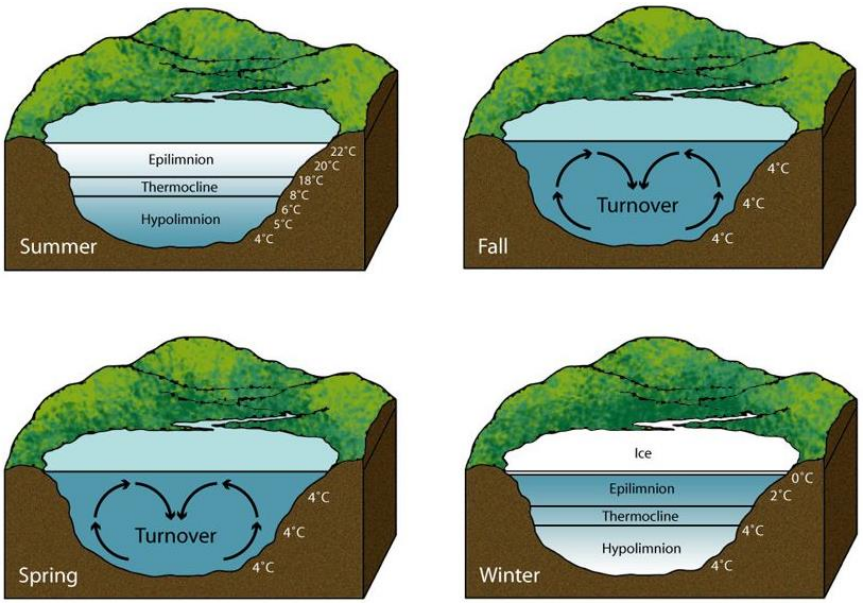

Figure 43. Lake turnover (National Geographic, 2011)

The situation in lakes can be sectioned by temperature distribution in four different conditions (Aittomäki, 1983):

- Winter stratification
- Spring turnover
- Summer stratification
- Fall turnover

3.4.2 **Seawater**

Seawater contains salt. Oceans have a salinity of 35 g per kilogram, expressed as a ratio of 35. The Baltic Sea is a mixture of ocean and fresh water, which salinity level is on average 7, but varies significantly by region and depth. In comparison to ocean seawater, the Baltic sea is known as brackish water, because it has different characteristics subject to location. The salinity at the surface water is around 20 % in the Danish straits, but it decreases gradually northwards, for example at the Gulf of Finland (GoF) the range is between 0 to 3 %. (Bruun, 2020) The freezing point of the surface water diverges depending on the salinity. The variation is between -0,17 °C to -0,33 °C from east to west at GoF. (Alenius, et al., 1998)

Stratification occurs both vertically and horizontally. Seasonal changes dominate the temperature variation of GoF, as in the entire Baltic Sea. The surface temperature begins to rise in April when the ice melts and solar radiation increases. When the surface temperature rises towards the maximum density temperature (2,5 to 3,5 °C), the surface water becomes heavier and triggers the start of vertical convection. When surface water exceeds the maximum density temperature, the seasonal thermocline begins to form all around the GoF in the summer period. This event keeps the water mass vertically homogenous. The upper layer is thermally almost homogenous, because of the wind mixing. Its thickness is between 10 to 20 meters. Underneath is the thermocline, where the temperature drops from about 15–20 °C at the surface to circa 2–4 °C at the bottom of the thermocline. The pool of cold water underneath the thermocline is also called old winter water. (Alenius, et al., 1998)

The surface temperature reaches its maximum in late July-early August. In late August, the vertical convection starts over again once the surface water temperature decreases. During fall the thermocline layer vanishes. The strong vertical salinity stratification stops the convection. Stormy winds, which create mechanical mixing in the ocean, have an important role in the desolation of the thermocline. (Alenius, et al., 1998)

Vertical stratification is called upwelling. The process transports water from deeper colder layers to the surface. Water wells up from a few tens of meters in the Baltic Sea. A characteristic upwelling event occurs along the coast where water currents created by winds cause the upwelling. The upwelling zone usually reaches 5 to 20 km from the shore to the open sea, which can easily be also seen from satellite images. Upwelling can likewise

accelerate the formation of blue-green algal blooms when nutrients are brought to the surface. This happens often in August when the possibility of stronger winds increases. (Bruun, 2020)

3.4.3 Sea and lake water plots

Measurements by the Finnish meteorological institute and the City of Helsinki provided temperature data from the Kruunuvuorenselkä measurement station. Measurement depths are 1,1 m, 2,8 m, 5,3 m, 7,3 m, and 9,6 m (in the bottom mud). For the case study was data over the year 2017 used. The seawater is at its coldest during the winter period. In spring the seawater temperature starts to rise and it reaches highest around august. The temperature starts decreasing after the summer period.

Lake water temperature data over Lankiluoto located in Vesijärvi, Lahti was also studied. The water temperature data were provided by Kalevi Salonen, University of Helsinki. The seasonal temperature change is similar to seawater. In Figure 44 sea and lake water temperatures are presented. The seawater temperature varies significantly in the summer between 2017 and 2018. The lake water stays more stable during the summer season. The year 2017 data is used in the case, which is presented in Chapter 5.

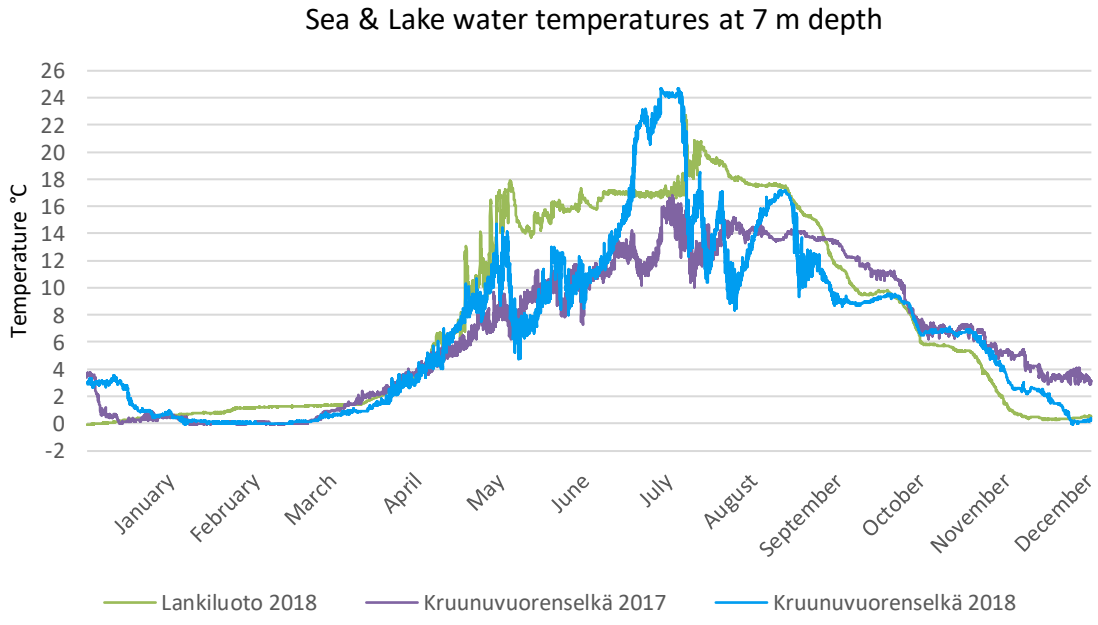

Figure 44 Sea and lake water temperatures over 2017 and 2018.

In a study of surface and close to bottom seawater temperatures at the coastal area of Helsinki, the probability for the seawater to exceed over 2 °C at the bottom levels was analyzed. The purpose of this study was to provide some background data to estimate the feasibility of seawater usage as a heat source for buildings. In Figure 45 depth zones over the coastal depths outside Helsinki are shown. The majority of the water areas are below depths of 10 m. The depth areas for 10-35 m are mostly located a couple of kilometers from the coastline. The depth areas above 35 m appear only in the open sea. (Vahtera, 2018)

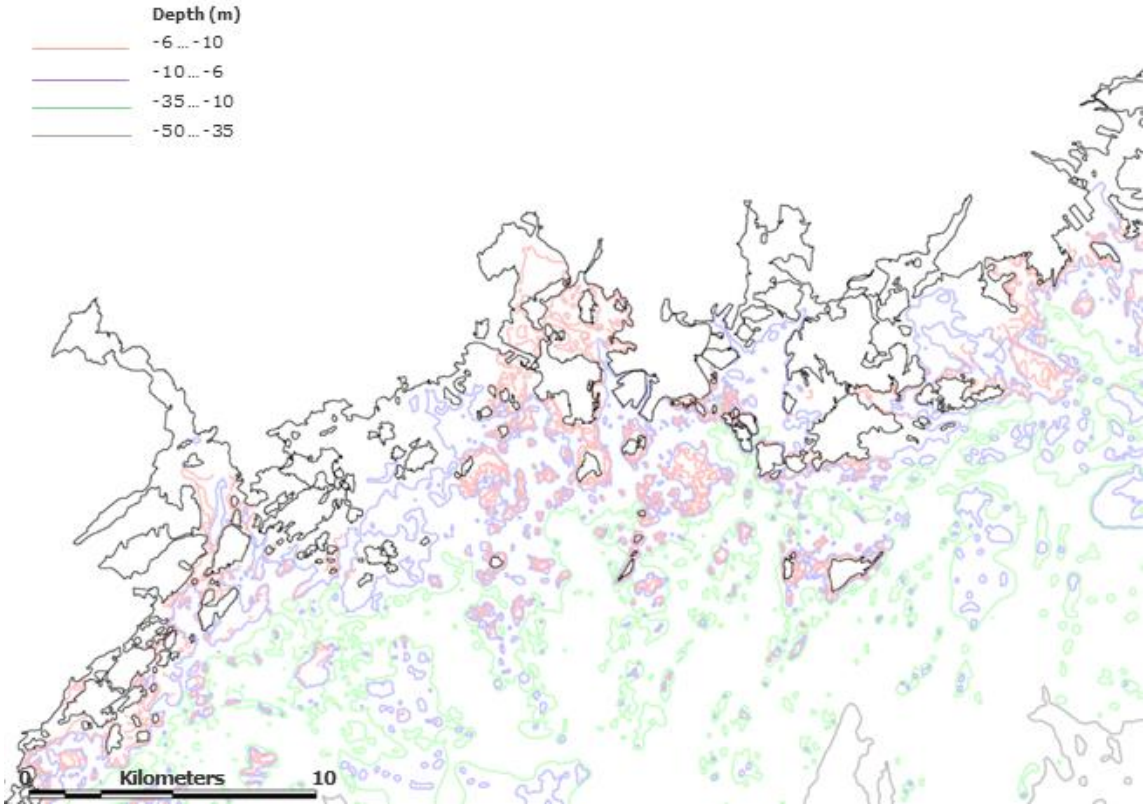

Figure 45. Capital region coastal depth zones. (Vahtera, 2018)

The study showed that in water areas with a depth less than 10 m the probability for near-bottom water temperatures exceeding 2 °C was insignificant from January to March. In April and May was the probability 90 % and 100 % correspondingly. In water areas within 10-35 m, the probability to exceed 2 °C temperature near the bottom was 60 % in April and over 90 % in May. From February to March the possibility was under 20 %. In deeper waters, 35 m and beyond, exceeding the near-bottom temperature of 2 °C was very likely from January to May. (Vahtera, 2018) In other words, in deeper waters, the temperatures are steadier and more optimal to use as a heat source. Figure 46 shows the probability for seawater to exceed 2 °C near-bottom layers of different depths.

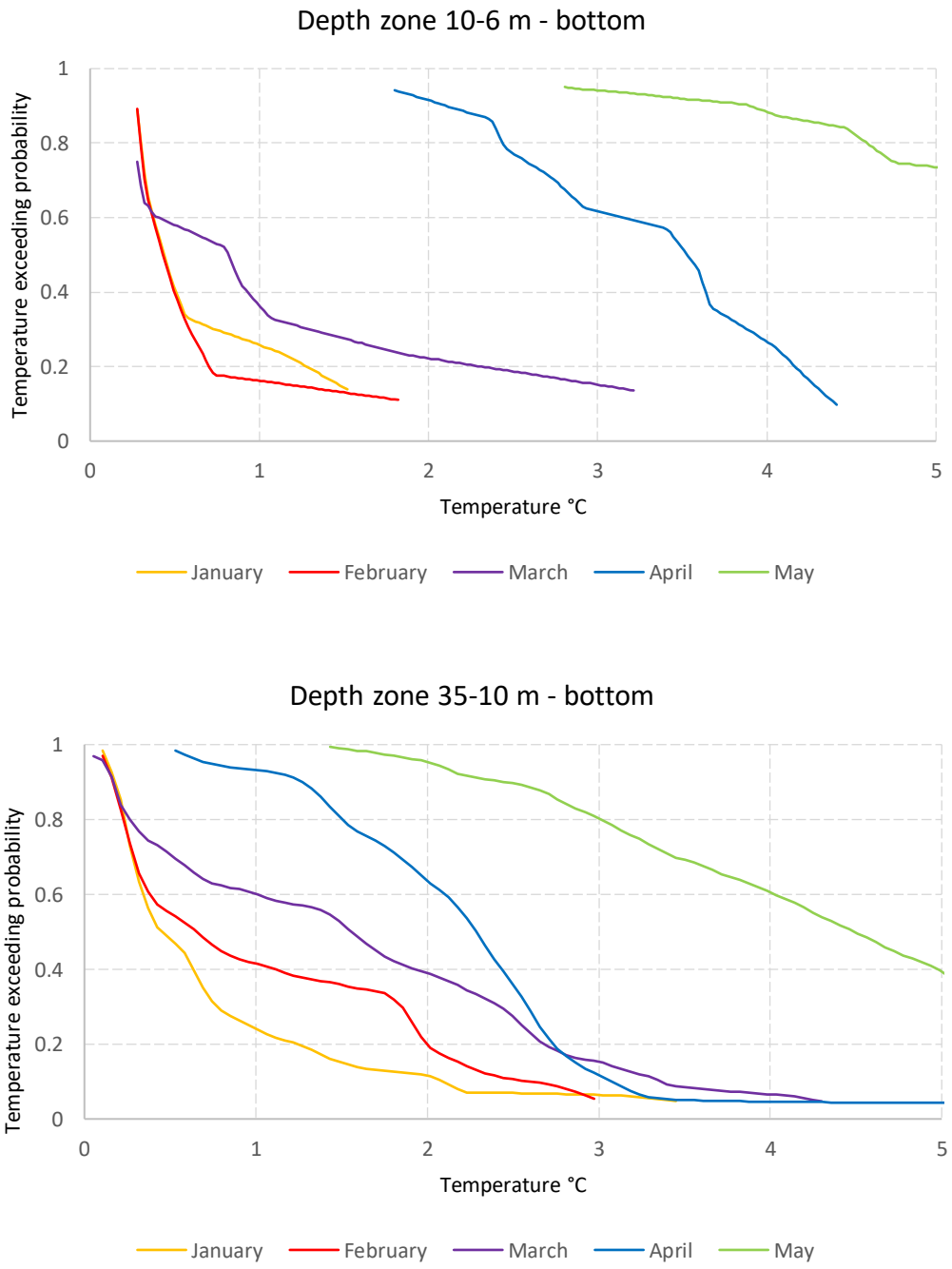

Figure 46. Probability to exceed 2 °C near-bottom layers. (Vahtera, 2018)

To further clarify what Figure 46 illustrates: In the 10-6 m depth zone is the probability for exceeding over 2 °C from January to February very poor, but in April is there a great chance, above 0,9 probability, of exceeding over 2 °C, because of the rapid water temperature increase.

4 ENVIRONMENTAL BOUNDARIES & RESTRICTIONS

4.1 Regulations

Three main acts: Environmental Protection Act, Water Act, Land Use and Building act regulate and contain the key factors that need to be fulfilled when taking to concern the surrounding environment.

4.1.1 Environmental Protection Act

The Environmental Protection Act (527/2014) is a general act on the prevention of pollution, which is applied to all actions that cause environmental damage. The main principles and duties of the Act are (L 27.4.2014/527. Environmental Protection Act)

- Principles to prevent or reduce harmful impacts
- The use of the best available technique (BAT)
- The use of best practices to prevent pollution
- Parties engaged in actions that stance a risk of pollution have a task to prevent or minimize harmful impacts

4.1.2 Water Act

The purpose of the Water Act (587/2011) is to promote, organize and coordinate the use of water resources and the maritime environment, so it remains socially, economically, and ecologically sustainable. Secondly, to prevent and reduce negative effects of water and the use of the maritime environment. A third purpose is to enhance the state of water resources and the maritime environment. (L 27.5.2011/587. Water Act.) This act also contains a permit requirement for activities, which alter water bodies in some way, including all physical construction and laying of pipelines.

4.1.3 Land use and Building Act

The Land Use and Building act (132/1999) concerns the use of land areas and building activities directed on them. The purpose is to produce a healthy, safe, and comfortable living environment that is socially functional and where different needs from various demographic groups are heard. The main principles and duties of the Act are:

- Organizing the use of land areas and building activities
- Encourage ecological, social, and culturally sustainable development
- Assuring that everyone has the right to contribute in the preparation of associated matters.
- Guarantee high quality and collaboration of planning, range of expertise, and sincere correspondence (Ministry of the Environment, 2020).

Land Use and Building act include different provisions, for example

- Town planning
- Municipal building ordinances
- Plot division
- General requirements on building (Ministry of the Environment, 2020).

4.2 Authorization

A permit is needed for executing a heat pump system for both seawater and ground source heat. The municipal action permit is applied in general for all cases. Ground heat exchangers that are planned on groundwater areas and SWHP systems are the Water Permit desired, which is applied and administered through the Regional State Administrative Agency (AVI). Several other things may require approval, for example, possible underground constructions in the region, groundwater zone, and safety distances to other buildings, plot borders, and other ground heat wells (Espoon Rakennusvalvonta, 2017). The Centres for Economic Development, Transport, and the Environment (ELY-Centres) have an essential part in the permit process as they provide expertise statements on each permit application. (Majuri, 2020)

Municipalities have broad practices in helping quality control throughout the action permit procedure. They may for example have recommendations for the location of the heat exchanger, an option of requiring a site manager and building inspectors may supervise some details at inspections. The level of expertise varied among building control officials depending on their interests and experience in Majuri's study from 2020. The same matters applied to AVIs. (Majuri, 2020) Permit schemes of ground heat exchangers are presented in Figure 47.

	Local administration	Regional administration
Legislation	Land Use and Building Act (Finnish statute 1999/132, section 126a)	Water Act (Finnish statute 2011/587, Chapter 3, section 2) Environmental Protection Act (Finnish statute 2014/527, section 17)
Competent authority	Municipal building control	Regional State Administrative Agency (AVI, Aluehallintovirasto)
Aim of legislation in relation to GHEs	Control installation of GHEs in relation to their potential impacts on natural conditions and surrounding land use	Groundwater protection
Application of legislation	In most municipalities each new GHE requires either (a) an Action Permit (a simplified building permit procedure applied to retrofits when only a geoenergy system is installed) or (b) a Building Permit (applies to larger projects, where the GHE is approved as a component of a construction project). However, a municipality may decide that permits are not needed, in which case (c) a notification procedure is usually applied.	If a planned GHE is located on a designated groundwater area, a permit from AVI is required. The municipal authority may request a statement on the need of a permit from the Centre for Economic Development, Transport and the Environment (ELY Centre).

Figure 47. Permit schemes for ground heat exchangers in Finland. (Majuri, 2020)

Systems that use water for producing heating or cooling with heat pumps require a Water Permit. This is a direct referred to Water Act (587/2011), where it is stated that when placing pipelines or pumping from a water source is the permit required. AVI administrates these permits and the applications should be directed to the regional agency that operates in the area where the system is designed to be built. Permission is also needed from the owner of the waters. The Water permit includes a comparison of interests, where benefits and disadvantages are put in weight. When the benefits are greater than the disadvantages, the permit can presumably be accepted. AVI has the authority to reject the owner of the water's posture if the water permit application fulfills the demands. (Suvanto, 2020)

During the application process of the Water Permit, it is common that the applicant has a dialogue with AVI of more detailed information for the permit documentation and magnitude. It is recommended in advance to inform AVI of the upcoming application for preparation and give some background information on the required content. In Water Act (587/2011) it is stated that a report over the detriment and effects on the waterway is required. It does not describe what should be contained, therefore is it AVIs task to provide more detailed information. Duration for the whole application process (preparation, hearing, admission) is about one year. (Suvanto, 2020)

This type of system does not bring presumably any major issues for authorization. However, lakes could be one exception, where the maritime biology and energy balance can be more sensitive, subject to the scale of the designed system and water body. Also, social apprehensions can have a significant role in the interest comparison in the subject of lakes. In one case study the potential of utilizing a lake for heating energy production was reviewed, where the interest groups had a stronger impact on the area. The reviewed lake was the only pure lake in the area, where many different social activities took place. If a SWHP system would have been designed on the lake area, the social activities would have suffered from that. (Laitinen, 2020) It is open to interpretations if an environmental permit is needed for these systems. One matter that could be interpreted differently is when ejecting colder return water back to the water body from the heat exchanger. If an environmental permit is needed in this case, it might depend on the water intake and ejection amounts and, what kind of water source it is. (Suvanto, 2020)

4.3 Environmental impact

Location and piping routes for the suction and discharge piping may bring some questioning from the waterway owner. A usual reaction is to exaggerate the scale of the work. Piping line routes, size of the construction, ignorance of the system, and unfamiliar contractors may arouse discussion. By clarifying to the owner in an early stage what is the purpose and scale of the planned work in the area would help in getting the approval. (Suvanto, 2020)

When exploring possible options for the piping lines, issues that affect water and sea activities should be concerned. To mention a few common matters sea routes, navigable routes, fishing areas, and recreational areas, and places where water activities are exercised. (Suvanto, 2020) Issues regarding SWHP systems are for example nature reserves or if the proposed area has reservations for other technical systems. (Laitinen, 2020)

Studies on the effects of hydrology, limnology, and biology on waterbodies can be performed during the design process for the system, especially when planning an industrial-size water pumping system that provides heating and cooling energy for a district. Central parameters that affect hydrology are the scale of the waterbody and the topology of the area. These parameters have an important role in the water discharge effect in the surrounding water area. A more detailed study on forecasting how the discharge flow is transferred in the

area can be performed via CFD simulations. Discharged cooling water distribution area during summer from the Vuosaari power plant without wind is shown in Figure 48.

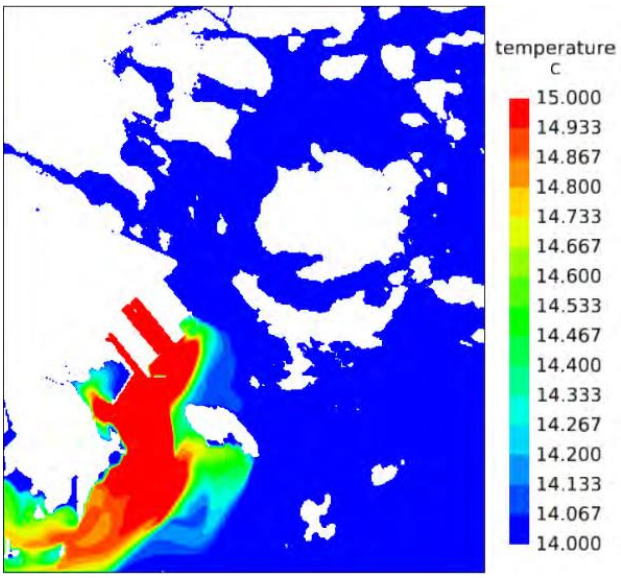

Figure 48 Vuosaari power plant discharged cooling water distribution area without wind during summer. (CFD-Finland Oy, 2013)

There are always uncertainties when creating models that correspond to a real state. Models usually are simplified to a certain degree for getting completed simulations. In these types of models can uncertainties occur for example in weather conditions, amount of released heat energy, surrounding flow conditions, and lack of topography information. (CFD-Finland Oy, 2013) (Helsingin Energia, 2014)

Different impacts on the waterbody may transpire when ejecting warmer water from a cooling process back to the source. A few possible impacts are listed in the following

- Wind circumstances in the area may have an impact on the water distribution flow from the plant.
- The increase in surface water temperature may decrease the ice layer thickness
- Discharge water does not include any straying matter that would increase eutrophication when only circulating seawater.
- Cloudiness near the discharge outlet is possible because of discharge flow
- Spring bloom can occur earlier, because of thinner ice layers, and plankton algae can periodically increase
- Close to the discharge area is an increase in vegetation abundance possible because of the temperature rise

- Impact on benthos community in the surroundings (Helsingin Energia, 2014).

Change in waterbody thermal balance may affect hydrology. Temperature decrease could extend the duration of the ice layer and affect the early stage survival of specific species. Temperature increase contributes to the release of nutrients, especially phosphor in the sediment, increase in eutrophication, and declining oxygen levels. A change in waterbody hydrodynamics could impact the water layers and bottom sediment when injecting and ejecting water. This might release nutrients and possible detrimental elements from the sediment to the upper layers closer to the surface. Also, the impact on endobenthic animals and their ecological state could be disturbed because of changes in hydrodynamics. Piping for the heat exchanger may affect recreational activities. (Ramboll, 2020) Surveillance is one part of the environmental monitoring when the plant is finished. Things that are in general monitored for example in lakes; water blurriness, water layer temperatures, and eutrophication, such as oxygen levels. (Laitinen, 2020)

5 CASE STUDY – GENERIC RESIDENTIAL BUILDING BLOCK

In this case study was examined the feasibility in practice of a SWHP systems heating and cooling potential, and profitability in a generic residential building block. A simulation model was created in IDA ICE for simulating the system energy production and consumption. The modeled system consists of heat pumps (HP) and district heating (DH), which function is to contribute to the required heating demands. The created model was then compared against a district heating-only system, which is a mature residential heating system used for decades. Compared factors were for instance heating and cooling production, electricity consumption, life cycle costing, and CO_2 emissions. Another goal was to have a working simulation model that can be used in future projects, where different energy systems are compared. One requirement was the option to adjust different parameters conveniently, mainly building demand and weather data, and heat pump sizing parameters.

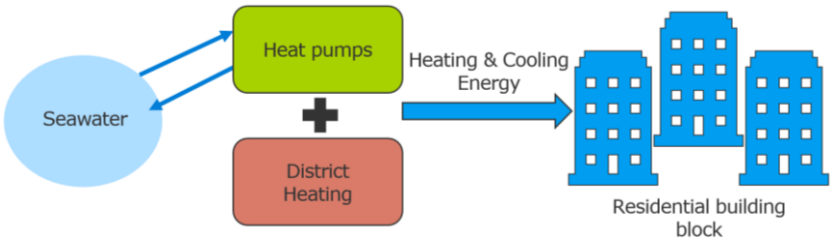

Figure 49. Basic system layout.

5.1 Building energy demand data

The energy demand data is based on hourly measured energy consumption of 50 apartment buildings located in Helsinki, which were constructed between 2014-2016. It includes energy demand data over space heating & cooling, and domestic water heating (DWH) demands in W/m^2 units over one year period. The space heating data contains also air handling unit (AHU) heating demand. The gross floor area (GFA) of 14 400 k-m^2 is used as a multiplication factor for representing a residential building block. Energy demands for the corresponding case are presented in Table 7.

Table 7. Energy demands over a 14 400 k-m^2 residential building block.

A_{GFA}	Peak space heating & AHU	Peak DWH	Peak space cooling
14 400 k-m^2	315 kW	169 kW	183 kW
$E_{th,tot}$	**Space heating & AHU**	**DWH**	**Space cooling**
1 270 MWh	798 MWh	427 MWh	45 MWh

The corresponding annual demand profiles are shown in the following figures. Space & AHU heating demand profile follows an ordinary curve, where the highest demands during the cold season are from November through March, as Figure 50 shows.

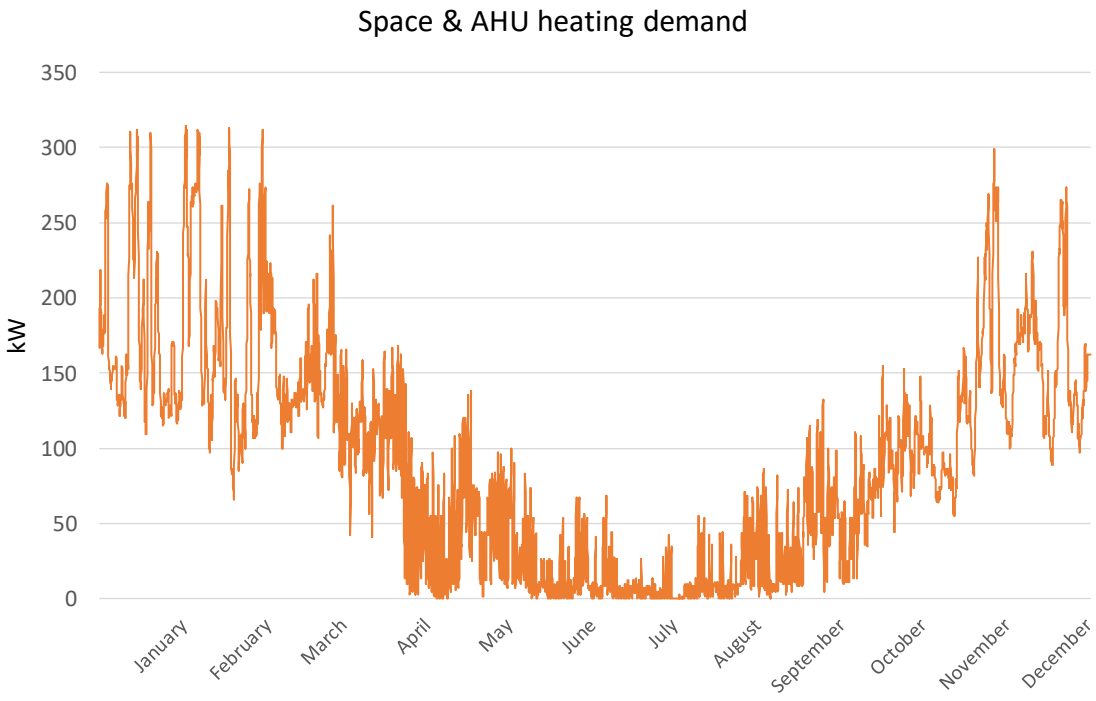

Figure 50. Yearly space heating and AHU heat demand.

The DWH demand has a more stable seasonal heating demand compared to the space heating profile. The demand curve is shown in Figure 51.

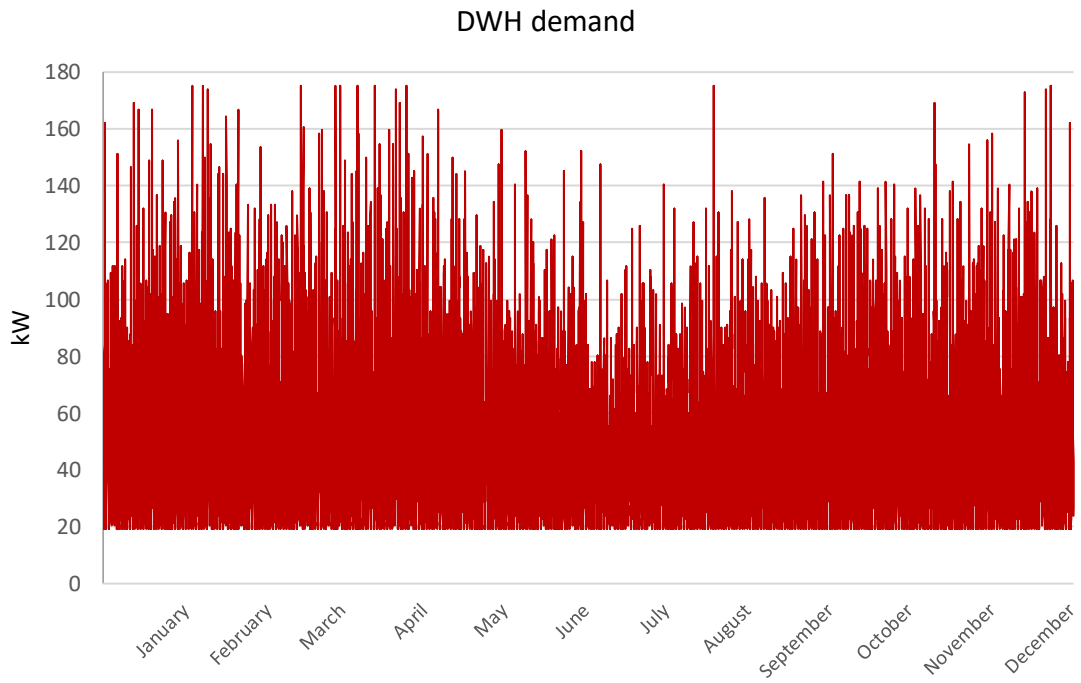

Figure 51. Yearly domestic water heating demand.

Space cooling demand takes place from late spring to early fall, but mostly during the summer season. The highest demand peaks are in the middle of the summer season, as Figure 52 shows. It can also be noticed that the space cooling energy demand is minor, but the required cooling power is much higher.

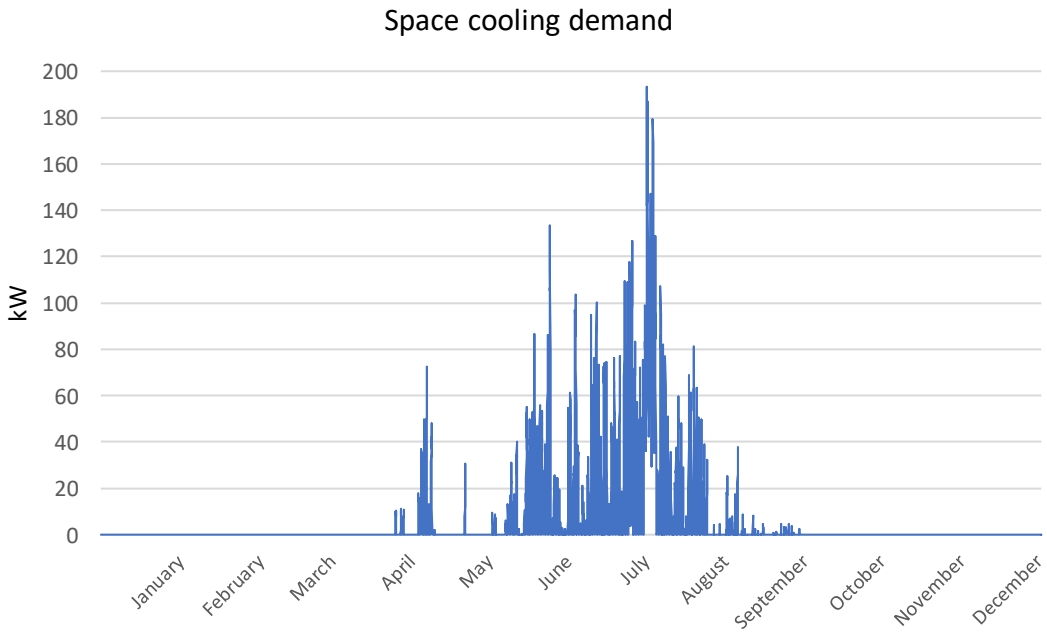

Figure 52. Yearly space cooling demand.

5.2 Main system application sizing

5.2.1 Heat pump sizing

The sizing of the heat pump was made by looking at the given heating demand curves. The general praxis for sizing is to set condenser capacity where yearly energy coverage is around 90 %. This sizing approach is commonly used, and it is found reasonable in terms of cost. Energy coverage describes the produced heat pump energy compared to the total energy demand. Separate heat pumps were chosen for both heating networks (space heating & DWH network), mainly for achieving better COP values for both units, and greater yearly energy coverage for the DWH network unit. Based on the given profile, condensing capacities were set at 200 kW for space heating and 100 kW for DWH.

COP and Capacity values were calculated with Oilon Selection Tool that suited for brine-to-brine solutions. The software calculates actual performance parameters for Oilon heat pumps with given condenser and evaporator inlet and outlet temperatures. (Oilon Group Oy, 2020) Entering and leaving temperature difference (ΔT) for evaporator and condenser were set as 5 °C and 10 °C, respectively.

Values for COP, EER, heating, and cooling capacity were logged from evaporator inlet temperatures between 0 to 18 °C, which referred to given seawater temperature data. The condenser temperature level was anticipated to represent a low-temperature space heating network, such as underfloor heating. The entering and leaving temperatures ($T_{cond,\ in}$–$T_{cond,\ out}$) was set as 20–30 °C, 25–35 °C, 30–40 °C, and 35–45 °C. This generated four different heat pump performance value sets depending on the condenser temperatures. Four condenser temperature levels were chosen to cover all the possible temperature ranges in the simulation. This enables the heat pump to operate more dynamically during the simulation. R-513A working fluid was chosen from the Oilon software because of the lower GWP value and better performance during the selection process. The heat pump design parameters are presented in Table 8.

Table 8. Heat pump design parameters.

Model	S180	S150
Capacity	180 kW	150 kW
Evaporator ΔT	5 °C	5 °C
Evaporator T_{out} max	-5 °C	-5 °C
Condenser ΔT	10 °C	30 °C
Condenser T_{out} max	45 °C	65 °C
Working fluid	R–513A (GWP 631)	R–513A (GWP 631)

Unit model capacity does not match the condensing power, that was estimated from the demand curves. The actual condensing power is dependent on the sizing temperatures and auxiliary equipment, such as sub-coolers and variable-frequency drives. COP for the 180 kW HP was between 2,9–6,8 and for the 150 kW HP between 2,5–3,5 based on the performance data. The lower performance of the DWH heat pump depends on the higher temperature difference between the evaporator and condenser which decreases COP.

5.2.2 Seawater heat exchanger

Selecting a proper heat exchanger for seawater purposes required a query with a couple of manufacturers. Vahterus and Alfa Laval recommended titanium plate heat exchangers. Titanium is recommended for corrosive fluids, such as seawater. Pricing for titanium compared to regular steel is over 1,7 times more expensive. After looking at the given dimensioning data provided by the manufacturers, was it decided to continue further discussions with the Vahterus Plate & Shell heat exchanger (PSHE) model.

The essential design criteria for a seawater heat exchanger is to achieve a low ΔT on the seawater side. A low-temperature difference enables cold seawater utilization when the water temperatures are between 1 to 4 °C. Secondly, for preventing freezing is high mass flow rate is endorsed, which derives from the low ΔT on the seawater side of the heat exchanger. Figure 53 illustrates how the mass flow rate increases when the temperature difference ($T_{plate,in}$-$T_{plate,out}$) decreases on the plate side. The mass flow rate starts to increase rapidly when the ΔT decreases below 1 °C. Great mass flow rates require large pumping powers, which affects notably the pump investment costs.

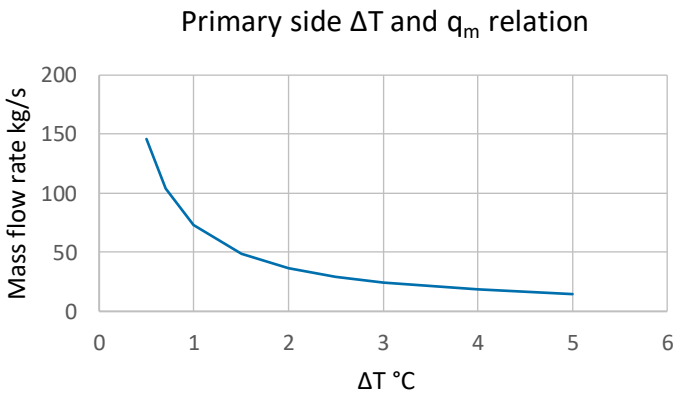

Figure 53. Relation between mass flow rate and primary (plate) side temperature difference.

Figure 54 presents the relation between seawater and ambient temperature compared to yearly heating demand. This illustrates the challenges of using seawater during the heating season where heating energy demand is high, and the heat source temperature is low. This sets a limit for utilizing seawater to a level where the heat exchanger has a high freezing risk. One benefit of seawater is the salinity which lowers slightly the freezing point. Experiments over how the heat exchanger performs around +/- 0 °C seawater temperatures have not been done in this kind of application. This arouses some uncertainty of the freezing risk in the heat exchanger. Therefore, one must make assumptions and rely on the computed performance data.

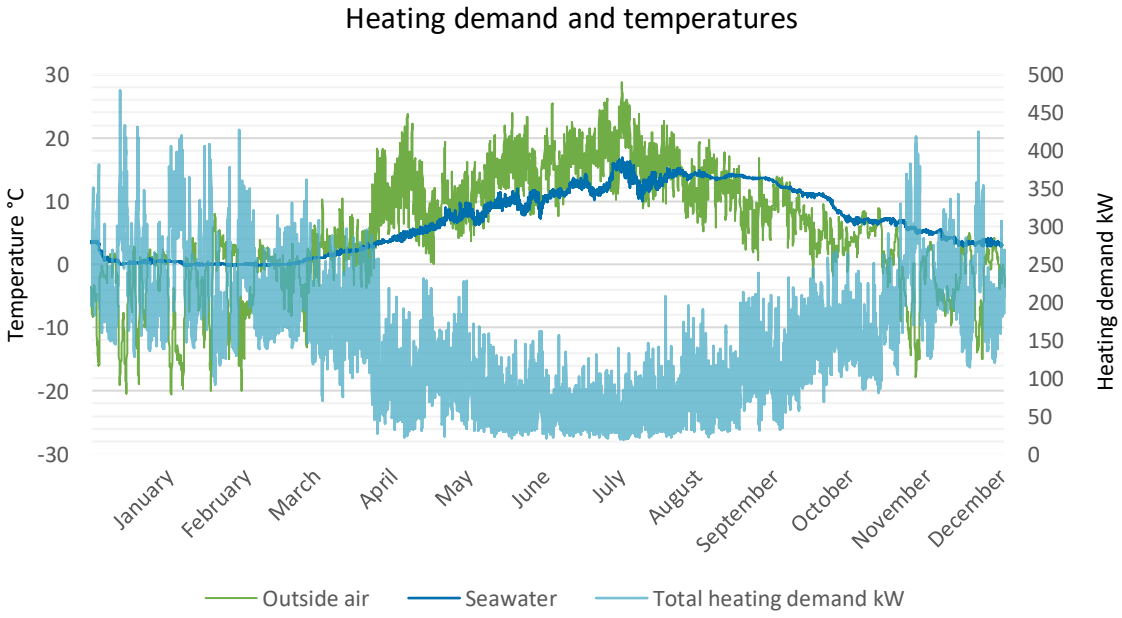

Figure 54. Chart of 2017 weather and seawater data including total heating demand of the case.

The design parameters are presented in Table 9 and the dimensions of the unit are shown in Figure 55.

Table 9. Vahterus PSHE design parameters.

	Value	**Explanatory sizing figure**
Capacity	300 kW	
Heat transfer area	59,7 m^2	
Logarithmic mean T	2,5 °C	
Mass flow rate	75,3 kg/s	
T Plate side (T_{in}-T_{out})	1 – 0 °C	
T Shell side (T_{in}-T_{out})	-5 – 0 °C	
Fluid Plate side	Seawater	
Fluid Shell side	Ethylene-glycol 30 %	
Pressure drop (p_{loss}) Plate side	95 kPa	
Pressure drop (p_{loss}) Shell side	14 kPa	
Connection sizes	DN 100	

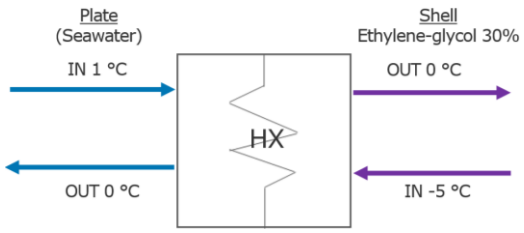

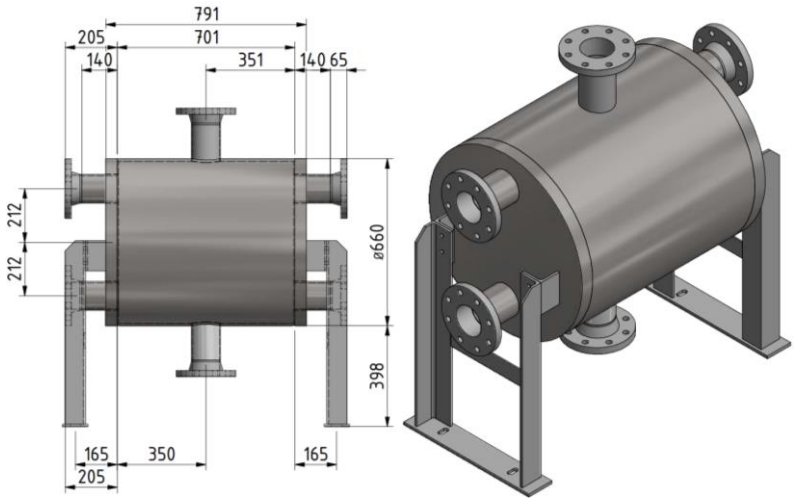

Figure 55. Dimensions of the Vahterus Plate & Shell heat exchanger. (Vahterus Oy, 2021)

5.2.3 **Circulation pumps**

Circulation pumps that were considered in the model are presented in Table 10 below. Different pump manufacturer P_e–q_m performance graphs were read to the simulation model and on the base of these were the yearly electricity consumption calculated. Seawater supply pump for the winter period is designed to work when seawater temperatures are close to 0°C and other-time supply pump cover the rest of the year. Circulation pumps for seawater have copper construction to improve corrosion resistance. Pressure loss was estimated equal to 100 kPa for all pumps, because of the case character.

Table 10 Table of circulation pump design values.

PU	q_m [kg/s]	P [kW]
Seawater, wintertime	75,5	13,5
Seawater, other-time	25	4,0
Ethylene-glycol network	30	4,4
Space heating network	12,5	1,96
DWH network	1,5	0,288
Space cooling network	9,1	1,3

5.3 Simulation model

IDA Indoor Climate and Energy (IDA ICE) software by EQUA Simulation Ab was used to create the simulation model. IDA Indoor Climate and Energy is a dynamic simulation tool to analyze building performance levels on a whole-year basis. IDA is capable of dynamic multi-zone simulations for the study of thermal indoor climate and energy consumption calculations of the whole building. An advanced level of this software was needed to create the simulation model, which is available in the Expert version. Advanced level or Plant has a schematic display interface, where you can modify and create new simulation models easily. (EQUA Simulation Ab, 2020) IDA ICE Plant requires always mass flow, temperature, and pressure when modeling systems. IDA solver engine requires that certain variables, for example, mass flow, should not equal to zero (0). The solver will otherwise produce a singular matrix and calculation is interrupted.

The model is based on different components and macro-objects that are connected via flow or signal links. Flow links contain mass flow, pressure, and temperature, where signal links read or send a single value. The designer can either use readymade components in Plant or create their own. In some conditions, creating your own components may result in a more stable simulation.

The modeled system consisted of heat pumps and DH substations where heat pumps covered most of the energy demands and district heating contributed to the peak demands and when the SWHP system was shut down. Space cooling demand was met by utilizing the cooling energy from the ethylene-glycol network. A water chiller unit was needed to cover the highest cooling demand peaks when the free cooling from the ethylene-glycol network was not sufficient. The district heating system consisted of only heating substations and a water

chiller unit for meeting the space cooling demand. The same model was used for simulating both systems and it is configured so that the SWHP components of the model could be excluded. Figure 56 presents the system layout of the simulation model. The general system and the DH-only system boundaries are marked with a hashed line.

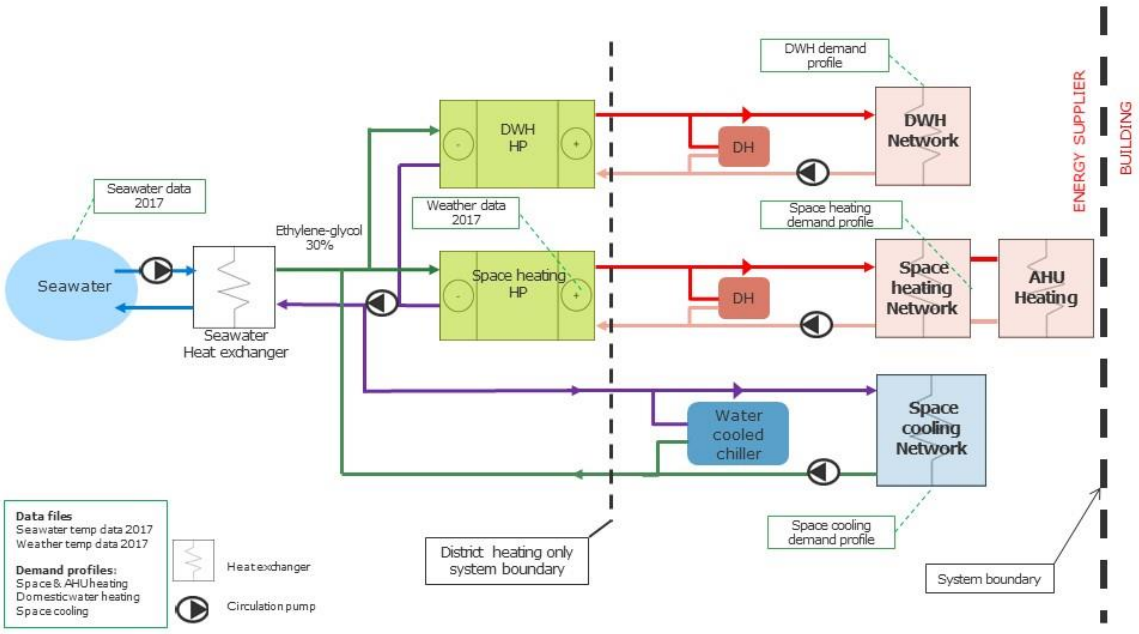

Figure 56 Simplified layout of the SWHP model in IDA ICE.

The system boundary for this model was delimited to the primary energy supply side of the building block, in other words, all the main technical applications that are required for heating and cooling between the heat source and building heat exchangers for the different networks. Apartment and common area electricity consumption were neglected. Piping lengths and sizes were not taken into concern in this model. This was due to the minor impact on the simulation results. Also, when the case was generic, there was no specific data on where the building block was placed.

The focus was on the primary side network between seawater and heat pump evaporators. This section is what differs a SWHP system from others, such as ground source heat pump systems. The secondary side between the condenser and building heat exchanger is a typical configuration that does not differ between models.

Starting values for the simulation model were heating demand data profiles, seawater, and ambient air temperature. 2017 was chosen as the reference year, where Kruunuvuorenselkä seawater temperature data at 7,3 m depth and outside air data from the Helsinki-Vantaa

weather station were used. The seawater depth of 7,3 m was chosen because the lower measurement point at 9,3 m was in the bottom mud, which would most likely cause blockage in the suction piping.

5.3.1 Heat pump simulation component

A simulation component was created to emulate heat pump operation. The component emulates a real heat pump unit, where the performance values change dynamically according to the simulation conditions. Option to modify the performance input data is also built in the component. The main reason to create an own simulation component was the complexity and risk of unstable simulations when using the readymade one. Also, this enabled the option to insert conveniently the performance data from the Oilon selection tool into the simulation model. Separate simulation components (macro objects) were created for both heat pumps. The inputs and outputs of the heat pump components are presented in Figure 57.

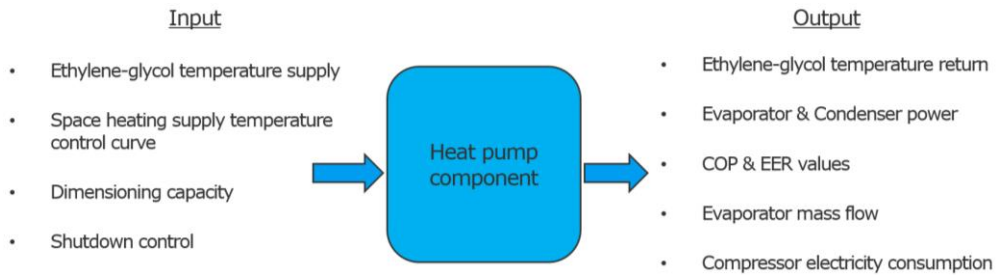

Figure 57 Plant macro object inputs and outputs.

Dimension capacity input refers to user input for the desired output power. Inside the heat pump component is a locked capacity value on which the performance data is based. The dimension capacity input either increases or decreases the output power, depending on the capacity value that is set in the component. The space heating supply temperature control is only for the space heating heat pump. The control curve is presented in section 5.3.4. The shutdown control switches the unit on or off depending on the anti-freeze signal from the primary side.

5.3.2 Primary network

Modeling of the primary network side between the seawater heat exchanger and heat pump evaporator is the most vital part of this system. The especially important part of this network is the heat exchanger temperature control by mass flow rate. The decision to create the model with an intermediate network enables the utilization of free cooling which is branched from this network to the space cooling network.

Three controls for regulating seawater mass flow depending on the seawater temperature were created. The first control is to keep the leaving ethylene-glycol fluid a few degrees colder than the entering seawater. Control 2 and 3 are active during the coldest seawater temperatures. The second control maintains the seawater outlet temperature above a certain degree of the reference freezing temperature. The third control, anti-freeze, shuts down the seawater supply pumps, ethylene-glycol network pump, and heat pumps if the seawater return temperature decrease below reference freezing temperature. Control 3 sends either signal 1 or 0 to the units that are connected to the control. Signal 0 activates the anti-freeze, which shuts down the units. Signal 1 turns the anti-freeze control off. The different controls are presented in Table 11 and illustrated in Figure 58.

Table 11. Primary side seawater mass flow control.

	Description	Value range
Control 1	The temperature difference between seawater inlet and secondary side outlet	-1…-5 °C
Control 2	Maintaining the seawater outlet temperature at a certain temperature above reference seawater freezing point (0°C)	0…1 °C
Control 3	Anti-freeze control: When the seawater outlet temperature decreases to freezing point temperature is the system shutdown. 1=Off 0=On	-0,2…+0,2 °C

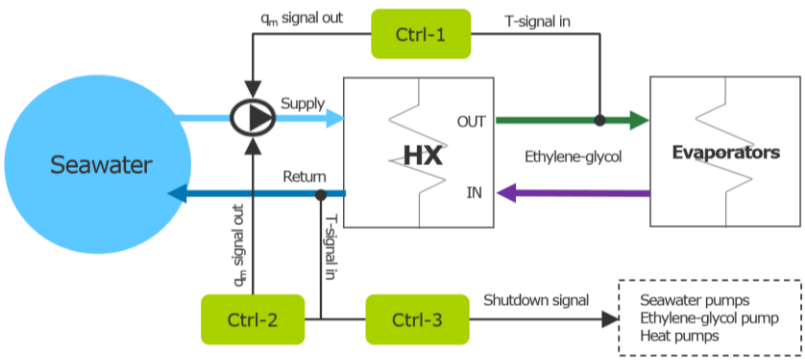

Figure 58. Primary side seawater mass flow control layout.

The temperature limit of 0 °C for shut down control was estimated to be a safe value, according to the earlier presented literature in 2.5.3 and 3.4.2. A practical approach to measuring accuracy has not been studied when estimating the control values. How fast should the changes be triggered in the units and how accurate temperature measurement is reasonable for unit control in real situations. Heat exchanger sizing data was read from Vahterus datasheets, where temperatures, pressure losses (P_{loss}), and capacity values were set in the heat exchanger component in IDA ICE. Seawater circulation pumps are controlled as following: $PU_{Wintertime}$ operates above 26 kg/s mass flow rate and the $PU_{other\text{-}time}$ is active up to 26 kg/s mass flow rate.

Figure 59 presents the supply and return temperatures for seawater (SW) and the ethylene-glycol (EG) network when Control 1 is set to -4 °C. From the end of January to the beginning of April are all presented temperatures constant, because the system is shut down most of the time.

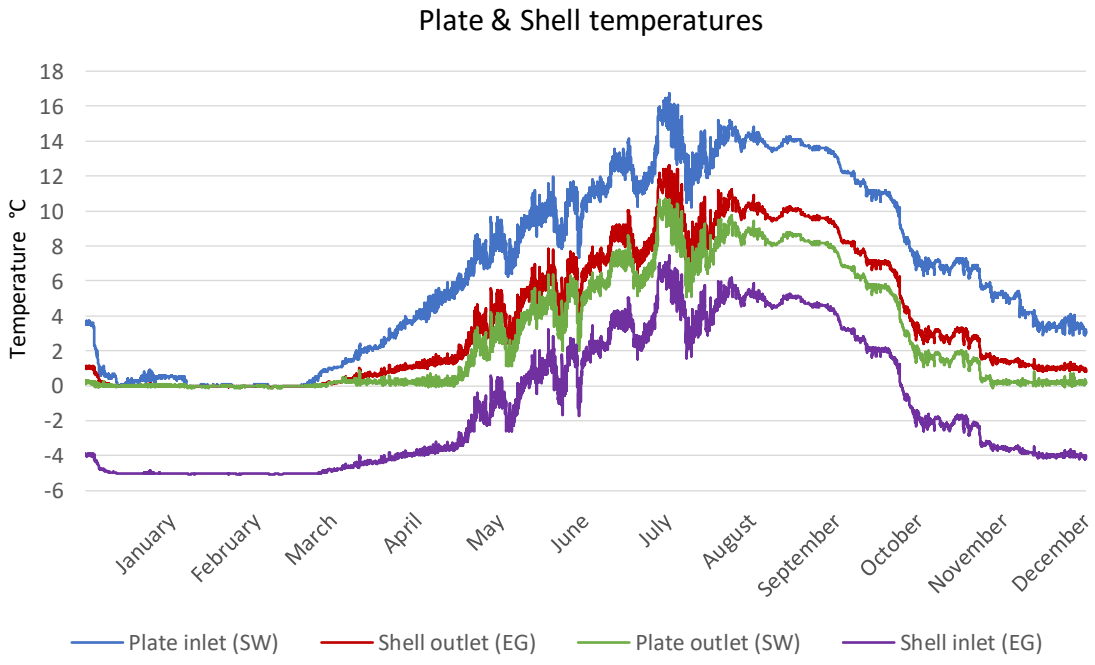

Figure 59. Primary network side temperatures when Control 1 set to -4°C.

The central design parameters for the primary network are introduced in Table 12.

Table 12. Main design parameters for the primary side network

	Value
$c_{p,seawater}$	4,0 kJ/kg K
$q_{m,seawater}$	75,5 kg/s
$c_{p,ethylene\text{-}glycol\ 30\%}$	3,7 kJ/kg K
ΔT_{HX} Plate to Shell	1 °C
Q_{HX}	300 kW
HX primary side p_{loss}	95 kPa
HX secondary side p_{loss}	14 kPa

5.3.3 Space cooling network

The space cooling network was designed in conjunction with the ethylene-glycol network, which enabled the free cooling option. The cooling supply was branched from the ethylene-glycol return side (HX secondary side inlet), and the cooling return was directed back to the ethylene-glycol supply (HX secondary side outlet) side. The cooling power derives from the heat pump evaporators, as the ethylene-glycol network is constantly active when heat pumps are producing heating power to the heating networks which enabled the use of evaporator capacity. Also, with this configuration can the evaporator supply temperature be increased. A water chiller unit was added to the network to meet the required cooling demand when free cooling capacity was not enough or available. The system layout is presented in Figure 60.

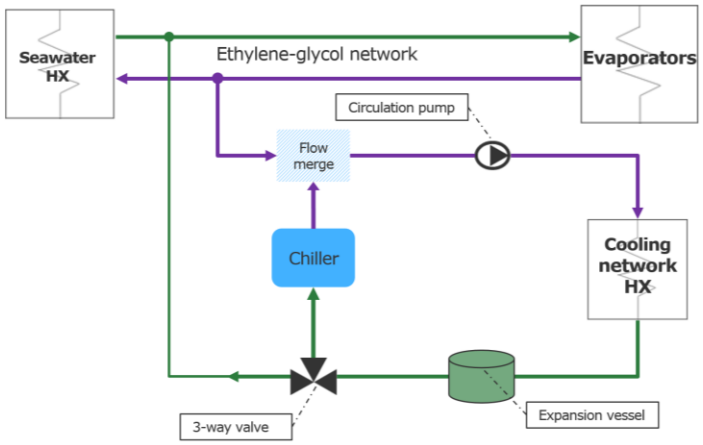

Figure 60. Simplified layout of the space cooling network.

The major cooling supply was provided by free cooling with an energy coverage of 89 %. Supply temperature varied as it was part of the ethylene-glycol network. The variation can be seen in Figure 59 shell inlet temperature plot. Return temperature was mainly constant

during the cooling period. In the DH-only system was no free cooling option available, therefore the cooling demand was produced entirely by the water chiller unit. A different network temperature of 7-12 °C was set for the DH-only system. The system design parameters are shown in Table 13.

Table 13. Space cooling network design values.

	Value
$Q_{cooling}$	183 kW
$E_{cooling}$	45 MWh
$q_{m,max}$	9,9 kg/s
EG_{return} temperature range	-5…+7,3 °C
SWHP system network temperature (T_{in}-T_{out})	5–10 °C
DH-only system network temperature (T_{in}-T_{out})	7–12 °C

5.3.4 Heating networks

The space heating & AHU and DWH networks shared the same system layout but used different demand profiles, temperatures, and mass flow rates. Space heating & AHU network supply temperature was regulated based on ambient temperature. The DWH network was set constant at 65 °C throughout the year for preventing legionella bacteria to develop in the network (Finnish Institute for Health and Welfare, 2021). The space heating was designed to represent an underfloor heating network, where supply and return temperatures are lower than in a radiator network. The system layout is presented in Figure 61 and the design parameters in Table 14.

Table 14. Main design parameters for secondary side

	Value
$Q_{space\ heating}$	315 kW
Q_{DWH}	169 kW
$q_{m,DWH}$	1,5 dm^3/s
$q_{m,space\ heating}$	12,5 dm^3/s
$\Delta T_{space\ heating}$	40–30 °C
ΔT_{DWH}	65–35 °C

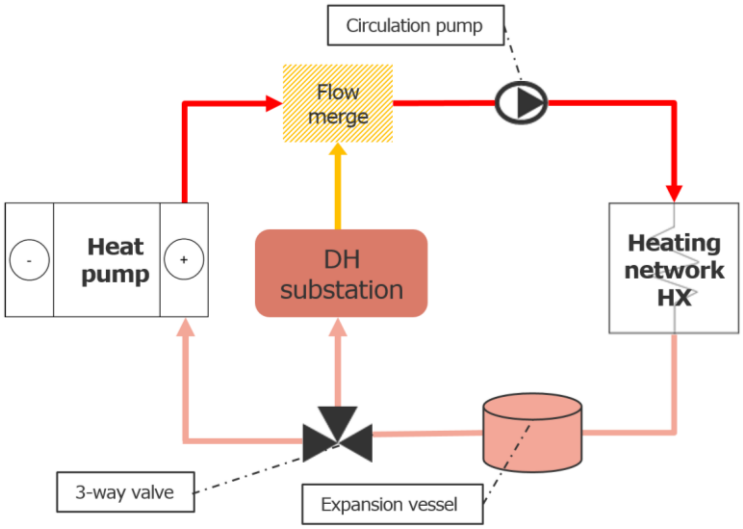

Figure 61. Simplified secondary side network.

The temperature difference in the heat exchanger is controlled by outside air temperature with a ΔT range from 4 to 10 °C. A three-way valve controls the flow rate between the heat pump and DH substation. Mass flow is directed to DH-substation when the heat pump power is not enough or when the unit is shut down.

The space heating demand profile included also AHU heating, which was not taken into concern when looking at the temperature levels. The focus was to model the network to respond dynamically to the heating demand and adjusting the supply temperature according to outdoor air. Another goal was to configure the heat pump as the main heating provider and DH as the supporting unit. This was mainly controlled by the heating supply control curve, presented in Figure 62. The control curve was adjusted to emulate a common temperature level which can be seen in ground source heat pump systems.

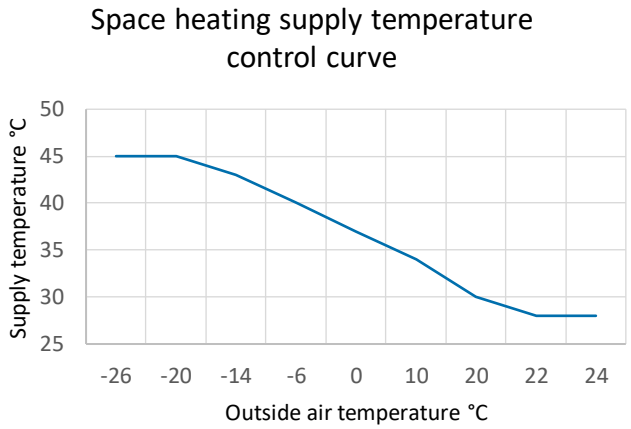

Figure 62. Supply temperature control curve.

The temperature plot for the space heating network is shown in Figure 63. DWH is excluded because of the constant temperature levels. The supply temperature is on average during heating season 35 °C and other times 30 °C. The higher supply temperature during the summer season derives from the bathroom underfloor or radiator heating. It can also be noticed that the supply temperature is rarely 45 °C, which derives from mild outdoor air temperatures of the year 2017 during the heating season. This temperature plot could represent future building stock heating network temperatures, where heat loads are decreasing when buildings are becoming more energy-efficient and smarter in controlling different energy loads.

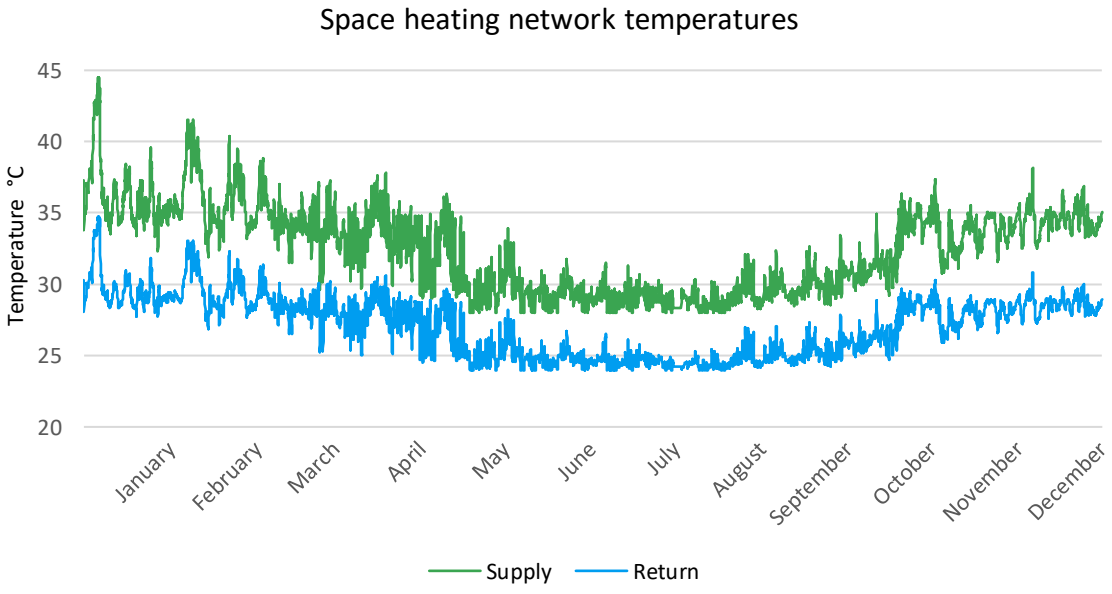

Figure 63. Space heating network temperature plot.

The distribution between HP and DH heating production is presented in Figure 64. It can be noticed that DH responds to the heating demand mostly during the first quarter of the year when the heat pumps are shut down. The figure presents the distribution with the final control values, which are presented in section 5.4.1.

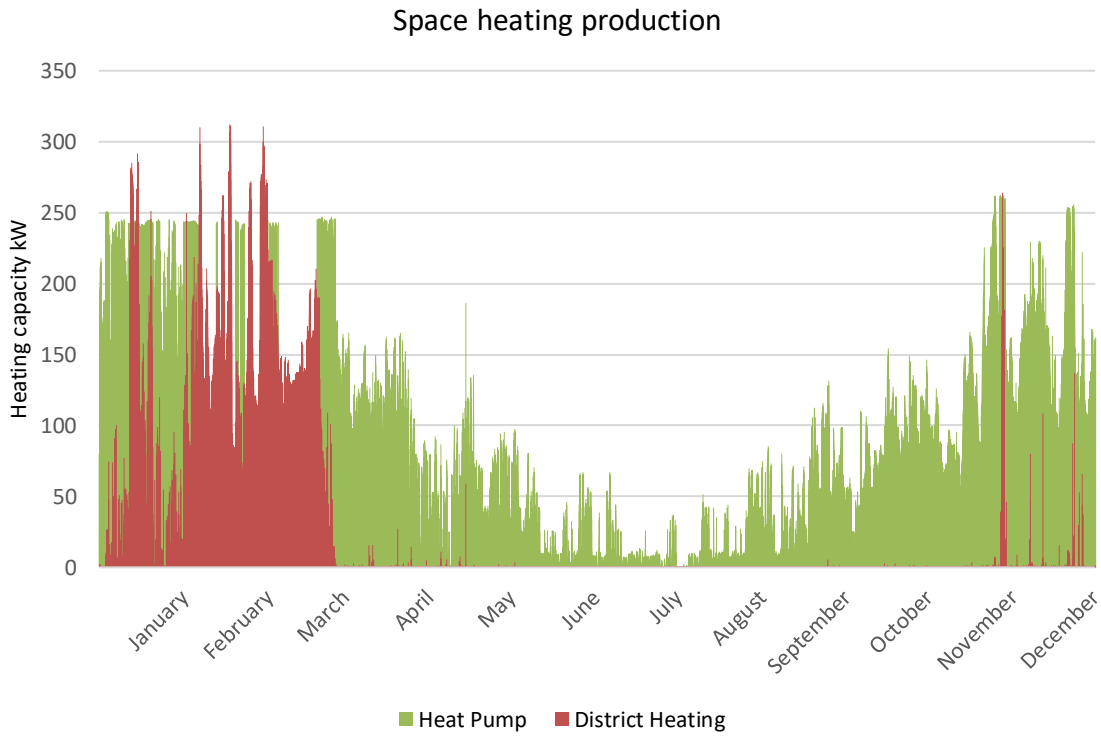

Figure 64. Space heating network heating distribution.

5.3.5 Output files and parametric run

Examining the functionality of the simulation model was done by logging variables into different output files. The output file consists of a plotted graph where the logged data is shown. The data can be transferred to Microsoft Excel if needed. For instance, are network supply and return temperatures typically logged into the same output-file. Combining the same network temperatures or mass flow into the same output file gave a quick overview of the simulation model if it worked as designed. The simulation run length is adjustable from one second to one year.

Parametric runs-function was used for executing multiple simulations with different parameters. Input and output values were required for creating a run. The input value is a chosen parameter whose effect on the model is examined. The output file is a logged result

of a variable, such as energy consumption. The number of simultaneous runs is restricted by the number of available CPU cores. The number of different values that were set in an input parameter increased the number of different combinations that had to be simulated.

The problem examined via parametric runs was the effect of seawater mass flow rate on system energy performance. The three primary side controls:

- Control 1: ΔT between seawater inlet and ethylene-glycol network supply temperature (HX second side outlet)
- Control 2: Maintaining the heat exchanger seawater outlet temperature above a certain temperature.
- Control 3: Temperature limit for the system shut down.

and maximum seawater mass flow rate was used as input values. The four input parameters are presented in Table 15. Results from the parametric run were studied for which control values and mass flow rates gave the best system performance and how the controls affected the different simulation components.

Table 15. Parametric run input values.

Input	Value range
$q_{m,seawater}$	75, 100, 150 [kg/s]
Control 1	-5 -4 -3 -2 -1 [°C]
Control 2	0,1 0,4 0,7 1,0 [°C]
Control 3	-0,2 -0,1 0,0 +0,1 +0,2 [°C]

The following output values were logged for instance:

- Heat pump energy coverages, heating energy production, COP, and compressor electricity consumption
- District heating production
- Circulation pump electricity consumption
- Cooling production

The results were exported to Microsoft Excel, where the results could be examined more easily. The results are shown in the next chapter 5.4.

5.4 Simulation results

The parametric run result data confirmed the significance of how minor temperature changes have a great impact on the whole system performance, especially heat pump production that affects the energy coverage. Already a 0,1 °C change in anti-freeze limit (Control 3) fluctuated the energy coverage substantially. Control 2 had an impact on the wintertime seawater pump. The higher the setpoint value for return water temperature was, the greater the annual electricity consumption. An increase in mass flow did not result in notable energy coverage improvement. The focus was to get a general view of how the different controls had an impact on the system performance. Figure 65 demonstrates the mass flow and anti-freeze control impacts on energy coverage.

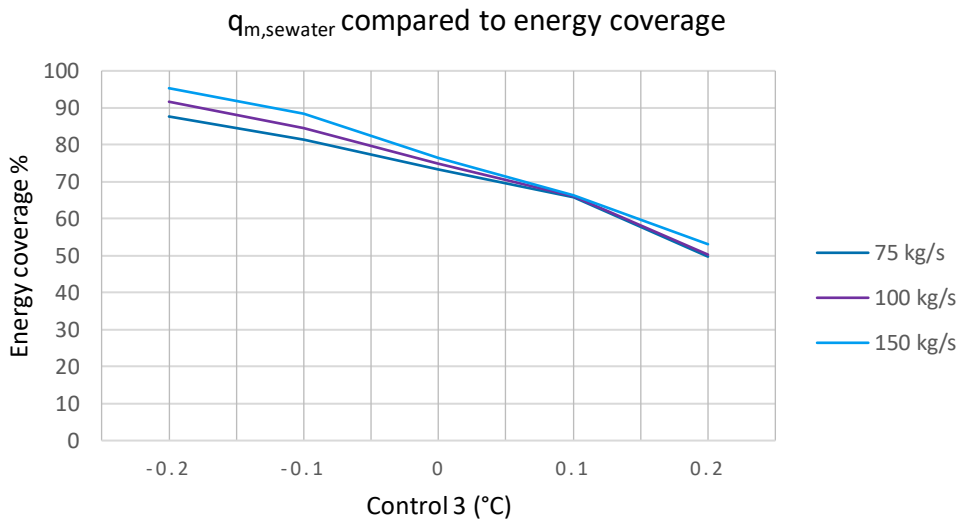

Figure 65. Mass flow rate and anti-freeze control impact on energy coverage.

The corresponding remark can be shown by comparing the distribution between the heat pumps and district heating production as Figure 66 presents.

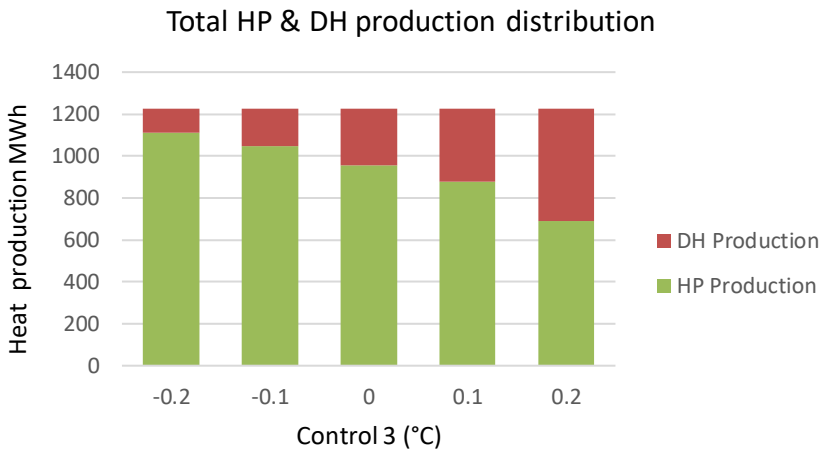

Figure 66. Anti-freeze control impact on heat production distribution.

The anti-freeze control operation is presented in Figure 67. It describes to a certain extent also the system running time. Variation occurs in the first quarter when the system is frequently shut down. This control is solely based on the incoming temperature signal, which may not be the most optimal way to control freezing. Shutting down frequently or ramping the power of the heat pump compressors and primary side circulation pumps will most likely affect the component durability, which will result in denser maintenance intervals. An engagement in how the real execution of this control would be done was not studied.

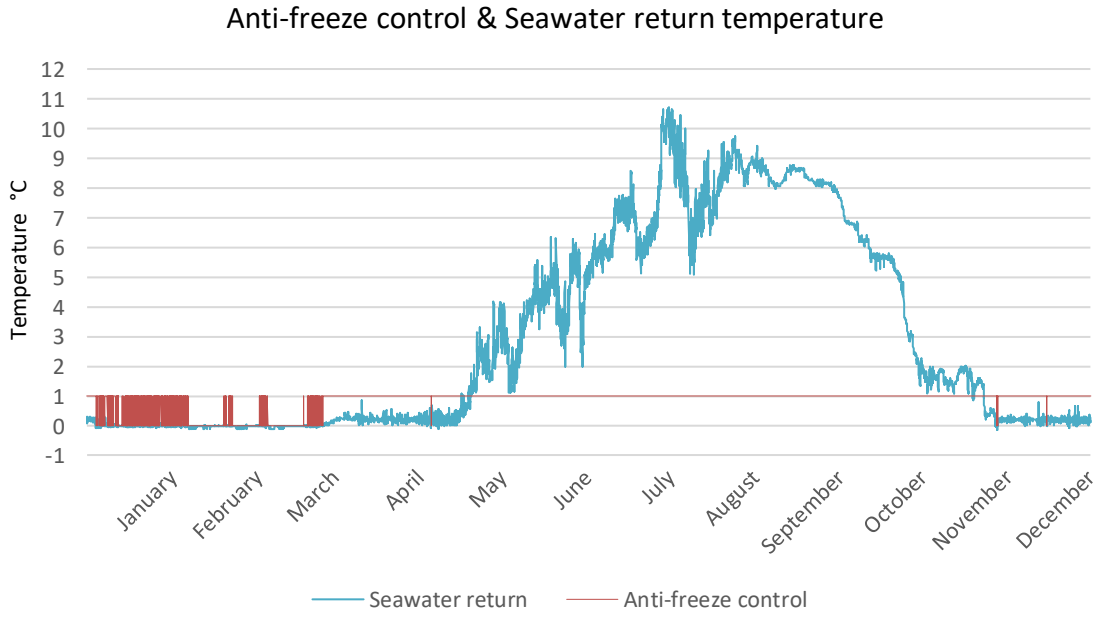

Figure 67. Anti-freeze control (1 = Control OFF, 0 = Control ON) with 0 °C limit contrary to seawater return temperature.

Another result was mass flow rate dependency on the temperature difference between seawater supply and ethylene-glycol (Control 1). Increasing the temperature difference resulted in lower mass flow rates that impacted pump sizing. Figure 68 presents the temperature difference impact on seawater mass flow. The curve for -1 ℃ does not plot because the mass flow exceeded the $PU_{other\text{-}time}$ and was directed to the $PU_{wintertime}$. The gap from January to March represents the wintertime seawater pump operation time. The chosen temperature difference for the final results was -4 °C.

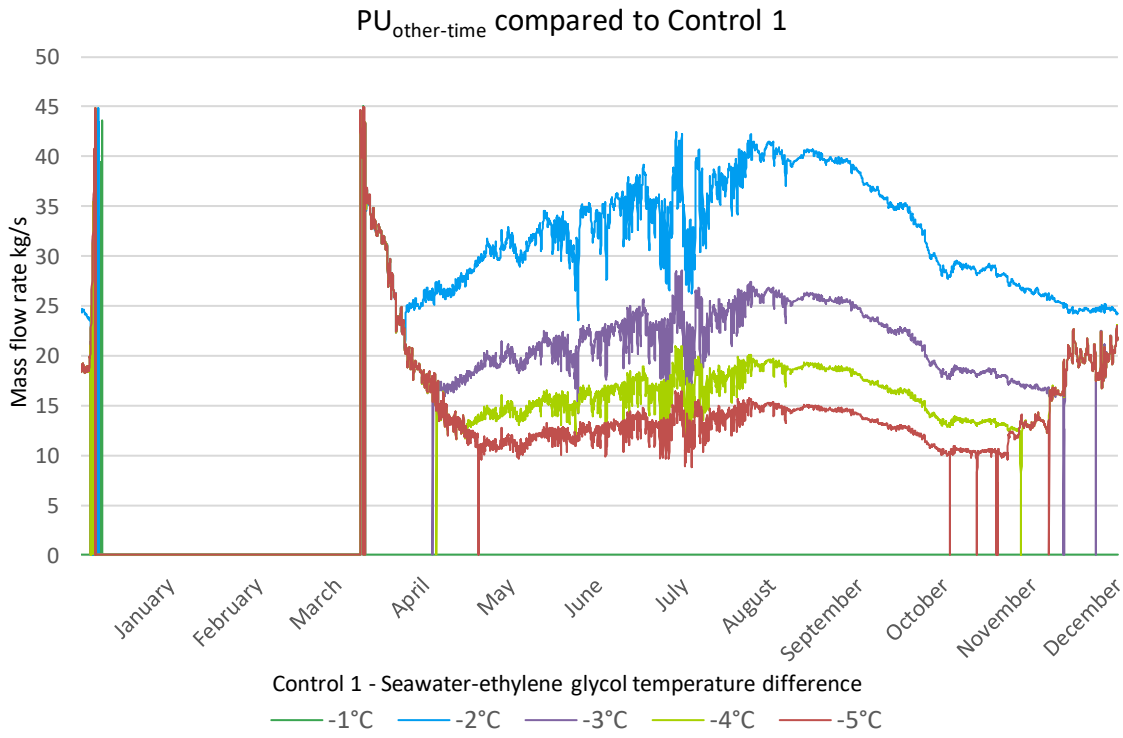

Figure 68. Control 1 impact on seawater pump other-time mass flow.

Control 2 affects the $PU_{wintertime}$ annual electricity consumption. This means that an increase in the seawater return temperature or setpoint value also increases the yearly electricity consumption of the circulation pump. The maximum q_m remained longer the higher the control setpoint was. This control contributed very diminutive to the increase in energy coverage.

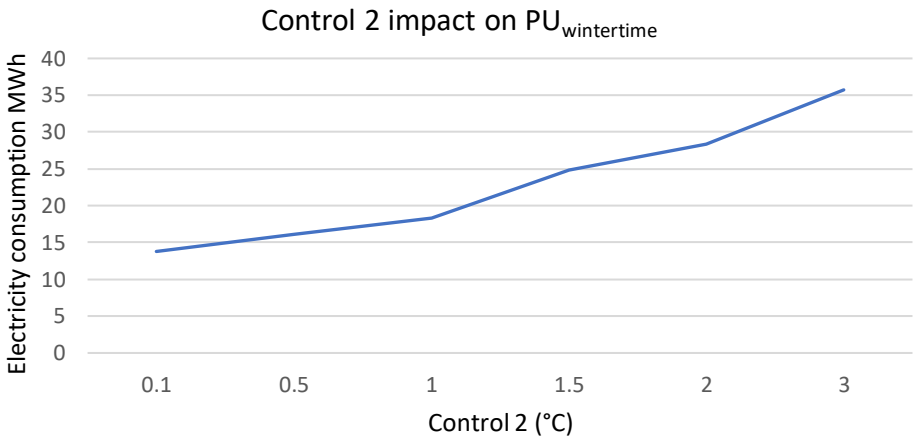

Figure 69. Control 2 impact.

Figure 70 presents primary network pumps mass flow rates. The temperature difference of the heat exchanger (HX) seawater side is also shown in the graph. The pump mass flows react according to the seawater return temperature. The smallest ΔT was during the coldest water temperatures and increased when seawater temperature rise. PU $_{wintertime}$ ramped up and down almost constantly, according to the anti-freeze control, but due to better visualization was it ignored.

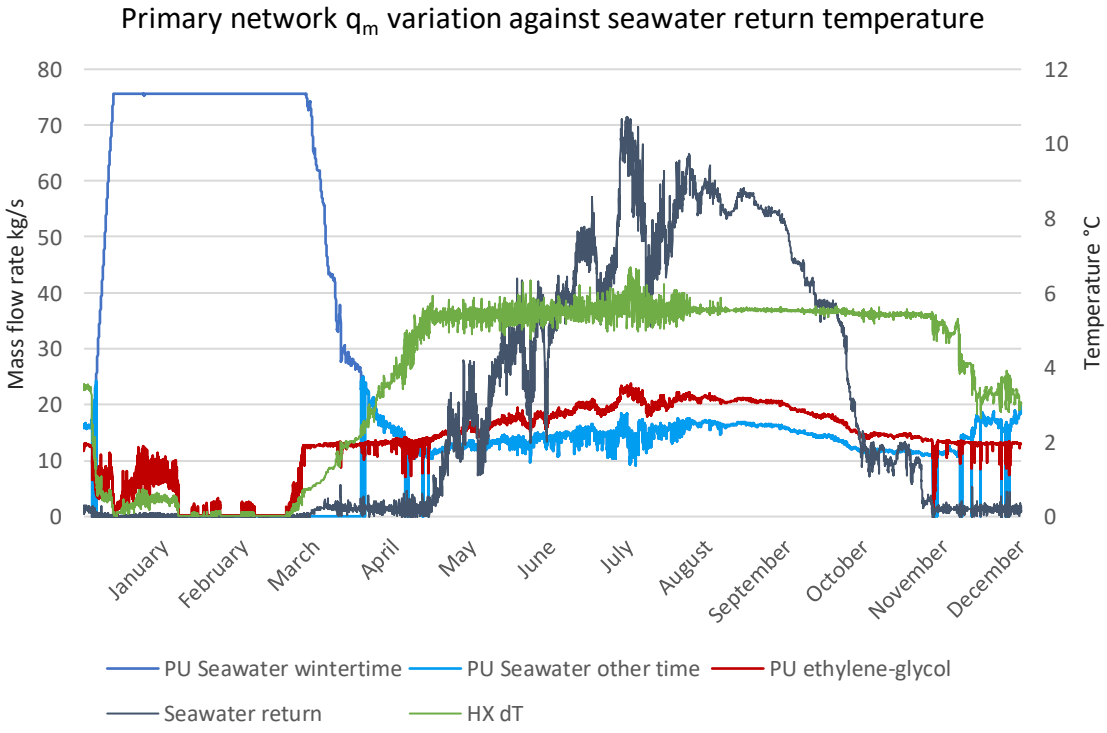

Figure 70. Primary network mass flow rates in contrast to seawater return temperature.

Figure 71 presents how the COP for both heat pumps is tied to the seawater temperature. The COP value emulated the seawater supply temperature, where the space heating & AHU HP showed the strongest impersonation. COP values ramped up and down in the first quarter, but due to better visualization was ignored.

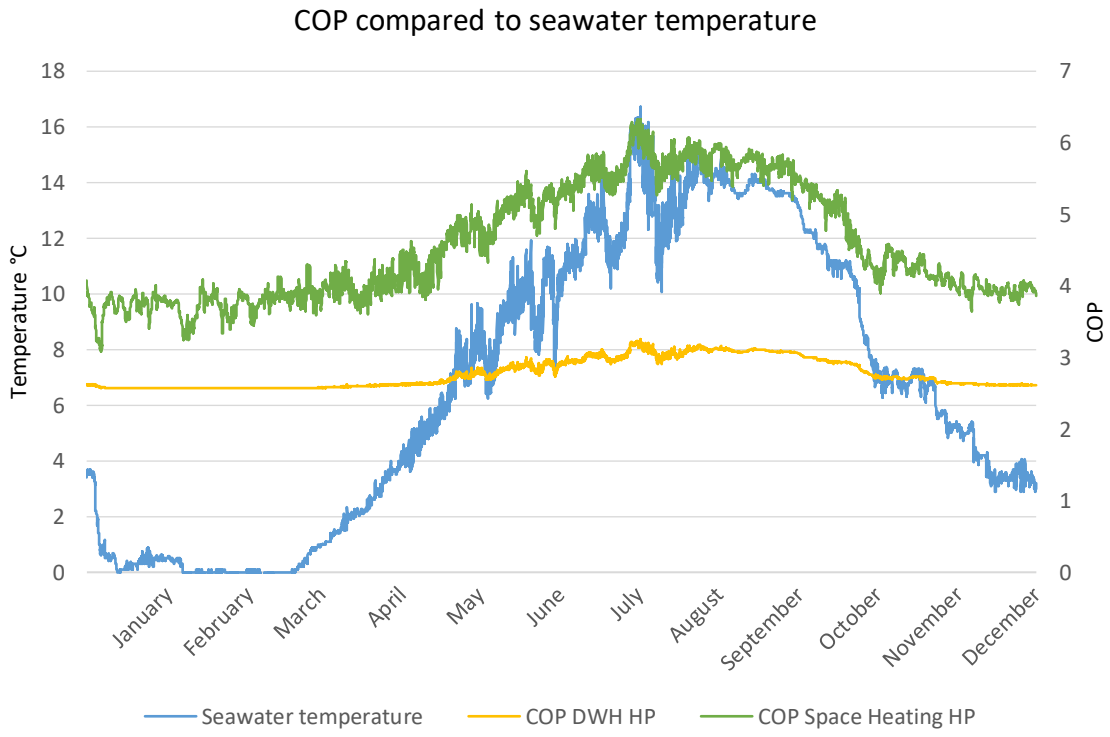

Figure 71. Yearly COP value variation in contrast to seawater temperature.

5.4.1 **Final parameter results**

Based on the examination of the different parametric runs the following values were chosen to be used in the final simulation:

- Control 1: -4,0 °C
- Control 2: 0,1 °C
- Control 3: 0,0 °C
- Seawater mass flow 75,5 kg/s.

Results from the simulations were used in the life cycle costing and emission calculations. Table 16 presents the simulation results.

Table 16. Key results of the concluding simulation.

	Value
Total system heating energy coverage	77 %
$HP_{space\ heating}$ energy coverage	74 %
HP_{DWH} energy coverage	87 %
Free cooling coverage	89 %
$E_{th,\ HP}$ production	950 MWh
$E_{th,\ DH}$ production	279 MWh
$E_{c,\ free}$ production	39,8 MWh
$E_{c,\ chiller}$ production	5 MWh
$E_{e,\ comp,space\ heating}$	141,6 MWh
$E_{e,\ comp,DWH}$	129,9 MWh
$E_{e,\ comp,\ chiller}$	1,8 MWh
$E_{e,\ pump}$ total	66 MWh
$COP_{\ avg,HP\ space\ heating}$	4,6
$COP_{\ avg,HP\ DWH}$	2,8

Most of the heating and cooling demands were produced by the heat pump network. District heating plays a minor role in this case. This was also the purpose of the system, that district heating had a supportive role. The available free cooling from the ethylene-glycol network covered most of the cooling demand. The production shares for both heating and cooling are presented in Figure 72.

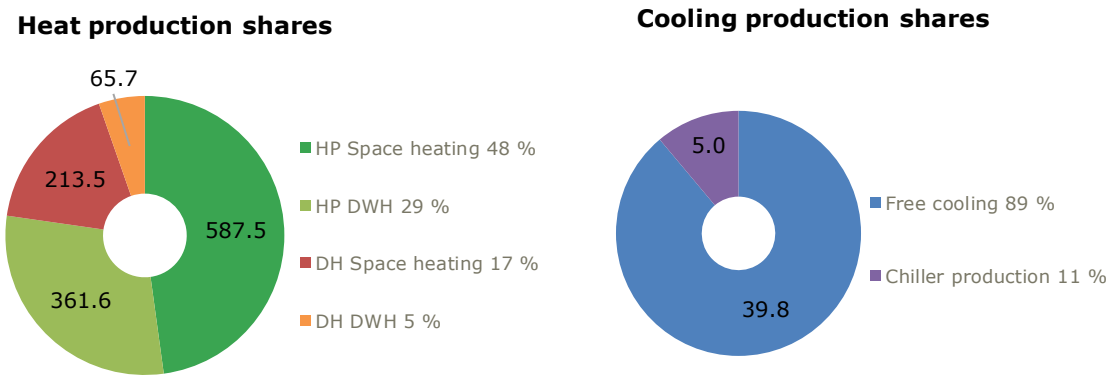

Figure 72. SWHP system heating and cooling production distribution in MWh and percentage.

The purchased energy, electricity, for heat pump compressors and circulation pumps, are shown in Figure 73 and Figure 74. Compressor electricity use takes the biggest share where the chiller has a minor yearly consumption. The primary side circulation pumps, seawater, and ethylene-glycol consumed most of the electricity. The secondary side heating and cooling networks' yearly electricity use is very small compared to the primary system.

The major components that should be given extra notice when sizing are the heat pumps and primary side circulation pumps for minimizing total electricity consumption.

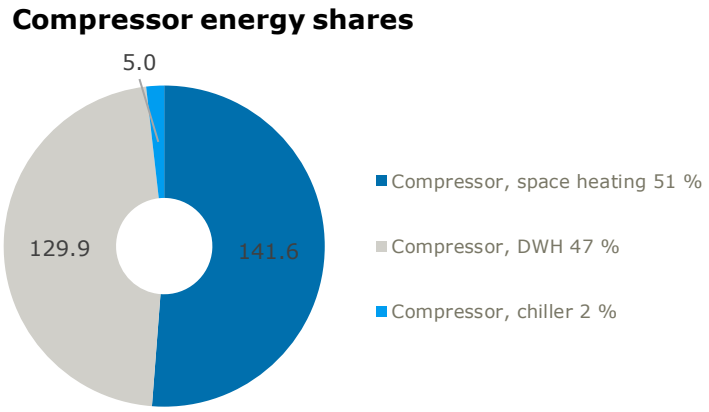

Figure 73. Compressor electricity consumption in MWh and percentage.

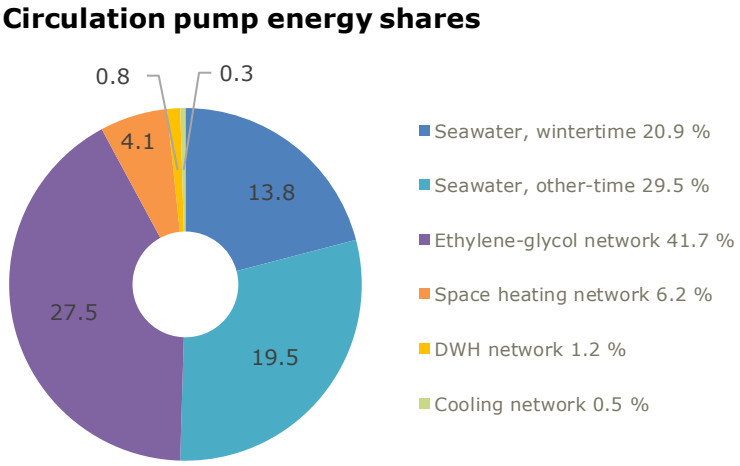

Figure 74. Circulation pumps electricity consumption in MWh and percentage.

5.5 Life cycle costing analysis

Method for study of profitability was done by life cycle costing (LCC) analysis. This method is widely used in economic evaluations of different systems. The analysis considers the capital and operation cost impacts by using net present value (NPV). (Sirén, 2015) The SWHP and DH systems are analyzed via the LCC method. Data of starting values are presented in Table 17.

Table 17. Main LCC calculation parameters

	Value
Lifetime	30 years
Inflation	1 %
Real interest rate	1,98 %
Energy escalation rate	2 %
Real escalation rate	0,98 %
Nominal interest rate	3 %
Electricity price	75,97 €/MWh

The common reference period for a heat pump system in LCC calculation is 30 years. Inflation, escalation, and rate of interest values were given. With the provided values was real interest and escalation rate calculated. Escalation can be expressed also as an increase in energy price. The same escalation rate is applied for both electricity and heating costs. The inflation rate is based on the consumer price index published by Statistics Finland. The index describes price development in products and services purchased by households. This index is used as a general inflation measure in Finland. (Statistics Finland, 2021) The described index is shown in Figure 75.

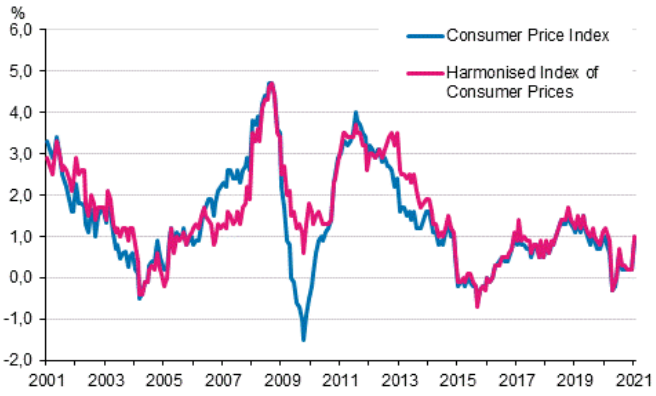

Figure 75. Consumer price index January 2001 to January 2021. (Statistics Finland, 2021)

Electricity price is based on the Vattenfall Oy housing company contract and Helen Sähköverkko Oy's low-voltage power distribution tariff pricing. (Vattenfall Oy, 2021) (Helen Sähköverkko Oy, 2021) District heating connection costs, water flow cost, and energy costs are based on pricing by Helen Oy. (Helen Oy, 2021) The seasonally changing energy cost was considered in the simulation model, where pricing change according to the season.

There are several ways to evaluate investment profitability. In the following sections are presented the used calculation methods, system investment costs, and results of the different methods. In the early stage of a project can profitability of the investment be estimated by a simple payback time (PBT) calculation. In the following is PBT presented:

$$PBT = \frac{\mathrm{I}}{A} \tag{9}$$

where

I starting investment

A yearly operation costs

Real inflation (*r*) and escalation rate(r_e): Where *f* is the inflation rate and f_e is escalation rate

$$r = \frac{i - f}{1 + f}, r_e = \frac{i - f_e}{1 + f_e} \tag{10}$$

where

i nominal interest rate

f inflation rate

f_e escalation rate

Discounting factor (a_n) for equivalent periodic performances can be calculated as follows:

$$a_n = \frac{1 - (1 + r)^{-n}}{r} \tag{11}$$

where

r real interest rate

n reference period

In the NPV method is all incomes, expenses, and investments discounted to present value and summarized. Reinvestments during the reference period must be included in the sum. The equation is as follows

$$NPV = I + \frac{q_1}{(1+i)^1} + \frac{q_2}{(1+i)^2} + \cdots + \frac{q_n}{(1+i)^n} + \frac{S}{(1+i)^n} \quad (12)$$

where

q	running costs and expenses
n	reference period
S	residual value in end of year n

By calculating the system energy price (C_{sys}) in €/MWh can it be compared against the purchased energy price or other system prices. It is as follows

$$C_{sys} = \frac{a'A + I_0}{a''E_{tot}} \quad (13)$$

where

a'	preset value factor including inflation
a''	preset value factor including escalation
E_{tot}	total heating and cooling energy demand
C_{sys}	system energy price

5.5.1 **Investments**

This section introduces investment costs and how the expenses are spread. The majority of Capital Expenditure (CAPEX) investment prices were read from manufacturer pricing lists or by approaching manufacturer sales representatives. All prices are without VAT. All major application investments were considered in this calculation. Piping costs for the separate networks and smaller devices, such as expansion vessels, valves, and measurement instruments were neglected.

The CAPEX costs for the SWHP system turned out to be comprehensive compared to the DH system. The investment difference was mainly derived from the number of different units that were required. Both systems share the same costs for secondary side circulation pumps, substations, and district heating connection costs. For the DH system was a larger water chiller was chosen to meet the peak space cooling demand.

DH connection costs included basic cost, line cost, water flow cost, and excavation costs. DH-substation prices were read from a cost database provided by the company. A seawater intake filter was required to prevent fouling in the seawater supply line. Energy accumulators were needed for storing excess heating energy from heat pumps and balancing the production. Seawater supply and return piping was estimated to be 100 m of polyethylene (PE) pipe. CAPEX investments for both systems are presented in Table 18.

Table 18. SWHP & DH CAPEX investment costs. VAT 0 %.

	SWHP		**District Heating**	
Product	**Amount**	**Total Cost [€]**	**Amount**	**Total Cost [€]**
Heat Pump 150kW	1	56 680		
Heat Pump 180kW	1	52 400		
Water chiller 183,7kW			1	57 800
Water chiller 145,4kW	1	53 400		
Seawater heat exchanger 300kW	1	35 000		
Seawater intake filter	1	14 500		
DH-Substation	1	20 295	1	20 295
PU Seawater wintertime	1	12 800		
PU Seawater other-time	1	11 400		
PU Ethylene-glycol	1	5 272		
PU DWH	1	1 499	1	1 499
PU Space heating	1	4 806	1	4 806
PU Cooling	1	3 399	1	3 399
Energy accumulator	4	27 200		
Seawater pipes PE DN200	100 m	5 712		
DH Connection costs		19 560		19 560
Total		**323 923**		**107 359**

Operating expenses (OPEX) for district heating are checked from price lists by Helen Oy. Service costs for DH substation were estimated at 500 €/a and heat pumps 2000 €/a per unit. The yearly electricity power tariff cost was calculated with an estimated electricity demand of 534 kW for the whole building block. The electricity price was calculated to 75,97 €/MWh. Total operating costs are lower for the SWHP system, even though the system consumes much more electricity. One major difference is in yearly district heating energy charge cost. All energy consumptions for electricity, heating, and cooling were read from the simulation model. Table 19 presents OPEX costs for compared systems.

Table 19. Annual SWHP & DH OPEX costs.

	SWHP		**District Heating**	
Expense	**Consumption [MWh/a]**	**Yearly costs [€/a]**	**Consumption [MWh/a]**	**Yearly Costs [€/a]**
District heating				
Energy charge		14 848		65 182
Water flow charge		12 870		12 870
Electricity tariff				
Annual basic charge cost		312		312
Annual Power tariff cost		28 836		28 836
HP Compressor space heating	141,6	10 760		
HP Compressor DWH	129,9	9 869		
Chiller Compressor	1,8	137	17,2	1 048
		0		
PU Seawater wintertime	13,8	1 050		
PU Seawater other-time	19,5	1 481		
PU ethylene-glycol	27,5	2 089		
PU Space heating	4,1	310	4,1	250
PU DWH	0,8	61	0,8	49
PU Cooling	0,3	24	0,3	21
Service cost		6 500		2 500
Total		**89 146**		**111 068**

Reinvestments, such as application renewals, were read from the instruction guide RT 18-10922. The guide contains information about the technical lifetime and maintenance period for heating, ventilation, and air-conditioning (HVAC). (Building Information Ltd, 2008) The maintenance periods were referenced from this document for circulation pumps and heat exchangers. Heat pump and chiller compressor renewal were estimated as 50 % of the unit investment cost. The following reinvestments were noticed:

- 15 years: Compressors for both heat pumps and chiller
- 20 years: Circulation pumps. DH-substations, Plate & Shell HX

Reinvestments excluded in the DH system were the heat pump compressors and Plate & Shell HX. These costs are included in the NPV calculation presented in section 5.5.2 Profitability.

5.5.2 **Profitability**

In this section are the results of the LCC calculation presented. The simplest PBT calculation gave the following result

$$PBT = \frac{CAPEX_{SWHP} - CAPEX_{DH}}{OPEX_{DH} - OPEX_{SWHP}} = 9{,}73\ years \quad (15)$$

By calculating the difference between the compared system OPEX and CAPEX results in a coarse estimation of PBT. Systems that include both heat pumps and DH substations have a PBT approximately of 10 years.

Recognizing the operation costs that affect inflation or escalation when implementing real interest and escalation rate to NPV calculations is needed. Separate NPV calculations were made for both systems OPEX where real inflation (r) and escalation (r_e) rates were implemented. NPV consist of starting investment expenses at year 0 to where OPEX is added cumulatively until the end of the reference period. Service costs are calculated with the real inflation rate. NPV graph is presented in Figure 76. The intersection indicates PBT for the SWHP investment. Higher start investment for the SWHP resulted in greater savings of 290 565 €. The small alternations on both curves represent the reinvestments where SWHP has greater reinvestments because of the more comprehensive system.

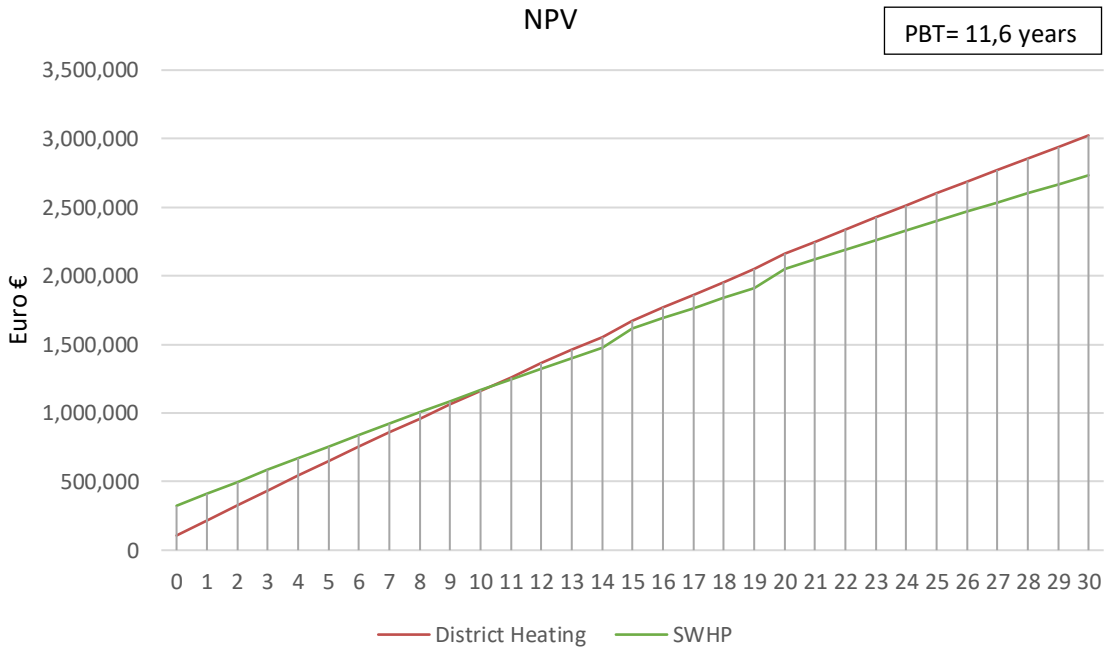

Figure 76. NPV over 30 years of the compared systems.

The PBT in NPV calculation is more accurate because the calculation takes the real inflation and escalation rates into account. Also, reinvestments of units have an impact on the final expenses. Before calculating the system prices for the compared systems was the discount factor (a_n) with real interest and escalation to be calculated. The following values were attained by using equation 11:

$$a'_n = 22{,}46$$
$$a''_n = 25{,}88$$

By inserting (a_n) in Equation 13 were the following system prices attained:

$$C_{sys,SWHP} = 70{,}80\,\frac{€}{MWh}$$
$$C_{sys,DH} = 79{,}42\,\frac{€}{MWh}$$

The price difference was 8,6 €/MWh between the compared systems. When the calculated system price is lower than the purchased energy price, is the investment more appealing, which the SWHP system price show. With all the previous calculation method results can it be seen that hybrid heat pump systems overall are reasonable investments, with a relatively short PBT.

5.6 Carbon dioxide (CO_2) emissions

The CO_2 emissions are calculated based on an emission database for construction developed by SYKE, commissioned by the Ministry of the Environment. The goal of this database is to complement the calculation of the climate impacts of buildings throughout their lifecycle. (Finnish Environment Institute SYKE, 2021). Table 20 shows the total CO_2 emissions and energy productions (heating and electricity) over the 30-year reference period. The SWHP system had 1 994 tons lower CO_2 emissions compared to the district heating-only system. Emissions from the district heating-only are over two times more than SWHP. With these results is the SWHP system evidently more attractive when looking from an emissions perspective.

Table 20. Total CO_2 emissions in tons and energy production in MWh over a 30-year lifetime of the compared systems. (Finnish Environment Institute SYKE, 2021)

System	Energy production [MWh]	Emissions [t]
SWHP	18 557	1 635
DH_{only}	37 418	3 629

The cumulative CO_2 emissions and energy production over the compared systems are presented in Figure 77, where the difference in energy and emission production can be observed clearly.

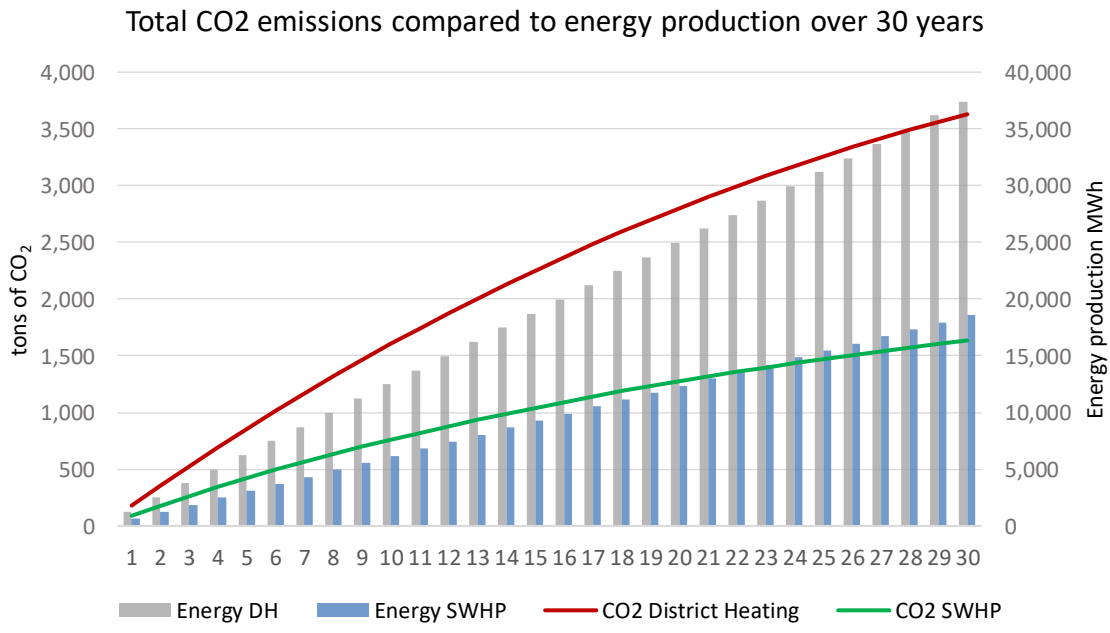

Figure 77. Cumulative CO_2 emissions in tons and total energy production in MWh of the compared systems.

6 CONCLUSIONS & SUMMARY

In this research, energy analysis was performed for a seawater water heat pump (SWHP) system that utilizes seawater as a heat source. A generic residential building block was used as the case study. A simulation model was created with IDA ICE, where the energy system consisted of heat pumps combined with district heating. The modeled energy system was compared to a district heating-only system via system performance, economic, and emission calculations. Systems in similar scale and weather conditions did not come across during this study.

A SWHP system differs from more common ground source heat pump systems by the primary side, where the heat source is a water body. Two methods for seawater utilization were presented: open and closed-loop, where open-loop uses a separate heat exchanger for seawater and closed-loop has a collector pipe system. Open-loop configuration can also be designed with direct evaporation, thus excluding the need for a separate heat exchanger.

In colder climates, for example in the Nordics, the biggest challenge is to use seawater or lake water for heating energy purposes during wintertime when the temperature close to the surface is around 0 °C. In deeper waters, around 35 m, where the temperature is higher (ca. 2 °C) and more stable seawater utilization conditions are better. The salinity of the seawater decreases slightly the freezing point of the seawater. Seawater also enables the utilization of free cooling which is a good option to produce nearly emission-free and reliable cooling energy.

Preliminary assumed concern in a SWHP system was the performance during wintertime, for example how cold water can be utilized until the heat exchanger starts to freeze. The risk for freezing can be addressed by taking the supply water from deeper levels, enabling great seawater mass flow rates and enough pressure loss in the heat exchanger. These two features enable great turbulent flow and large shear forces in the heat exchanger that decrease the risk of freezing. The Plate & Shell heat exchanger (PSHE) has the features mentioned earlier and is, therefore, a valid option when designing a system that utilizes seawater. Pre-heating of seawater could solve freezing issues, by circulating for instance seawater through an application that requires cooling. The warmer return water could then pass through the heat exchanger and then be ejected back to the sea. Only direct use of seawater was utilized in this case and no pre-heating was modeled.

Systems that use water for producing heating or cooling with heat pumps require a Water Permit. This is a direct referral to Water Act (587/2011), where it is stated that when placing pipelines or pumping from a water source a permit is required. AVI administrates these permits and the applications should be directed to the regional agency that operates in the area where the system is designed to be built. Permission is also needed from the owner of the waters. This type of system does not bring presumably any major issues for authorization. However, lakes could be one exception, where the maritime biology and energy balance can be more sensitive, subject to the scale of the designed system and water body. Also, social apprehensions can have a significant role in the interest comparison in the subject of lakes. When exploring possible options for the piping lines, issues that affect water and sea activities should be concerned. To mention a few common matters sea routes, navigable routes, fishing areas, recreational areas, and places where water activities are exercised.

The generic residential building block of 14 400 k-m^2 had an annual heating demand of 1225 MWh and 45 MWh of cooling demand. The given energy demand data was based on measurement data over 50 apartment buildings built between 2014-2016 in Helsinki. It contained hourly data over space heating, DWH and space cooling. With the building demand data, seawater temperature data from Kruunuvuorenselkä in Helsinki, and weather data from Helsinki-Vantaa functioned as starting values for the simulation model. The created simulation model consisted of a seawater heat exchanger, separate heat pumps for both heating systems, free cooling from an ethylene-glycol network combined with a water chiller to meet the cooling demand, and district heating to cover the peak heating demands. All the main components of the system were modeled, and real performance data was used to emulate a real SWHP system performance.

The created controls for seawater mass flow control resulted in a couple of noteworthy remarks with trivial parameter adjustments in the controls. Two seawater pumps were used. One for the cold seawater period from January to April, where high seawater flow was applied. The second pump was active the rest of the year. The most responsive control was the anti-freeze control, where the heat exchanger return temperature was measured (Control 3). Already a 0,1°C change had a distinct impact on energy coverage. The lower the set point for system shut down, the higher was the energy coverage. At this stage, the question can be asked once again: how low can the return water be before any signs of frosting occur in the heat exchanger? One indicator would be the more specific freezing

point of the source when dimensioning the heat exchanger. The Gulf of Finland has a freezing point between -0,17 °C to -0,33 °C. Control for maintaining ethylene-glycol fluid colder than seawater supply (Control 1) impacted the mass flow rate during the warmer seawater return temperatures from April to December. Smaller temperature differences resulted in a higher seawater mass flow rate. Evaluating an optimal temperature difference will have a beneficial effect on seawater pump energy consumption.

The benefit of free cooling comes along with the intermediate ethylene-glycol network, from where most of the space cooling demand was utilized. The major issue to solve is the control of supply and return temperature limits for seawater. Real limits must be experimentally discovered by heat exchanger testing in order to verify its performance close at seawater freezing points. Practical measurement accuracy for the anti-freeze control is also an important issue that requires experimental proceedings. Shutting down frequently or ramping the power of the heat pump compressors and primary side circulation pumps will most likely affect the component durability, which will result in more frequent maintenance intervals.

In general, the seawater mass flow rate had a trivial impact on the whole system's performance. Doubling the mass flow rate from the dimensioned had a minor influence on energy coverage. The most significant control was the anti-freeze control, which had a remarkable impact on the heat pump energy coverage.

Results from the SWHP simulation model demonstrated a reasonable performance in heating production. With a total heating energy coverage of 77 %, this system is realizable and has the potential to be a valid solution towards carbon-neutral heating production. The most difficult time for the system performance was during the coldest seawater temperatures, from January to April. During that period was district heating covering the heating energy demands. Free cooling from the ethylene-glycol network between the seawater heat exchanger and heat pump evaporators reached an energy coverage of 89 %. The average COP for space heating and DWH heat pumps were 4,6 and 2,8. The ethylene-glycol circulation pump had the biggest electricity consumption by covering almost half of the 66 MWh total pump electricity usage. Through LCC analysis became the results more concrete, when comparing the investment and operating costs for both systems.

SWHP investment cost (CAPEX) turned out to be three times more expensive than the DH system. The operating costs (OPEX) were favorable for SWHP, where the DH system had higher expenses, mostly of greater district heating energy charge costs. As a result, the SWHP system became a more profitable investment when the reference period of 30-years was used. Payback time resulted in 11,6 years and a system energy price of 70,8 €/MWh. As the purchased energy price was 76 €/MWh, was the investment more favorable for the SWHP system compared to the DH-only with a 79,4 €/MWh system energy price. Savings after 30 years were 290 569 €. Total CO_2 emissions were over two times lower for the SWHP system. Over the 30 years were the total emissions 1365 t for SWHP and 3629 t for district heating-only. When comparing different energy systems, it is worth remembering that emissions are an important factor when energy production emissions are concerned.

Nowadays residential building block areas are becoming more self-sufficient for instance with ground source heating. Consequently, SWHP could be a considerable option in the case of optimal location and size of the water body. We are surrounded by lakes and seas, that have a substantial potential to be utilized in heating and cooling production at different scales. The technology is available and becoming more mature over time. Nevertheless, there is a necessity for a sustainable system design, which would be tailored to work around the year, especially during colder seasons. To conclude the performed thesis work, seawater and lake water could play an important role in heating & cooling energy production, which would increase the share of cleaner energy production and steer forward carbon-neutral urban environment.

A topic for further research could be to perform an experimental test on how the mass flow rate affects a seawater heat exchanger. Test of the unit performance with the created controls in the simulation model at low-temperature conditions would give perception into how the simulated results are in line with the measured data. The experimental test would also give perspective on the freezing risks in the heat exchanger and measurement data over temperature when freezing starts to occur. The next step would be to create a pilot SWHP system to get data over the whole system performance. A pilot system would provide fundamental data on what kind of measurement accuracy could be optimal for the system operation controls. Also, a study on how water intake depth would affect energy production and system running time with the pilot system.

REFERENCES

Abdesselam, H. et al., 2008. Performance Study of a Water-to-Water Heat Pump Using Non-azeotropic Refrigerant Mixtures R407C. *International Energy Journal,* Volume 9, p. 267–274.

Aittomäki, A., 1983. *Maaperä ja vesistöt lämmönlähteinä,* Tampere: Tampere University of Technology, Department of Mechanical Engineering, Thermal Engineering, Report 37.

Aittomäki, A. et al., 2012. *Kylmätekniikka.* 4th ed. Helsinki: Suomen Kylmäyhdistys Ry.

Alenius, P., Myrberg, K. & Nekrasov, A., 1998. The physical oceanography of the Gulf of Finland: a review. *BOREAL ENVIRONMENT RESEARCH,* Volume 3, pp. 97-125.

Arpagaus, C. et al., 2018. High temperature heat pumps: Market overview, state of the art, research status, refrigerants, and application potentials. *Energy,* Volume 152, pp. 985-1010.

Arsenyeva, O. P. et al., 2016. Two types of welded plate heat exchangers for efficient heat recovery in industry. *Applied Thermal Engineering,* Volume 105, pp. 763-773.

ASHRAE, 2018. *ASHRAE Guide for Sustainable Refrigerated Facilities and Refrigeration Systems.* Atlanta,GA: ASHRAE.

Awad, M. M., 2011. *Fouling of Heat Transfer Surfaces, Heat Transfer - Theoretical Analysis,Experimental Investigations and Industrial SystemProf. Aziz Belmiloudi (Ed.).* [Online]
Available at: http://www.intechopen.com/books/heat-transfer-theoretical-analysis-experimental-
[Accessed 16 December 2020].

Bruun, J.-E., 2020. *MarineFinland.fi.* [Online]
Available at: https://www.marinefinland.fi/en-US/Nature_and_how_it_changes/The_unique_Baltic_Sea
[Accessed 29 June 2020].

Building Information Ltd, 2008. *Kiinteistön tekniset käyttöiät ja kunnossapitojakso.* [Online] Available at: https://kortistot.rakennustieto.fi/kortit/RT%2018-10922 [Accessed 1 February 2021].

Cengel, Y. A. & Boles, M. A., 2011. *Thermodynamics - An engineering approach.* 7th ed. New York: McGraw-Hill.

Cengel, Y. A. & Ghajar, A. J., 2015. *Heat And Mass Transfer:Fundamentals And Applications.* 5th ed. New York: McGraw-Hill Education.

CFD-Finland Oy, 2013. *Liite 4a - Vuosaaren voimalaitoksen jäähdytysvesien leviämismalliselvitys (CFD-Finland Oy 2013),* Helsinki: Helsingin Energia.

EHPA, 2020. *Heat pump sales overview.* [Online] Available at: http://www.stats.ehpa.org/hp_sales/story_sales/ [Accessed 12 May 2021].

EHPA, 2021. *Market Data.* [Online] Available at: https://www.ehpa.org/market-data/ [Accessed 12 May 2021].

EQUA Simulation Ab, 2020. *IDA Indoor Climate and Energy*. [Online] Available at: https://www.equa.se/en/ida-ice [Accessed 18 March 2021].

Eskafi, M., Asmundsson, R. & Steingrímur, J., 2019. Feasibility of seawater heat extraction from sub-Arctic coastal water; a case study of Onundarfjordur, northwest Iceland. *Renewable Energy,* Volume 134, pp. 95-102.

Espoon Rakennusvalvonta, 2017. *Rakennusvalvonnan ohje-Maalämpökaivon poraus tai lämmönkeruuputkiston asentaminen.* Espoo: City Of Espoo.

European Commission - EU Science Hub, 2019. *Renewable Energy – Recast to 2030 (RED II).* [Online] Available at: https://ec.europa.eu/jrc/en/jec/renewable-energy-recast-2030-red-ii [Accessed 24 October 2020].

European Commission, 2020a. *Renewable energy directive.* [Online] Available at: https://ec.europa.eu/energy/topics/renewable-energy/renewable-energy-directive/overview_en#timeline-for-renewable-energy-in-the-eu
[Accessed 24 October 2020].

European Commission, 2020b. *Energy efficiecy directive.* [Online] Available at: https://ec.europa.eu/energy/topics/energy-efficiency/targets-directive-and-rules/energy-efficiency-directive_fi
[Accessed 24 October 2020].

European Commission, 2020c. *National action plans and annual progress reports.* [Online] Available at: https://ec.europa.eu/energy/topics/energy-efficiency/targets-directive-and-rules/national-energy-efficiency-action-plans_en
[Accessed 24 October 2020].

European Commission, 2020d. *In focus: Energy efficiency in buildings.* [Online] Available at: https://ec.europa.eu/info/news/focus-energy-efficiency-buildings-2020-feb-17_en
[Accessed 25 October 2020].

European Commission, 2020e. *Energy performance of buildings directive.* [Online] Available at: https://ec.europa.eu/energy/topics/energy-efficiency/energy-efficient-buildings/energy-performance-buildings-directive_en
[Accessed 25 October 2020].

Eurostat Newsrelease, 2020a. *Eurostat-Newsrelease- Renewable energy in the EU in 2018 Share of renewable energy in the EU up to 18.0%.* [Online] Available at: https://ec.europa.eu/eurostat/documents/2995521/10335438/8-23012020-AP-EN.pdf/292cf2e5-8870-4525-7ad7-188864ba0c29
[Accessed 23 October 2020].

Finnish Energy, 2021. *Energy Year 2020 - District Heating.* [Online] Available at: https://energia.fi/en/newsroom/publications/energy_year_2020_-_district_heating.html#material-view
[Accessed 12 May 2021].

Finnish Environment Institute SYKE, 2021. *Emissions database for construction.* [Online] Available at: https://co2data.fi/ [Accessed 19 March 2021].

Finnish Institute for Health and Welfare, 2021. *Legislation and guidelines relating to legionellae.* [Online] Available at: https://thl.fi/en/web/environmental-health/water/legionella-bacteria-in-water-systems/legislation-and-guidelines-relating-to-legionellae [Accessed 1 March 2021].

Forsén, M., 2005. *Heat pumps technology and environmental impact,* s.l.: European Heat Pump Association.

Frate, G. F., Ferrari, L. & Desideri, U., 2019. Analysis of suitability ranges of high temperature heat pump working fluids. *Applied Thermal Engineering,* Volume 150, p. 628–640.

Green Building Council Finland, 2020. *Ympäristöluokitukset.* [Online] Available at: https://figbc.fi/ymparistoluokitukset/ [Accessed 2 December 2020].

Hansen, M., 2011. *Experimental testing and analysis of surface water heat exchangers,* Stillwater: Oklahoma State University.

Helen Oy, 2021. *District heat prices.* [Online] Available at: https://www.helen.fi/en/heating-and-cooling/district-heat/district-heat-prices [Accessed 1 March 2021].

Helen Sähköverkko Oy, 2021. *Electricity distribution prices.* [Online] Available at: https://www.helensahkoverkko.fi/en/services/electricity-distribution-prices [Accessed 1 March 2021].

Helsingin Energia, 2014. *Biopolttoaineiden käytön lisääminen Helsingin energiantuotannossa - YMPÄRISTÖVAIKUTUSTEN ARVIOINTISELOSTUS,* Helsinki: Helsingin Energia.

Hundy, G. F., Trott, A. R. & Welch, T. C., 2016. *Refrigeration, Air Condition and Heat Pumps.* 5 ed. s.l.:ElSevier.

Hundy, G., Welch, T. & Trott, A., 2008. *Refrigeration and Air-Conditioning,* Amsterdam: Butterworth-Heinemann.

IEA-Heat pump technologies, 2020. *Efficiency and heat pumping application.* [Online] Available at: https://heatpumpingtechnologies.org/market-technology/refrigerants/ [Accessed 10 January 2020].

Kapanen, M., 2017. *Kylmäainetilanne 2017,* s.l.: Suomen Kylmäaineyhdistys ry.

Kavanaugh, S. P. & Rafferty, K. D., 2014. *Geothermal Heating and Cooling : Design of Ground-source Heat Pump Systems.* Atlanta: ASHRAE.

Kavvadias, K., Jiménez-Navarro, J. & Thomassen, G., 2019. *Decarbonising the EU heating sector - Integration of the power,* Luxembourg: Publications Office of the European Union.

Kärkkäinen, S., 2012. *Heat pumps for cooling and heating,* s.l.: International Energy Agency Demand-Side Management Programme.

L 27.4.2014/527. Environmental Protection Act, 2014. *Environmental Protection Act.* [Online]
Available at: https://finlex.fi/en/laki/kaannokset/2014/en20140527_20190049.pdf [Accessed 26 October 2020].

L 27.5.2011/587. Water Act., 2011. *Water Act.*. [Online] Available at: http://www.finlex.fi/fi/laki/ajantasa/2011/20110587 [Accessed 11 July 2020].

Laitinen, A., Rämä, M. & Airaksinen, M., 2016. *Jäähdytyksen teknologiset ratkaisut,* Espoo: VTT Teknologian tutkimuskeskus.

Laitinen, J., 2020. *Environmental aspects on heat pumps with water as heat source* [Interview] (3 July 2020).

Leppävirta, M., Virta, J. & Huttula, T., 2017. *Hydrologian Perusteet.* Helsinki: Helsingin yliopisto, Fysiikan laitos.

Liu, L., Wang, M. & Chen, Y., 2019. A practical research on capillaries used as a front-end heat exchanger of seawater-source heat pump. *Energy,* Volume 171, p. 170–179.

Longhini, M., 2015. *Next generation of refrigerants for residential heat pump systems,* Lisboa: Instituto Superior Técnico.

Majuri, P., 2020. *Geoenergy and sustainable development – Perspectives on environmental challenges and governance of geoenergy installations, Doctoral Disseration,* Turku: Univeristy Of Turku-Faculty of Science and Engineering-Department of Biology Environmental science.

Makhntach, P. & Khodabandeh, R., 2014. The role of environmental metrics (GWP, TEWI, LCCP) in the selection of low GWP refrigerant.. *Energy Procedia,* Volume 61, p. 2460–2463.

Ministry of Economic Affairs and Employment, 2019. *Finland's Integrated Energy and Climate Plan,* Helsinki: Ministry of Economic Affairs and Employment.

Ministry of the Environment and Statistics Finland, 2017. Finland's Seventh National Communication under the United Nations Framework Convention on Climate Change. In: Helsinki: Ministry of the Environment and Statistics Finland, p. 314.

Ministry of the Environment, 2020. *Land Use and Building Act.* [Online] Available at: https://ym.fi/en/land-use-and-building-act [Accessed 28 October 2020].

Mitchell, M. S. & Spitler, J. D., 2013. Open-loop direct surface water cooling and surface water heat pump systems—A review. *HVAC&R Research,* Volume 19, pp. 125-140.

Monti, A. & Romera, B. M., 2020. Fifty shades of binding: Appraising the enforcement toolkit for the EU's 2030 renewable energy targets. *Review of European Community and International Environmental Law (RECIEL),* 29(2), pp. 221-231.

Morrow, S. J., 2010. *Unicode number 0216 (ALT+ Number) Diameter.* Lancaster, ITT Corporation, Industrial Process.

National Geographic, 2011. *Lake Turnover.* [Online] Available at: https://www.nationalgeographic.org/media/lake-turnover/ [Accessed 13 May 2020].

NIBE, 2014. *Pientalojen maalämpöpumppu opas,* Vantaa: NIBE.

Nordman, R., 2012. *Seasonal Performance factor and Monitoring for heat pump systems in the building sector SEPEMO-Build Final Report,* Borås: SEPEMO-build.

Nowak, T., 2018. *Heat Pumps - Integrating technologies to decarbonise heating and cooling,* Brussels: European Copper Institute.

Oilon Group Oy, 2020. *Oilon Selection Tool.* [Online] Available at: https://oilon.com/en-gb/products-gb/oilon-selection-tool/ [Accessed 18 March 2021].

Ramboll, 2020. *Project notes.* Tampere: Ramboll.

REHVA, 2016. *Federation of European Heating, Ventilation and Air Conditioning Associations position paper on the European Commission review of the ENERGY PERFORMANCE OF BUILDINGS DIRECTIVE,* Brussels: REHVA.

Reikko, T., 2020. *Kylmäaineet lämpöpumpuissa* [Interview] (26 November 2020).

REN21, 2018. *Renewables 2018 Global Status Report,* Paris: REN21 Secretariat.

Schneider, 2017. *White Paper 254: The Different Types of Cooling Compressors,* s.l.: Schneider Electric.

Shah, R. K. & P. Sekulić, D., 2003. *Fundamentals of Heat Exchanger Design.* Hoboken: John Wiley & Sons.

Sidat, S., 2018. *The importance of refrigerants in heat pump selection.* [Online] Available at: https://www.wsp.com/en-GB/insights/the-importance-of-refrigerants-in-

heat-pump-selection
[Accessed 1 September 2020].

Sirén, K., 2015. *Rakennusten Energiainvestointien Kannattavuuden Laskenta,* Espoo: Aalto Yliopisto.

Statistics Finland, 2021. *Consumer price index.* [Online] Available at: http://www.stat.fi/til/khi/index_en.html [Accessed 8 March 2021].

Su, C. et al., 2020. Seawater heat pumps in China, a spatial analysis. *Energy Conversion and Management,* Volume 203, pp. 1-15.

Suomen Maalämpötukku, 2021. *Keruupiiripaketit.* [Online] Available at: https://www.maalampotukku.fi/category/287/keruupiiripaketit [Accessed 31 March 2021].

Suvanto, S., 2020. *Authorization and permits for surface water heat pumps* [Interview] (20 October 2020).

SWEP, 2019. *Refrigerant handbook.* [Online] Available at: https://www.swep.net/refrigerant-handbook/refrigerant-handbook/ [Accessed 20 August 2020].

Teiniranta, L., 2010. *Heating and Cooling with a Heat Pump,* Jyväskylä: University of Jyväskylä - Department of Physics.

The Finnish Heat Pump Association (SULPU), 2021a. *Heat pump market in Finland 2020, slides,* Turku: SULPU.

The Finnish Heat Pump Association (SULPU), 2021b. *Press Release 1/2021 - In Finland another peak year for heat pumps. More than 100,000 pumps were sold,* Turku: SULPU.

Thomaßen, G., Kavvadias, K. & Navarro, J. P. J., 2021. The decarbonisation of the EU heating sector through electrification: A parametric analysis. *Energy Policy,* Volume 148, pp. 1-17.

Vahtera, E., 2018. *Meriveden lämpötila Helsingin edustalla,* Helsinki: Helsingin Kaupunki-Kaupunkiympäristön toimiala.

Vahterus Oy, 2021b. *Email and phone conversations with Miikka Ailama.* Helsinki: -.

Vahterus Oy, 2021c. *The Original Plate & Shell Heat Exchanger.* [Online] Available at: https://vahterus.com/products/ [Accessed 5 May 2021].

Vahterus Oy, 2021. *Plate & Shell Heat Exchanger,* Kalanti: Vahterus Oy.

Wang, Y. et al., 2012. Improvement of energy efficiency for an open-loop surface water source heat pump system via optimal design of water-intake. *Energy and Buildings,* Volume 51, p. 93–100.

Vattenfall Oy, 2021. *Asunto-osakeyhtiöt.* [Online] Available at: https://www.vattenfall.fi/yritysasiakkaat/asunto-osakeyhtiot/ [Accessed 28 April 2021].

Volkova, A. et al., 2019. Small low-temperature district heating network development prospects. *Energy,* Volume 178, pp. 714-722.

Xin, J., Lin, D. & Haiwen, S., 2018. Large-area seepage and heat transfer model of beach well infiltration intake system for seawater source heat pump. *Energy and Buildings,* Volume 158, pp. 1593-1601.

Zahid, A., 2016. Worlds Largest Ammonia Heat Pump (14MWh) for District Heating in Norway - A Case Study. *Heat Transfer Engineering,* Volume 37, pp. 382-386.

Zheng, W., Wu, Z., You, S. & Zhang, H., 2020. Model development and performance investigation of staggered tube-bundle heat exchanger for seawater source heat pump. *Applied Energy,* Volume 262, pp. 1-11.